CHAPTER IV
RESULTS AND DISCUSSION

1. Solid lipid nanoparticles (SLN)

1.1 Formulation of drug-free SLN

1.1.1 Preparation of drug-free SLN by warm microemulsion method (WME)

In preliminary study by WME, various solid lipids were used; Dynasan 114, stearic acid, GB and GP. From the results, both GB and GP could form SLN dispersions whereas the other two could not or displayed white precipitate after dilution. The surfactants used were Solutrol® HS15, Brij 72, Brij 98, M52, M53, M59, Tw20, Tw80, CreRH and CreEL. The latter three surfactants produced good physical results for several formulations while all of the formers could not stabilize SLN at all; therefore, they were excluded from further study. PG, Gly, PEG and Butanol were selected to be used as co-surfactant. Butanol with chosen solid lipid and surfactant could not form microemulsion that phase separation was shown. Hence, the three former co-surfactants were used in this experiment.

Physical appearance

The physical appearances of both SLN dispersions, GB-SLN and GP-SLN with various 1:1 surfactant and co-surfactant ratios are shown in Tables 10 and 11 respectively.

Effect of solid lipid

Various GB-SLN with Tw80 and three co-surfactants could not be prepared. Precipitation occurred especially when using PG as co-surfactant. This might be due to the long carbon chain length of GB which much difference between the melting point and room temperature could promote rapid lipid recrystallization. In contrast, GP-SLN could be obtained in all formulations. Morever the appearance of GP-SLN was clearer than that from GB-SLN indicating of the smaller particle size of

Table10 Physical appearances of SLN dispersions containing 10% GB as solid lipid with different types and amounts of surfactants and co-surfactants prepared by WME method

Formulation	Macroscopic		Formulation	Macroscopic		Formulation	Macroscopic	
	a	b		a	b		a	b
(Tw80+Gly):W			(Tw80+PG):W			(Tw80+PEG):W		
(15+15):60	-	-	(15+15):60	P	-	(15+15):60	-	-
(20+20):50	-	-	(20+20):50	P	-	(20+20):50	+	P3M
(25+25):40	+	P3M	(25+25):40	P	-	(25+25):40	+	P3M
(30+30):30	+	P3M	(30+30):30	P	-	(30+30):30	+	P3M
(35+35):20	+	P3M	(35+35):20	P	-	(35+35):20	+	P3M
(CreEL+Gly):W			(CreEL+PG):W			(CreEL+PEG):W		
(15+15):60	-	-	(15+15):60	+	-	(15+15):60	+	P3M
(20+20):50	+	P3M	(20+20):50	+	P1M	(20+20):50	+	P3M
(25+25):40	+	P3M	(25+25):40	+	P1M	(25+25):40	P	-
(30+30):30	+	P3M	(30+30):30	+	P1M	(30+30):30	P	-
(35+35):20	-	-	(35+35):20	P	-	(35+35):20	P	-
(CreRH+Gly):W			(CreRH+PG):W			(CreRH+PEG):W		
(15+15):60	+	P3M	(15+15):60	+	P1M	(15+15):60	+	+
(20+20):50	+	+	(20+20):50	+	P1M	(20+20):50	+	+
(25+25):40	+	P3M	(25+25):40	+	P1M	(25+25):40	+	P3M
(30+30):30	+	P3M	(30+30):30	+	G3M	(30+30):30	+	P3M
(35+35):20	-	-	(35+35):20	+	G3M	(35+35):20	-	-

a, b: initial and after storage at 4°C for 6 months; -,+: could not be prepared, white fluid dispersion; P, P1M, P3M: precipitation appeared at initial, and after 1, 3 months; G3M: gel formation within 3 months.

Table 11 Physical appearances of SLN dispersions containing 10% GP as solid lipid with different types and amounts of surfactants and co-surfactants prepared by WME method

Formulation	Macroscopic		Formulation	Macroscopic		Formulation	Macroscopic	
	a	b		a	b		a	b
(Tw80+Gly):W			(Tw80+PG):W			(Tw80+Gly):W		
(15+15):60	+	P3M	(15+15):60	+	P3M	(15+15):60	+	P3M
(20+20):50	+	P6M	(20+20):50	+	+	(20+20):50	+	P6M
(25+25):40	+	P3M	(25+25):40	+	+	(25+25):40	+	P3M
(30+30):30	+	P3M	(30+30):30	+	P3M	(30+30):30	+	P3M
(35+35):20	+	P3M	(35+35):20	+	P3M	(35+35):20	+	P3M
(CreEL+Gly):W			(CreEL+PG):W			(CreEL+Gly):W		
(15+15):60	+	P3M	(15+15):60	+	P3M	(15+15):60	+	P3M
(20+20):50	+	P3M	(20+20):50	+	P3M	(20+20):50	+	P3M
(25+25):40	+	P3M	(25+25):40	+	P3M	(25+25):40	+	P3M
(30+30):30	+	P3M	(30+30):30	+	P3M	(30+30):30	+	P3M
(35+35):20	+	P3M	(35+35):20	+	P3M	(35+35):20	+	P3M
(CreRH+Gly):W			(CreRH+PG):W			(CreRH+Gly):W		
(15+15):60	+	P3M	(15+15):60	+	P3M	(15+15):60	+	P3M
(20+20):50	+	+	(20+20):50	+	+	(20+20):50	+	+
(25+25):40	+	+	(25+25):40	+	+	(25+25):40	+	+
(30+30):30	+	+	(30+30):30	+	+	(30+30):30	+	+
(35+35):20	+	P3M	(35+35):20	+	+	(35+35):20	+	P3M

a, b: initial and after storage at 4°C for 6 months; +: white fluid dispersion; P3M, P6M: precipitation appeared after 3, 6 month

the former SLN. Since a wide range of surfactant and co-surfactant could be use to obtain good physical stability, GP-SLN was selected to further load the drug.

Effect of surfactant

Tw80 could not stabilize GB-SLN at all but could stabilize GP-SLN when using either PG or PEG as co-surfactant, particularly at the amount of 20% and 25%. When using CreEL as surfactant, the preparations of GB-SLN and GP-SLN with any tested co-surfactants showed physical instability. In contrast, CreRH was an excellent stabilizer at the amount of 20-30%. Although both CreEL and CreRH are polyoxyethylene castor oil derivatives, they had different hydrophilic-lipophilic balance (HLB) values. HLB of CreRH is between 14-16 while 12-16 is noted for CreEL (Kibbe, 2000; Strickley, 2004). For this reason, the o/w microemulsion stabilized by CreRH was more stable than that of CreEL. In addition, the small molecules of hydrophilic co-surfactant could possibly intercalate between the molecules of more hydrophilic CreRH at the o/w interface better than those of CreEL.

Effect of co-surfactant

For GB-SLN dispersions, 20% Gly and PEG as co-surfactant with CreRH provided good physical stability while PG showed poor results. In contrast, all co-surfactants with CreRH at the concentration of 20-30% could stabilize GP-SLN dispersions. Gly with Tw80 could not stabilize GP-SLN that white precipitate appeared after storage for 3-6 months whereas 20-25% of PG and PEG with Tw80 displayed good physical stability. Therefore, type and amount of co-surfactant affect the formation and stability of SLN. One of the conditions necessary for microemulsion formation is the high fluidity of the interface. The interfacial fluidity and low interfacial tension can be achieved by using a proper co-surfactant or an optimum temperature. However, the amount of co-surfactant should be quantitatively considered in order to stabilize the formulations.

Particle size

Size determination was generally used as a characterization tool. When the composition, the technique, or the process parameters (time, temperature, pressure, equipment type, sterilization and lyophilization conditions) were modified in an attempt to optimize the conditions, particle sizing was chosen as a quality response parameter (Heurtault et al., 2003). With regarding to the amount of surfactant and co-surfactant in parenteral formulations, the preparations containing 10% of GP with 20 and 25% of each surfactant/co-surfactant were chosen to determine the particle size by PCS and the results are shown in Figure 5. The particle sizes of preparations containing 20% CreEL with Gly, PG or PEG were 26.3±0.3, 22.2±0.2 or 46.5±1.0 nm respectively, while the particles of the preparations 25% of surfactant were 26.8±0.4, 21.7±0.6 or 81.9±0.2 nm, respectively. The obtained particle sizes were less than 100 nm and yielded the lowest values whereas those from GP-SLN containing Tw80 and CreRH with all co-surfactants were significantly larger ($p < 0.05$, ANOVA). It could be seen that surfactant played an important role to reduce the size of droplets as described in terms of nature and structure of surfactant and critical micelle concentration (CMC). Application of Cremophor® in the marketed microemulsion-based cyclosporin A provided very small droplet size, thus enhanced the bioavailability of drug (Gao et al., 1998). In addition, microemulsion with polyoxyethylene hydrogenated castor oil as surfactant did not require a co-surfactant (Lawrence, 1996). Although CreEL had the lower CMC value than CreRH (0.009 and 0.039%, respectively), the concentration of both surfactants in the system were much higher than their CMC. The added surfactant forms micelles and the adsorption to the interface did not increase with surfactant concentration. Therefore, CMC parameter could not describe the difference of the obtained particle sizes. On the other hand, it might be associated with the structure of surfactant. The structure of CreEL is smaller and more lipophilic than CreRH. It prefers to be adsorbed toward the oil/water rather than an oil/air interface (Friberg and Kayali, 1991). Thus, the formulation consisted of CreEL might exhibit more a tendency to form globular structure than that of CreRH which showed less particle size.

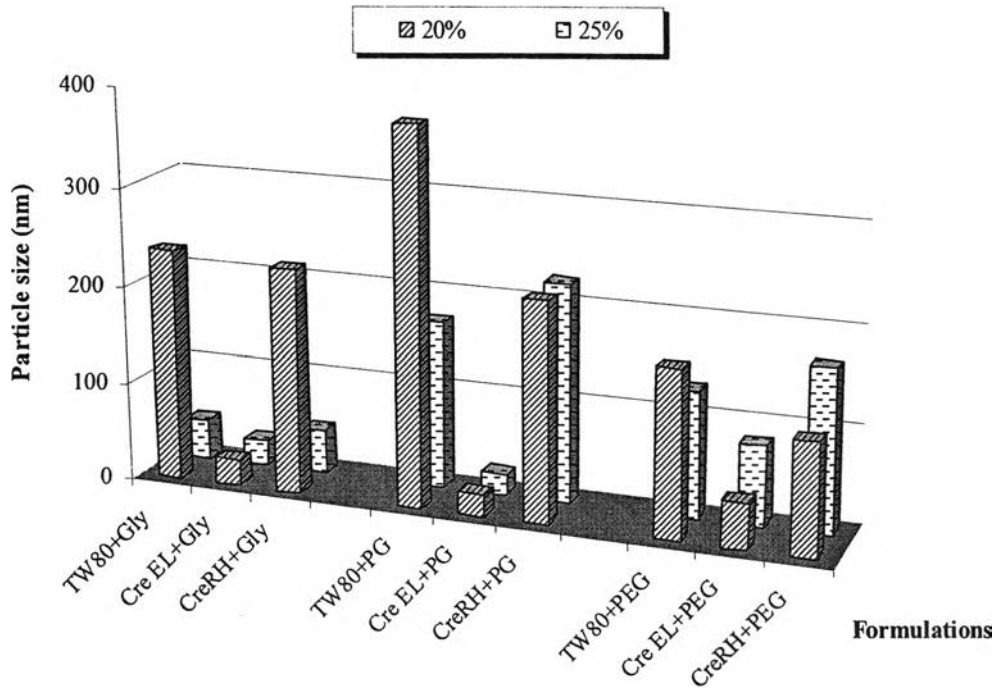

Figure 5 The particle sizes of drug-free SLN dispersions containing 10%GP as solid lipid with 20% and 25%of surfactant/co-surfactant prepared by WME method.

pH measurement and Osmolality

The pH of drug-free SLN preparations with GB and GP as solid lipid are shown in Figure 6. All preparations showed weakly acidic values (4.93 - 6.94). Due to the nature of solid lipid in the system, the hydrolysis of GB or GP leading to the formation of free fatty acids might occur which gradually reduced the pH. The obtained pH of GB-SLN were slightly lower than those of GP-SLN due to the more fatty acid to be hydrolysed leading to the less pH values. It was also found that the pH of SLN formulations were concentration-independent of surfactant/co-surfactant.

The osmolalities of drug-free GB-SLN and GP-SLN with various types and amount of surfactants/co-surfactants are shown in Figure 7. The osmolality was strongly affected by the composition of SLN. The regression coefficients (r^2) between the osmolality and amount of surfactant/co-surfactant were 0.9913-0.9996 and 0.9836-0.9997 for drug-free GB-SLN and GP-SLN, respectively. The type and amount of co-surfactants had an influence on the osmolality while the type of lipids and amount of surfactants had no effect. The influence of co-surfactants on the

osmolality was ranked: PG > Gly >> PEG. The osmolality was osmotic pressure of the dissolved substance calculated by molecule per kilogram of water (Viagas and Henry, 1998). PG, Gly and PEG had molecular weights of 76, 92 and 380-420, respectively (Kibbe, A.H., 2000). At the same co-surfacant concentration, the preparations which contained PEG would have the fewer molecules in water leading to produce the lowest osmolality value.

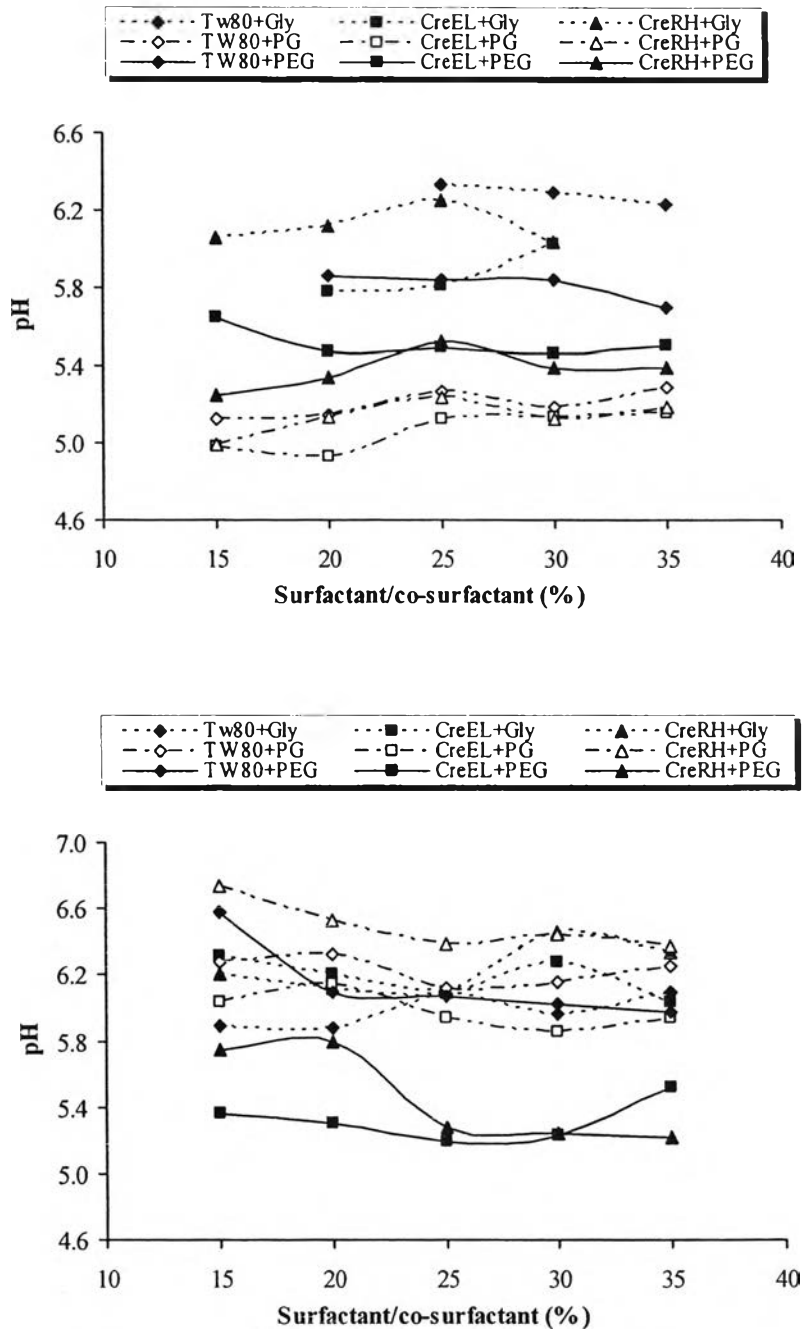

Figure 6 The pH of drug-free SLN dispersions with various types and amount of surfactants/co-surfactants prepared by WME; GB-SLN (top), GP-SLN (bottom).

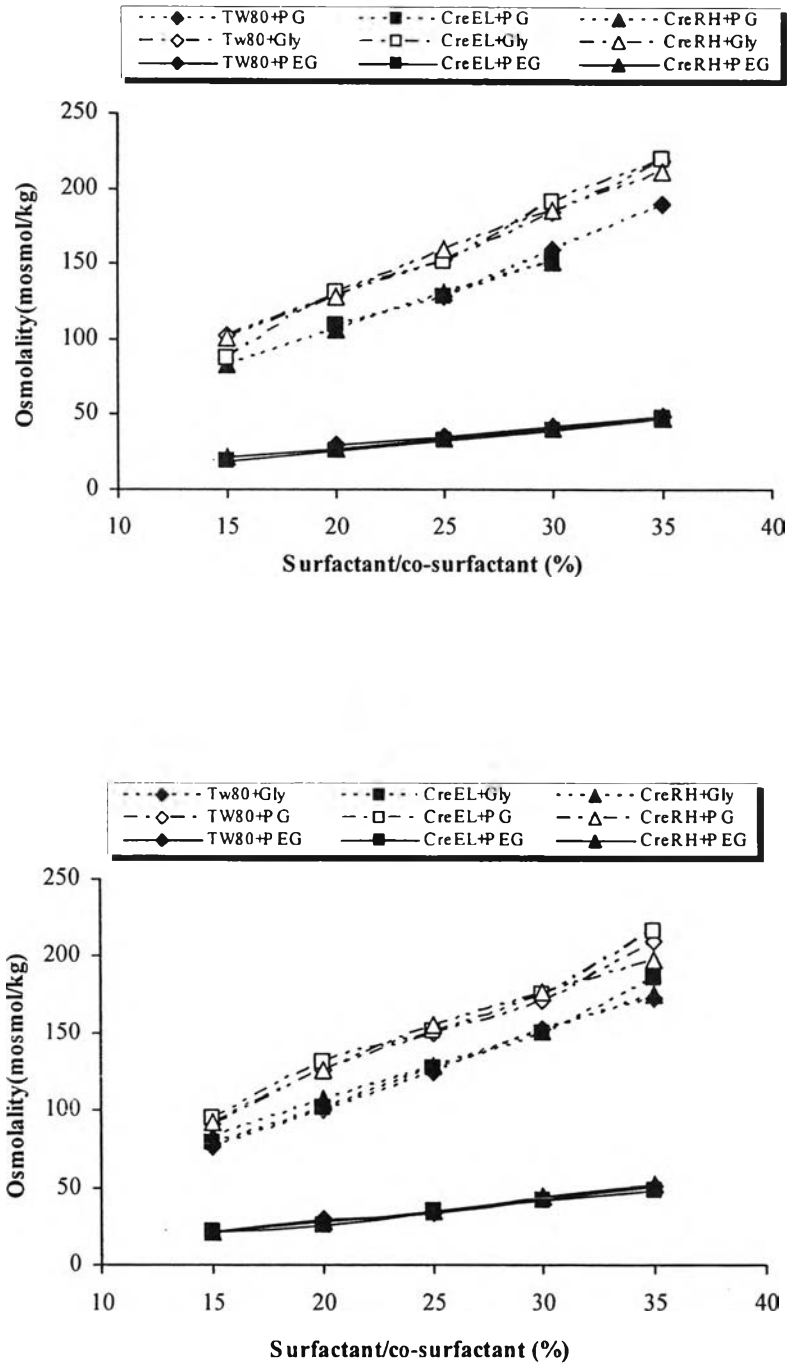

Figure 7 The osmolality of drug-free SLN with various types and amount of surfactants/co-surfactants prepared by WME; GB-SLN (top), GP-SLN (bottom).

1.1.2 Preparation of drug-free SLN by high pressure homogenization (HPH)

In the preliminary study, 3, 5 and 10% of GB with 1-5% Tw80 as a model were to prepare the pre mix emulsion by probe sonication and reducing the particle size into nanometer size range by high pressure homogenizer. The results showed that 3 and 5% GB with 1-5% stabilizer could display good physical appearance but not 10% GB with stabilizer. Since AmB is amphiphilic in nature, it has low solubility in both oil and water. High concentration of solid lipid was unnecessary; therefore, 3% of solid lipid was selected for further study. Similar to drug free SLN prepared by WME method, GB and GP were also chosen in HPH method. The former method had limitation on types of stabilizer. For HPH method, several parenterally approved stabilizers could be selected including polyoxyethylene stearates and polyoxyethylene-polyoxypropylene coblock polymer.

Physical appearance

A. Tween

The visual observations of SLN containing both 3% GB and GP with either 1-5% Tw20 or Tw80 are shown in Table 12. White translucent fluid dispersion was obtained even after 6 months-storage for GB-SLN with both stabilizers. GP-SLN with these stabilizers initially showed bluish white clear dispersion. However, gelatinous phenomenon occurred in formulation with 1% stabilizer and phase separation was shown in those of 3-5% stabilizer after storage for 3 months. Therefore, SLN containing 2% of stabilizer was selected for loading the drug. The stabilization mechanism tween was steric stabilization (Pichayakorn, 1999).

B. Cremophor

The physical appearances of both GB-SLN and GP-SLN containing 1-5% CreEL and CreRH are shown in Table 12. White translucent fluid dispersion was still obtained after 6 months storage for GB-SLN with CreEL as stabilizer, while gel formation was noted after storage for 1 month on the preparations of 4-5% CreRH. On the other hand, GP-SLN with various amount of CreEL showed separation

Table 12 The physical appearances of 3% GB-SLN and GP-SLN with 1-5% of Tw20, Tw80, CreEL and CreRH prepared by HPH method

Formulation	Macroscopic observation		Formulation	Macroscopic observation	
	a	b		a	b
3GB+1Tw20	+	+	3GB+1Tw80	+	+
3GB+2Tw20	++	++	3GB+2Tw80	+	+
3GB+3Tw20	+	+	3GB+3Tw80	+	+
3GB+4Tw20	+	+	3GB+4Tw80	+	+
3GB+5Tw20	+	+	3GB+5Tw80	+	G3M
3GP+1Tw20	++	G3M	3GP+1Tw80	+	G3M
3GP+2Tw20	++	++	3GP+2Tw80	++	++
3GP+3Tw20	++	S3M	3GP+3Tw80	+	S3M
3GP+4Tw20	++	S3M	3GP+4Tw80	+	S3M
3GP+5Tw20	++	S3M	3GP+5Tw80	+	S3M
3GB+1CreEL	+	G2M	3GB+1CreRH	+	+
3GB+2CreEL	++	++	3GB+2CreRH	+	+
3GB+3CreEL	++	++	3GB+3CreRH	++	++
3GB+4CreEL	++	++	3GB+4CreRH	++	G1M
3GB+5CreEL	++	++	3GB+5CreRH	++	G1M
3GP+1CreEL	+	G2M	3GP+1CreRH	+	+
3GP+2CreEL	++	S2M	3GP+2CreRH	++	++
3GP+3CreEL	++	S2M	3GP+3CreRH	++	++
3GP+4CreEL	++	S2M	3GP+4CreRH	++	++
3GP+5CreEL	++	S2M	3GP+5CreRH	++	++

a, b: initial and after storage at 4°C for 6 months; +,++: white fluid dispersion, bluish white fluid dispersion; G1M, G2M, G3M, G6M: gel formation within 1, 2, 3, 6 months; S2M, S3M: sedimentation after storage for 2, 3 months.

after storage for 3 months, while with CreRH, the SLN displayed good physical appearance for more than 6 months. The possible explanation was might be due to the nature of the substances. Cremophor is pegylated castor oil or hydrogenated castor oil and is a complex mixture of relatively hydrophobic and hydrophilic molecules. CreEL is a mixture of 83% relatively hydrophobic and 17% relatively hydrophilic components whereas CreRH is a mixture of approximately 75% relatively hydrophobic (Strickley, 2004). It was probably that the less of both hydrophilic portion and HLB value of CreEL was not enough to stabilize the colloidal systems thus showed phase separation after storage.

C. Poloxamer

The visual appearances of SLN containing both 3% GB and GP with 1-5% P188 or P407 are shown in Table 13, respectively. White fluid dispersions were observed in all preparations. P188 and P407 could maintain good physical stability of both GB-SLN and GP-SLN for more than 6 months except the preparation of 1% stabilizer which formed highly viscous gel. In most cases, gel formation was irreversible. At low concentration of poloxamer, a large surface area of the solid lipids was available for adsorption of stabilizer. Bridging between particles occurred as a result of the simultaneous adsorption of poloxamer molecules onto the surfaces of different solid lipid nanoparticles. However, the number of particle-particle bridges was relative low. Therefore, these systems had uncovered lipid surface particles which could contact other particles and resulted in gel formation. The higher concentrations of poloxamer of 2-5% on particle surface could prevent close attraction of the particles via the phenomenon of steric stabilization and therefore gel formation could be retarded (Viriyaroj, 2001). However when using 5% P407, coalescence occurred after 6 month storage but not 5% P118. P407 possessed higher molecular weight and larger propylene oxide than P118. The propylene portion imparted lipophilicity which located at the surface particles might interact and fused into large particles led to coalescence.

D. Myrj

The physical appearances of SLN containing 1-5% M52 and M59 with those lipids are shown in Table 13. White translucent fluid dispersion was shown in all preparations. The appearance of SLN containing GP is brighter than that of GB. SLN composed of GB with 3-5% of M52 and M59 formed gel formation and phase separation after 1 month storage, respectively. GP-SLN with 2-4% stabilizers could maintain satisfactory physical stability for more than 6 months. The SLN dispersions with M52 seemed to be more stable than those with M59. This was due to the fewer oxyethylene unit of M52 ($\cong$ 40) than that of M59 ($\cong$ 100). Therefore, the excess hydrophobic portion of the latter might be fused and separated to the continuous phase.

Table 13 The physical appearances of 3% GB-SLN and GP-SLN with 1-5% of P188, P407, M52 and M59 prepared by HPH method.

Formulation	Macroscopic observation		Formulation	Macroscopic observation	
	a	b		a	b
3GB+1P188	+	G6M	3GB+1P407	+	G6M
3GB+2P188	+	+	3GB+2P407	+	+
3GB+3P188	+	+	3GB+3P407	+	+
3GB+4P188	+	+	3GB+4P407	+	+
3GB+5P188	+	+	3GB+5P407	+	C6M
3GP+1P188	+	G6M	3GP+1P407	+	G6M
3GP+2P188	+	+	3GP+2P407	+	+
3GP+3P188	+	+	3GP+3P407	+	+
3GP+4P188	+	+	3GP+4P407	+	+
3GP+5P188	+	+	3GP+5P407	+	C6M
3GB+1M52	+	+	3GB+1M59	+	+
3GB+2M52	+	+	3GB+2M59	+	+
3GB+3M52	+	G1M	3GB+3M59	+	G1M
3GB+4M52	+	G1M	3GB+4M59	+	S3M
3GB+5M52	+	G1M	3GB+5M59	+	S3M
3GP+1M52	+	G3M	3GP+1M59	+	G3M
3GP+2M52	++	++	3GP+2M59	+	+
3GP+3M52	++	++	3GP+3M59	++	++
3GP+4M52	++	++	3GP+4M59	++	++
3GP+5M52	++	G6M	3GP+5M59	++	G6M

a, b: initial and after storage for 4°C for 6 months; +,++: white fluid dispersion, bluish white fluid dispersion; G1M, G3M, G6M: gel formation within 1, 3, 6 months; S3M: sedimentation after storage for 3 months; C6M: coalescence after 6 months.

Particle size

The particle sizes determined by PCS of drug-free GB-SLN and GP-SLN with 2% of various types of surfactants prepared by HPH method are shown in Figure 8. The mean diameters of all preparations were in nanometer range. The particles obtained by GB-SLN and GP-SLN dispersions with cremophor (37.2–78.5 nm) were lower than those of other surfactants. It was possible that cremophor could stabilize by decreasing the surface area of dispersed solid lipids with higher coverage of molecules of it at the interface. On the other hand, the particles obtained by both GB-SLN and GP-SLN dispersions with poloxamer gave the highest values

(199.1-276.3 nm). This was due to steric stabilization by poloxamer which was block copolymer.

The particle sizes of SLN prepared by WME and HPH were different. Mostly the particle sizes of SLN preparations from WME process were smaller than those from HPH process. It indicated that the formulation process and the excipient composition had an influence on the average particle diameter of SLN dispersions (Heurtault et al., 2003). In this experiment, the comparison between different preparation procedures could not be conducted directly due to the difference in types and amounts of ingredients. The higher lipid content should result in larger particles and broader particle size distribution (Mehnert and Mäder, 2001). Due to the WME method used larger amount of surfactant calculated to total solid lipid than those used in HPH method, high surface of the emulsifier reduced the surface tension and facilitate the particle partition during preparation led to decrease in particle size. Moreover, the influence of co-surfactant composition on the average particle size was described by Boltri et al (1995). The presence of co-surfactant in the formulation of SLN led to smaller particles due to the stabilizing effect on the microemulsion interface and probably as a consequence of its effect on steric crystallization, growth over time minimal.

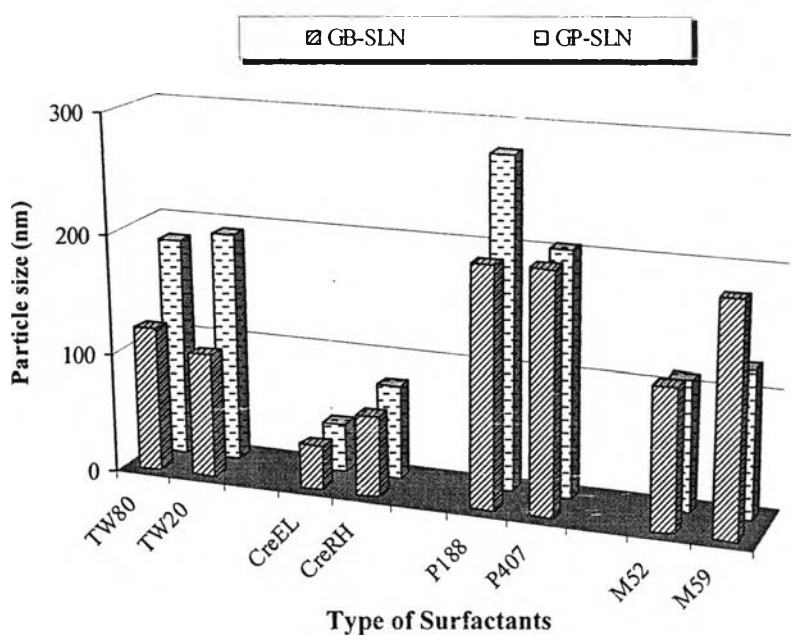

Figure 8 The particle sizes of drug-free SLN dispersions containing 3% GB and GP as solid lipid with 2% of various surfactants prepared by HPH method.

pH measurement and Osmolarity

Figure 9 shows the pH of drug-free GB-SLN and GP-SLN with various types and amount of surfactants prepared by HPH method. All preparations were weakly acidic. The lower pH might be influenced from the degradation product of solid lipid which was acidic compound while the neutral surfactants did not affect the pH. The relationship of the observed pH and the amount of surfactants was poorly concentration-dependent. However, the pH was mostly decreased when the amount of surfactants increased especially, the formulations with M59 as surfactant which exhibited the lowest pH.

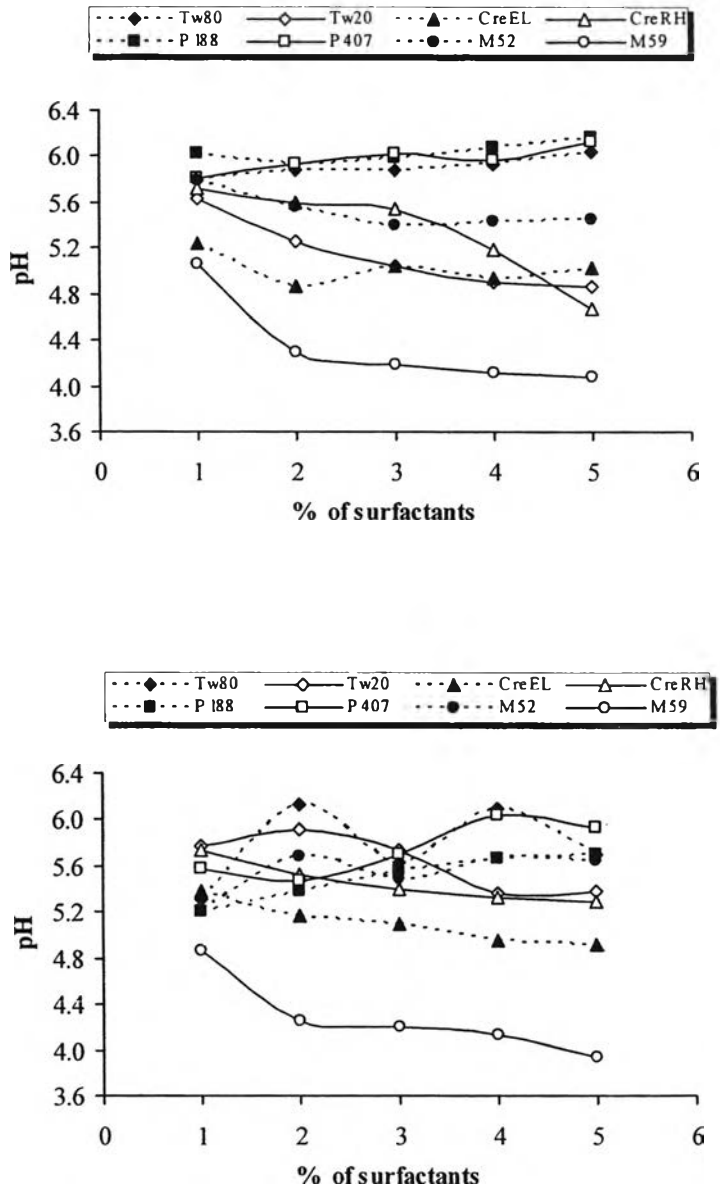

Figure 9 The pH of drug-free SLN dispersions with various types and amount of surfactants prepared by HPH; GB-SLN (top), GP-SLN (bottom).

The osmolality of drug-free GB-SLN and GP-SLN prepared by HPH is shown in Figure 10. Due to the large molecular weight, both solid lipids did not affect the osmolality. Increasing the amount of surfactants, the higher osmolality was observed with linearity. Linear regression analysis of GB-SLN and GP-SLN was performed with the coefficient of determination (r^2) of 0.9573-0.9923 and 0.9657-0.9933, respectively. However, the result showed very low osmolality of these preparations.

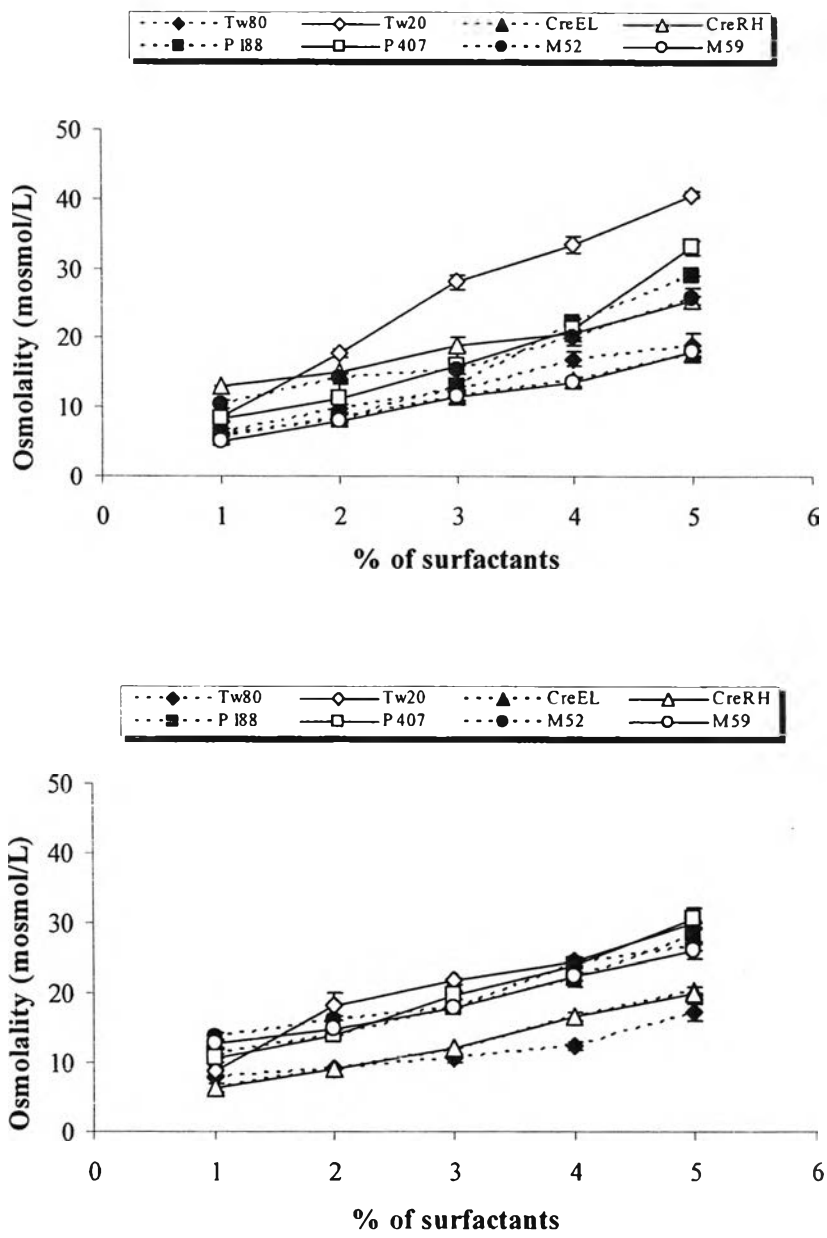

Figure 10 The osmolality of drug-free SLN with various types and amount of surfactants prepared by HPH; GB-SLN (top), GP-SLN (bottom).

1.2 Formulation of amphotericin B (AmB) loaded SLN (AmB-SLN)

1.2.1 AmB-SLN formulations prepared by WME method

From the results of drug-free GB-SLN and GP-SLN dispersions, satisfactory formulations contained 10% GP with 20-30% of surfactant and co-surfactant. The SLN containing 10% GP with 20% of various surfactants/co-surfactants were selected to load AmB due to the lowest amount for sufficiently stabilizing the system.

Physical appearance

The physical stability of dispersions of GP-SLN containing AmB that was solubilized by 0.1N NaOH and DMSO are shown in Table 14. Yellowish colloidal dispersions were obtained according to the color of AmB. The results of physical stability when using 0.1N NaOH and DMSO were similar in all preparations. In case of using Tw80, the color of all preparations that used Gly, PG or PEG as co-surfactant faded after 1-month storage and white precipitate appeared after storage for 2 months at 4°C. For preparations using CreEL or CreRH, color fading occurred when using PEG as co-surfactant while those with Gly and PG maintained yellowish color. In comparison between CreEL and CreRH, the preparations prepared by using CreEL with all co-surfactants displayed white precipitate after 1-month storage whereas those of CreRH with Gly and PG showed no alteration after storage for 3 months. Similar to the drug-free preparations, the GP-SLN dispersions containing drug prepared by using CreRH as stabilizer showed good physical stability.

Particle size

The particle sizes of SLN containing AmB which solubilized by 0.1N NaOH and DMSO, 10% GP and 20% of various surfactant/co-surfactant are shown in Table 15. The obtained particle size was determined by PCS method. It could not be examined by LD technique because the obsculation range was too low to measure. Results of all of preparations prepared by solubilizing AmB in 0.1N NaOH or with

Table 14 The physical appearances of SLN containing AmB which solubilized by 0.1N NaOH and DMSO, 10% GP and 20% of various surfactant/co-surfactant prepared by WME method

Formulation	Macroscopic observation			
	0.1N NaOH		DMSO	
	a	b	a	b
AmB:GP:(Tw80+Gly):W	+	F1M, P2M	+	F1M, P2M
AmB:GP:(CreEL+Gly):W	+	P1M	+	P1M
AmB:GP:(CreRH+Gly):W	+	+	+	+
AmB:GP:(Tw80+PG):W	+	F2M, P1M	+	F2M, P1M
AmB:GP:(CreEL+PG):W	+	P1M	+	P1M
AmB:GP:(CreRH+PG):W	+	P2M	+	+
AmB:GP:(Tw80+PEG):W	+	F2M, P2M	+	F2M, P2M
AmB:GP:(CreEL+PEG):W	+	F1M, P1M	+	F1M, P1M
AmB:GP:(CreRH+PEG):W	+	F2M	+	F2M

a, b: initial and after storage at 4°C for 3 months; +: yellowish fluid dispersion; F1M, F2M: fade in color within 1, 2 months; P1M, P2M: precipitation within 1, 2 months

the aid of DMSO were in the same trend. The particles of the preparations obtained by using CreEL with either Gly or PG as co-surfactant were 74.4, 27.0 nm and 37.9, 46.6 nm when drug solubilized in 0.1N NaOH and DMSO, respectively. They were significantly smaller than those with other surfactant ($p<0.05$). These preparations of CreEL yielded the particle size were less than 100 nm which was in accordance with the result of drug-free GP-SLN. Thus, the incorporation of AmB did not affect the particle size of the preparation. The particle sizes of formulations with other surfactants were also in the nanometer range with narrow size distribution and lower than 1 μm that was suitable for parenteral products. Among co-surfactants, the particle sizes of SLN with all stabilizers and PEG were not different ($p>0.05$) while those with the other two co-surfactants showed different particle size. It was possible that the small structure of PG and Gly could rapidly exchange and distribute themselves among the interface of oil phase and waster. This dynamic process which generated energy into smaller particles depended on the nature of surfactants. For large structure polymer, PEG could stabilize the particles by steric stabilization, therefore the particle sizes of the formulations with different surfactants were nearly the same.

Table 15 The particle sizes of SLN containing AmB which solubilized by 0.1N NaOH and DMSO, 10% GP and 20% of various surfactant/co-surfactant prepared by WME method

Formulation	Mean particle size by PCS (nm)			
	0.1N NaOH		DMSO	
	Z value ± SD	PI	Z value ± SD	PI
AmB:GP:(Tw80+Gly):W	288.6 ± 2.5	0.297	48.5 ± 1.0	0.268
AmB:GP:(CreEL+Gly):W	74.4 ± 1.3	0.187	37.9 ± 1.3	0.265
AmB:GP:(CreRH+Gly):W	124.4 ± 7.8	0.347	51.2 ± 0.4	0.208
AmB:GP:(Tw80+PG):W	407.6 ± 6.1	0.339	218.7 ± 3.0	0.392
AmB:GP:(CreEL+PG):W	27.0 ± 0.5	0.210	46.6 ± 3.2	0.337
AmB:GP:(CreRH+PG):W	609.2 ± 40.5	0.248	147.4 ± 14.7	0.288
AmB:GP:(Tw80+PEG):W	109.2 ± 2.7	0.309	105.4 ± 1.1	0.294
AmB:GP:(CreEL+PEG):W	68.7 ± 1.2	0.280	92.9 ± 1.6	0.291
AmB:GP:(CreRH+PEG):W	69.1 ± 0.5	0.253	97.9 ± 1.1	0.248

pH , osmolality zeta and potential

The pH, osmolality and zeta potential of AmB loaded SLN dispersions are shown in Table 16. The pH of all preparations were weakly acidic to neutral and was higher than that of drug free preparations when using 0.1N NaOH as solubilizing agent. In contrast, using DMSO did not affect the pH of the preparations. The pH of the preparations using CreEL are the lowest when compared with the others ($p<0.05$). Although their pH were different, they were in the range for optimum clarity and stability.

Considering to the osmolality of SLN dispersions, 0.1N NaOH did not affect the osmolality of AmB loaded SLN dispersions when compared with drug-free SLN dispersions. On the other hand, solubilization of AmB by DMSO gave higher osmolality than unloaded preparations ($p<0.05$). Type of surfactants in preparations had no effect on the osmolality ($p>0.05$). For co-surfactant, the formulations obtained by using PG gave the highest osmolality while using PEG showed the lowest similarly to the results of drug-free preparations. Nevertheless, the osmolality of all preparations were obviously low which was inappropriate to physiological fluid.

Thus, selected preparations should add osmolality agents such as glycerol or be added to intravenous fluids for i.v. infusion before used.

Zeta potential is an important and useful indicator of particle surface charge, which can be used to predict and control the stability of colloidal suspensions or emulsions. The zeta potentials of selected formulations were measured. These formulations showed the negative charge in the range of -17.30 to -23.27 millivolts which were mild to moderate zeta potential for good stability.

Table 16 The pH, osmolality and zeta potential of SLN containing AmB which solubilized by 0.1N NaOH and DMSO, 10% GP and 20% of various surfactant/co-surfactant prepared by WME method

Formulation	pH	Osmolality (mosmol/kg)	Zeta potential (mV)
AmB:GP:(Tw80+Gly):W*	7.02 ±0.01	101.3 ± 1.5	ND
AmB:GP:(CreEL+Gly):W*	6.89 ±0.01	107.7 ±1.5	ND
AmB:GP:(CreRH+Gly):W*	6.98 ±0.02	111.7 ± 0.6	-23.27
AmB:GP:(Tw80+PG):W*	7.05 ±0.02	137.3 ± 1.5	ND
AmB:GP:(CreEL+PG):W*	6.78 ±0.02	137.7 ± 4.5	ND
AmB:GP:(CreRH+PG):W*	7.01 ±0.02	134.3 ± 4.2	ND
AmB:GP:(Tw80+PEG):W*	6.35 ±0.02	30.3 ± 0.6	ND
AmB:GP:(CreEL+PEG):W*	6.21 ±0.02	30.0 ± 0.0	ND
AmB:GP:(CreRH+PEG):W*	6.31 ±0.02	32.3 ± 0.6	-19.58
AmB:GP:(Tw80+Gly):W**	6.55 ±0.01	158.0 ± 5.3	ND
AmB:GP:(CreEL+Gly):W**	6.27 ±0.01	162.0 ±3.0	ND
AmB:GP:(CreRH+Gly):W**	6.32 ±0.01	180.7 ± 1.5	-17.30
AmB:GP:(Tw80+PG):W**	6.38 ±0.01	187.7 ± 4.2	ND
AmB:GP:(CreEL+PG):W**	5.98 ±0.02	188.0 ± 5.0	ND
AmB:GP:(CreRH+PG):W**	6.20 ±0.01	186.7 ± 3.5	ND
AmB:GP:(Tw80+PEG):W**	5.92 ±0.02	84.0 ± 0.0	ND
AmB:GP:(CreEL+PEG):W**	5.69 ±0.02	83.7 ± 0.6	ND
AmB:GP:(CreRH+PEG):W**	5.75 ±0.02	83.7 ± 2.3	-22.27

*,**: AmB solubilized by 0.1N NaOH, DMSO; ND: Not determined.

1.2.2 AmB-SLN formulations prepared by HPH method

Due to no difference in physical properties between using 0.1N NaOH and DMSO as solubilizing agent in the WME method; therefore, 0.1N NaOH was selected to be used in the HPH method to avoid the toxicity of organic solvent. From the data of drug-free SLN containing both GB and GP with various surfactants prepared by HPH method, formulation of 2% surfactants was selected to load the drug due to sufficient amount for stabilizing the system.

Physical appearance

The visual observation of the SLN dispersions containing 1% AmB, 3% GB or GP, and 2% of various surfactants and both at initial and after storage for 3 months are listed in Table 17. The color of AmB-SLN containing GP was brighter than that of GB. Due to the higher triglycerides fraction of GB, the visual observation of the AmB loaded GB-SLN dispersions could be interfered. Indeed, the formulations consisted of poloxamer which had large polymeric side chains could be disturbed by naked eyes. Both GB-SLN and GP-SLN had similar physical appearance after storage at 4 °C for 3 months. The preparations using either Tw80 or CreEL as stabilizer were physically unstable. The color of AmB faded in case of using Tw80 as stabilizer while the color of AmB faded and the dispersion turned to white precipitate after 1-month storage when using CreEL. In addition, GP-SLN formulations which used Tw20 was unstable with prepipitate appeared.

Particle size

Table 18 shows the particle size of AmB-SLN containing GB and GP with various types of surfactants measured by two different techniques, LD and PCS. The type of lipid had an effect on their particle sizes. From the result of particle size determined by LD, AmB-SLN containing GP obtained the smaller particle size and narrower size distribution than that containing GB. GP contains the mixture of mono-, di-and triglycerides of C_{16} and C_{18} which are shorter than those of GB; therefore, they

exist as smaller particles similarly to the reported of Videira et al (2005). Ahlin et al (1998) also reported the influence of lipid composition on particle size.

Table 17 The physical appearances of 1% AmB loaded GB-SLN and GP-SLN dispersions with various stabilizers prepared by HPH method

Formulation	Macroscopic observation		Formulation	Macroscopic observation	
	a	b		a	b
AmB+3GB+2Tw80	+	F1M	AmB+3GP+2Tw80	+	F1M
AmB+3GB+2Tw20	+	+	AmB+3GP+2Tw20	+	P3M
AmB+3GB+2CreEL	+	F,P1M	AmB+3GP+2CreEL	+	F,P1M
AmB+3GB+2CreRH	+	+	AmB+3GP+2CreRH	+	+
AmB+3GB+2P118	+	+	AmB+3GP+2P118	+	+
AmB+3GB+2P407	+	+	AmB+3GP+2P407	+	+
AmB+3GB+2M52	+	+	AmB+3GP+2M52	+	+
AmB+3GB+2M59	+	+	AmB+3GP+2M59	+	+

a, b: initial and after on storage at 4°C for 3 months; +: yellowish fluid dispersion; F1M: fade in color within 1 month; F,P1M: fade in color and precipitation within 1 month; P3M: precipitation within 3 months.

The particle size distributions determined by LD of SLN containing GB or GP with different surfactants were shown in Figure 11. It was clearly concluded that the GB-SLN displayed bimodal size distribution while GP-SLN showed monomodal size distribution. In addition, GB-SLN containing poloxamer and myrj gave higher median diameter than GB-SLN with cremophor and tween. This might due to the larger molecule of surfactant, thus the larger particle size of formulations was obtained. In case of the particle size and size distribution determined by PCS, the mean diameter and polydispersity index of most GB-SLN and GP-SLN were not different and showed monomodal size distribution. PCS technique can define the particle size lower than 100 nm while the LD technique had limitation. PCS measures the fluctuation of the intensity of scattered light caused by particle movement while the LD method is based on the dependence of the diffraction angle on the particle radius. Due to the difference in the principle of measurement, different results could be obtained (Heurtault et al., 2003).

Table 18 Particle sizes of 1% AmB loaded GB-SLN and GP-SLN dispersions with various stabilizers prepared by HPH method, determined by LD and PCS.

Formulation	Volume particle size			
	by LD (μm)		by PCS (nm)	
	D(v,0.5)	uniformity	Z value ± SD	PI
AmB+3GB+2Tw80	0.279	1.390	58.2 ± 5.2	0.261
AmB+3GB+2Tw20	0.229	1.340	142.8 ± 12.6	0.326
AmB+3GB+2CreEL	0.234	1.410	238.8 ± 17.1	0.322
AmB+3GB+2CreRH	0.271	1.510	137.6 ± 3.4	0.326
AmB+3GB+2P118	0.810	0.647	251.7 ± 4.8	0.361
AmB+3GB+2P407	0.732	0.703	250.2 ± 2.8	0.249
AmB+3GB+2M52	0.619	0.619	253.7 ± 3.2	0.217
AmB+3GB+2M59	0.554	0.728	114.0 ± 6.8	0.184
AmB+3GP+2Tw80	0.174	0.209	170.8 ± 8.0	0.315
AmB+3GP+2Tw20	0.167	0.156	92.4 ± 2.2	0.178
AmB+3GP+2CreEL	0.174	0.213	ND	ND
AmB+3GP+2CreRH	0.174	0.212	115.7 ± 5.0	0.274
AmB+3GP+2P118	0.222	0.337	267.8 ± 8.8	0.340
AmB+3GP+2P407	0.177	0.221	201.6 ± 3.5	0.145
AmB+3GP+2M52	0.180	0.228	263.0 ± 9.2	0.279
AmB+3GP+2M59	0.172	0.181	250.8 ± 4.3	0.362

ND: Not determined

Well-formulated systems should display narrow particle size distribution in the submicron range. Furthermore, particles greater than 1 μm and the increase of size with time can be an indicator of physical instability. Intravenous injection of particles with an average diameter above 5 μm might cause death due to embolism. Thus, size control and the avoidance of nanoparticle growth are important considerations in preparing dispersions and particular attention is paid to size. However, particle sizes of both GP-SLN and GB-SLN detected by PCS were in the nanometer range.

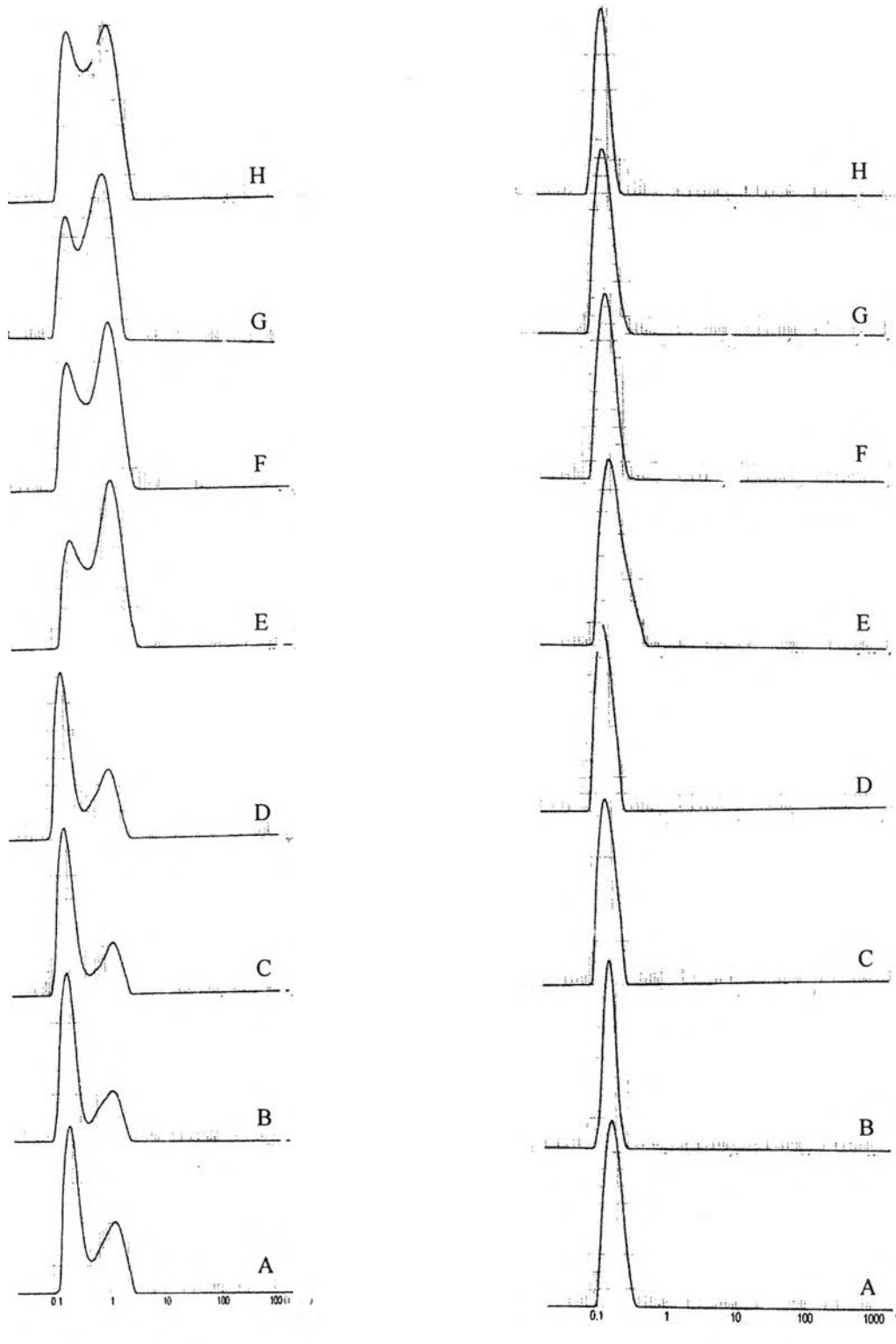

Figure 11 The particle size distribution determined by LD of 1% AmB loaded GB-SLN (I) and GP-SLN (II) with various surfactants prepared by HPH method; Tw80(A), Tw20(B), CreEL(C), CreRH(D), P188(E), P407(F), M52(G), M59(H).

pH , osmolality and zeta potential

Table 19 shows the pH, osmolality and zeta potential of SLN dispersions containing GB or GP as solid lipid with different surfactants. The pH of most AmB-SLN formulations was in the range of 6-7 which was optimum for chemical stability. The pH below 6 may cause the drug loss in activity. In this study, the formulations of AmB loaded in SLN dispersions containing GB and Tw80 or CreEL gave the pH values of 5.88 or 5.51, respectively which might affect the drug stability. With regarding to the type of lipid, the pH of GB-SLN formulations were lower than that of GP-SLN. GB had longer chain triglyceride thus was susceptible to more fatty acid hydrolysis than GP.

The osmolality of AmB-SLN dispersion prepared by HPH method was still too low to be used in intravenous administration. Thus, it was necessary to add some osmotic agents before used. However, the physical incompatibility and chemical stability of the intravenous mixtures should be examined further in order to assure of safety in clinical use.

The zeta potentials of selected SLN preparations were between -14.74 and -26.77 mV which meant mild to moderate physical stability. SLN dispersions containing poloxamer as stabilizer had the lowest zeta potential. This low zeta potential value was affected by the presence of PEO chain of poloxamer on the surface. It was able to form network structures as a plasticizer and a gelling agent. Free water could be incorporated intralamellar which would explain the hardening of the gel with time (Freitas et al., 1998b). The zeta potentials of GB-SLN were higher than those of GP-SLN especially SLN stabilized by P407. The proposal of this result might be due to the fast recrystallized GB which could still predominantly present the hydroxyl charge of AmB on the surface.

Table 19 The pH, osmolality and zeta potential of 1% AmB loaded GB-SLN and GP-SLN with various surfactants prepared by HPH method

Formulation	pH	Osmolality (mosmol/kg)	Zeta potential (mV)
AmB+3GB+2Tw80	5.88±0.05	10.7±0.6	ND
AmB+3GB+2Tw20	6.68±0.04	16.0±1.0	-28.21
AmB+3GB+2CreEL	5.51±0.04	9.7±0.6	ND
AmB+3GB+2CreRH	6.50±0.01	10.0±1.0	-36.13
AmB+3GB+2P118	7.07±0.02	8.7±1.2	ND
AmB+3GB+2P407	7.11±0.03	10.0±0.0	-39.46
AmB+3GB+2M52	7.25±0.02	9.0±1.0	-29.19
AmB+3GB+2M59	6.68±0.02	7.0±0.0	ND
AmB+3GP+2Tw80	6.96±0.02	8.7±0.6	ND
AmB+3GP+2Tw20	7.02±0.02	14.7±0.6	-26.77
AmB+3GP+2CreEL	6.68±0.02	9.0±0.0	ND
AmB+3GP+2CreRH	7.08±0.03	10.0±0.0	-24.96
AmB+3GP+2P118	6.97±0.02	8.0±0.0	ND
AmB+3GP+2P407	7.07±0.01	8.0±0.0	-14.74
AmB+3GP+2M52	7.30±0.03	8.3±0.6	-19.66
AmB+3GP+2M59	6.55±0.02	7.3±0.6	ND

ND = Not determined

1.3 Preparation of freeze dried SLN products

The optimized AmB-SLN formulation prepared by WME method consisted of GP+CreRH+Gly was selected to study the selection of bulking agents. The preparation yield, particle size and chemical stability of all AmB-SLN formulations prepared by WME and some AmB-SLN dispersions with good physical appearance prepared by HPH were investigated.

Selection of bulking agents

The protective effect of bulking agents has been widely investigated. The effects of type and amount of bulking agents on the physical properties, speed of redispersion, the ratio of the particle size of reconstituted freeze-dried product (Sf) to the particle size of colloidal dispersions (Sc) and the particle size uniformity are

shown in Table 20. According to the physical properties, redispersion speed, and the Sf/Sc ratio, it could be seen that mannitol was the better bulking agent than sucrose and fructose. All freeze-dried SLN were readily redispersed in water under mechanical stirring. Their particle sizes after reconstitution were 16-19 times of unlyophilized ones while using sucrose and fructose as bulking agents yielded larger particle size of 60-80 times. On the contrary, with regarding to the particle size uniformity, the former gave the widest size distribution. Therefore, the combination of bulking agents would be more effective. The optimized combination of bulking agents was 7.5% mannitol and 5% sucrose. The lyophilized products had excellent physical properties and could disperse in distilled water but still gave the particle sizes much larger than the unlyophilized ones. The results indicated that these bulking agents were insufficiently effective in preventing particle growth in the simple freeze-drying process.

Table 20 Effects of the nature of the bulking agents on the morphological characteristics of reconstituted AmB-SLN from freeze-dried products

No.	Bulking agents (%)			Physical properties[a]	Speed of redispersion[b]	Ratio Sf/Sc	Particle size uniformity
	Sucrose	Mannitol	Fructose				
1	12.5	-	-	_	+	58.26	1.090
2	10.0	-	-	_ _	+	59.72	1.000
3	7.5	-	-	_ _	+	68.81	0.873
4	-	12.5	-	+++	++	17.83	4.760
5	-	10.0	-	+++	++	16.17	3.740
6	-	7.5	-	+++	++	19.26	3.080
7	-	-	12.5	_	_	63.41	0.648
8	-	-	10.0	_ _	_	80.03	0.639
9	-	-	7.5	_ _	_	60.72	0.693
10	7.5	5.0	-	+	++	30.25	0.996
11	7.5	-	5.0	_	++	66.64	1.050
12	-	7.5	5.0	++	++	40.02	1.970
13	5.0	7.5	-	++	++	24.85	1.860
14	5.0	-	7.5	_ _	_	65.91	0.871
15	-	5.0	7.5	+	_	49.01	0.858

[a]The physical properties was graded as -,- -: bad, very bad; +++,++,+: excellent, very good, good.

[b]The speed of redispersion was graded as ++,+,-: moderate, slow, very slow.

Preparation yield

Tables 21 and 22 show the preparation yields in lyophilized form of various SLN preparations which produced by WME and HPH method, respectively. The preparation yields of the solid lipid nanoparticles obtained by the WME and HPH techniques were found to be in the range of 96.84% -104.95% and 101.00%-109.20%, respectively indicating that there was no loss in the preparation method.

Table 21 The preparation yields of AmB freeze-drid products from GP-SLN dispersions containing 10%GP with 20% of various surfactants and co-surfactants prepared by WME method.

Formulation	0.1N NaOH		DMSO	
	weight of particles obtained (g)	% yield	weight of particles obtained (g)	% yield
Tw80+Gly	1.5239	101.46	1.5412	102.61
CreEL+Gly	1.5291	101.80	1.5392	102.48
CreRH+Gly	1.5387	102.44	1.5347	102.18
Tw80+PG	1.5644	104.15	1.5031	100.07
CreEL+PG	1.4732	98.08	1.4894	99.16
CreRH+PG	1.4546	96.84	1.4783	98.42
Tw80+PEG	1.5277	101.71	1.5543	103.48
CreEL+PEG	1.5260	101.60	1.5405	102.56
CreRH+PEG	1.5390	102.46	1.5764	104.95

Table 22 The preparation yields of AmB freeze-drid products from GB-SLN and GP-SLN dispersions prepared by HPH method

Formulations	3GB		3GP	
	weight of particles obtained (g)	% yield	weight of particles obtained (g)	% yield
AmB+2Tw20	1.7156	107.09	1.6181	101.00
AmB+2CreRH	1.7140	106.99	1.6241	101.38
AmB+2P407	1.7131	106.94	1.7494	109.20
AmB+2M52	1.7180	107.24	1.6306	101.79

Particle size

Size measurements of reconstituted SLN by LD are shown in Tables 23 and 24. There was a marked increase in their average diameter and polydispersity index than the initial ones. The obtained average diameters were mostly larger than 5 μm which was unsuitable and prohibited for i.v. injection. This was probably due to the presence of aggregates between nanoparticles. The conditions of the freeze-drying process and the removal of the water probably promoted aggregation among SLN (Cavalli et al., 1997). These results were in accordance with those observed in a previous study of the particle sizes of Compritol-SLN and Dynasan-SLN after lyophilization by Schwarz et al (1997). However, changes in particle size during lyophilization could be minimized by optimizing the parameters of the lyophilization process such as bulking agents, freezing velocity, and thermal treatment (Yang and Zhu, 2002; Zimmermann et al., 2000).

Table 23 Particle sizes of AmB freeze-dried products from GP-SLN dispersions prepared by WME method

Formulation	Volume particle size (μm)			
	0.1N NaOH		DMSO	
	D(v,0.5)	uniformity	D(v,0.5)	uniformity
AmB:GP:(Tw80+Gly)	3.984	1.280	5.413	1.280
AmB:GP:(CreEL+Gly)	5.827	0.897	5.037	0.875
AmB:GP:(CreRH+Gly)	7.667	0.813	6.026	0.821
AmB:GP:(Tw80+PG)	6.055	1.220	5.587	0.774
AmB:GP:(CreEL+PG)	6.496	1.120	4.813	0.993
AmB:GP:(CreRH+PG)	6.435	0.852	6.111	1.300
AmB:GP:(Tw80+PEG)	5.510	0.847	5.140	1.060
AmB:GP:(CreEL+PEG)	8.588	0.749	5.690	1.280
AmB:GP:(CreRH+PEG)	5.286	1.890	6.467	0.889

Table 24 Particle sizes of AmB freeze-dried products from GB-SLN and GP-SLN dispersions prepared by HPH method

Formulation	Volume particle size (μm)			
	3GB		3GP	
	D(v,0.5)	uniformity	D(v,0.5)	uniformity
AmB+2Tw20	12.408	0.643	6.599	0.624
AmB+2CreRH	13.520	0.630	7.915	0.575
AmB+2P407	7.845	0.581	7.228	0.496
AmB+2M52	12.586	0.637	8.528	0.511

2. Nanostructured lipid carriers (NLC)

Formulation of AmB loaded nanostructured lipid carriers (AmB-NLC)

Physical appearance

NLC are produced by controlled mixing of solid lipid with spatially incompatible liquid lipids leading to special nanostructures with improved drug incorporation and release properties. In this experiment, NLC prepared by WME method showed the particle size in micrometer range and had poor physical stability; thus, it was excluded from this study. Nevertheless, NLC formulations could be prepared by HPH providing a special nanostructure with better drug accommodation facility when compared with conventional SLN formulations.

Table 25 shows the physical appearances of AmB loaded GB-NLC and GP-NLC with 30% MCT oil calculated to total solid lipid, respectively. They displayed yellowish colloidal dispersions and no alteration in color after storage for more than 3 months. The preparations using GB showed the lighter yellow color of AmB than those of preparations containing GP. This was due to the longer chain length of GB than GP.

Table 25 The physical appearances of AmB loaded GB-NLC and GP-NLC with various stabilizers prepared by HPH method

Formulation	Macroscopic observation			
	2.1GB		2.1GP	
	a	b	a	b
1AmB+0.9MCT+2Tw20	+	+	+	+
1AmB+0.9MCT+2CreRH	+	+	+	+
1AmB+0.9MCT+2P407	+	+	+	+
1AmB+0.9MCT+2M52	+	+	+	+

a, b: initial and stability after storage at 4°C for 3 months; +: Yellowish colloidal dispersions

Particle size

According to the particle size and size distribution determined by LD technique, there was no clear correlation between particle size and their compositions. Therefore, in this experiment, PCS was the method to describe the differences of particle sizes of NLC formulations. The mean diameter and polydispersity index measured by PCS of AmB loaded GB-NLC and GP-NLC are shown in Table 26. The type of lipids affected the particle sizes similar to that of AmB-SLN preparations which the formulations of GB gave larger particle than that of GP. However, they were in the nanometer range that was acceptable for i.v. therapy.

Most AmB-NLC preparations displayed the particle sizes slightly smaller than those of the corresponding SLN. The results were similar to the study of SLN and NLC using stearic acid, a mixture of stearic acid and oleic acid that the particle size was dependent on the oleic acid content in formulation (Hu et al., 2005).

pH, osmolality and zeta potential

The pH, osmolality, and zeta potential of AmB loaded NLC formulations which using GB and GP as solid lipid are shown in Table 27.

The pH of the preparations were in the appropriate range for drug stability. The osmolality of the preparation using Tw20 as surfactant gave the highest value but it was still too low to be used in parenteral administration.

Table 26 Particle sizes of AmB loaded GB-NLC and GP-NLC with various stabilizers prepared by HPH method

Formulation	Mean particle size by PCS (nm)			
	2.1GB		2.1GP	
	Z value ± SD	PI	Z value ± SD	PI
1AmB+0.9MCT+2Tw20	191.1 ± 0.7	0.278	112.4 ± 0.7	1.317
1AmB+0.9MCT+2CreRH	173.2 ± 2.4	0.357	108.8 ± 3.7	0.145
1AmB+0.9MCT+2P407	247.7 ± 1.7	0.336	127.6 ± 3.7	0.346
1AmB+0.9MCT+2M52	202.7 ± 4.8	0.323	156.1 ± 0.6	0.320

Table 27 The pH, osmolality and zeta potential of AmB loaded GB-NLC and GP-NLC with various stabilizers prepared by HPH method

Formulation	pH	Osmolality (mosmol/kg)	Zeta potential (mV)
1AmB+2.1GB+0.9MCT+2Tw20	6.86±0.01	17.3±0.6	-19.58
1AmB+2.1GB+0.9MCT+2CreRH	7.00±0.01	10.3±0.6	-16.46
1AmB+2.1GB+0.9MCT+2P407	7.11±0.02	7.7±0.6	-20.71
1AmB+2.1GB+0.9MCT+2M52	7.23±0.01	7.3±0.6	-15.35
1AmB+2.1GP+0.9MCT+2Tw20	6.48±0.02	13.7±0.6	-19.07
1AmB+2.1GP+0.9MCT+2CreRH	6.58±0.01	8.3±0.6	-27.57
1AmB+2.1GP+0.9MCT+2P407	6.74±0.01	8.0±0.0	-27.17
1AmB+2.1GP+0.9MCT+2M52	6.72±0.02	7.3±0.6	-20.02

The zeta potential of AmB-NLC formulations showed the negative charge in the range of -15.35 to -27.57 millivolts which were moderate zeta potential for good stability. The zeta potential of AmB-NLC results, using GB as solid lipid were significantly lower than those of SLN formulations indicating that the oil incorporated in the system affected on the stability, Nevertheless, the addition of oil had no effect on the zeta potentials of both SLN and NLC formulations that used GP as solid lipid. The result was in accordance to the investigation on SLN consisted of 100% Dynasan®116 and NLC consisted of 70% Dynasan®116 and 30% Miglyol 812 (Souto et al., 2004a). From the results, it might be concluded that the changes in zeta potential when oil was added to the system depended on the type of solid lipid which affect the recrystallization after process preparation.

3. Determination of drug content by HPLC method

Analysis of AmB from different dosage forms has been reported employing various methods such as UV-Vis spectrophotometry (Tiyaboonchai et al., 2001), Microbial assays (USP25, 2002) and high performance liquid chromatography (HPLC) (Lopez-Galera et al., 1995; Echevarr'ia et al., 1998; Egger et al., 2001; Eldem and Arican-Cellat et al., 2001).The precise route of the decomposition of this antibiotic has never been fully elucidated. However, HPLC is the most suitable method to determine the active ingredient of the formulations because of its high sensitivity, specificity and accuracy for detecting small amount of drug. In addition, a number of methods utilizing HPLC have been reported for AmB which separated the AmB from its decomposition products and the minor component amphotericin A. A prerequisite for the assessment of the stability of AmB in the SLN dispersion was modified by a method for quantitative extraction of the AmB from the Orabase® formulation. (Wilkinson, 1998)

Analytical method validation is a process to evaluate that the method are suitable and consistent for application. The analytical parameters considered in this validation study were specificity, precision, accuracy and linearity. From these satisfactory validation results and capable of separating AmB from its exipients, this HPLC condition was employed for the quantitative determination of the amount of drug from preparations in this study (Appendix C).

3.1 AmB content in SLN formulations

Figure 12 shows the AmB content in various SLN dispersions prepared by WME method which used 0.1N NaOH and DMSO as solubilizing agents, respectively. There was no significant difference or slightly lower in the content of drug for the former than the latter in most cases. All formulations showed the content of drug determined by HPLC over 70% calculated on the drug added basis. The drug might be degraded during process preparation. The presence of oxygen and heat exposure affected the content of drug (Müller et al., 2004).

The content of AmB in various SLN formulations containing GB or GP as solid lipid which prepared by HPH method are shown in Figure 13. The drug content was in the range of 78.07-89.77% and 68.95-85.11% of GB-SLN and GP-SLN, respectively. With regarding to the type of lipid, at the initial the drug

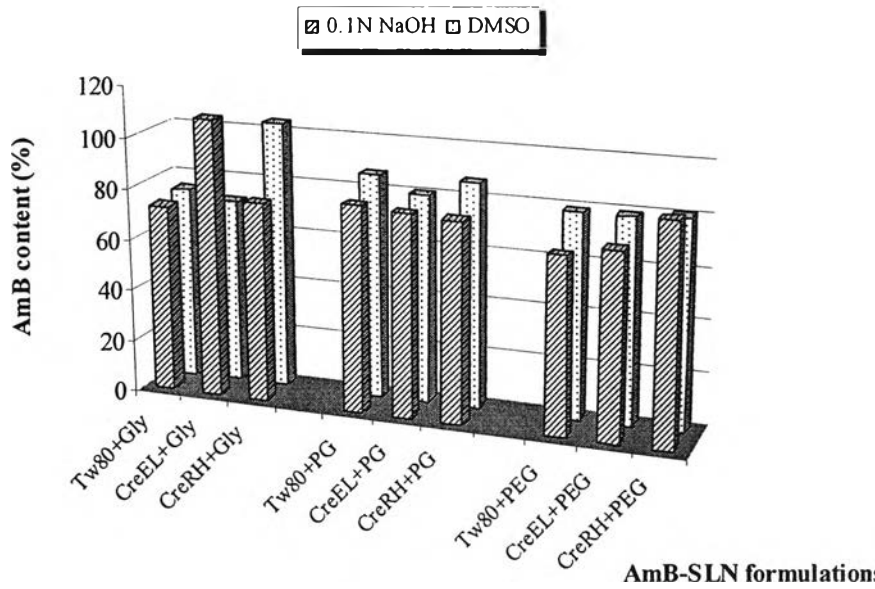

Figure 12 The percentage of AmB content using 0.1N NaOH and DMSO as solubilizing agent in various GP-SLN formulations prepared by WME method

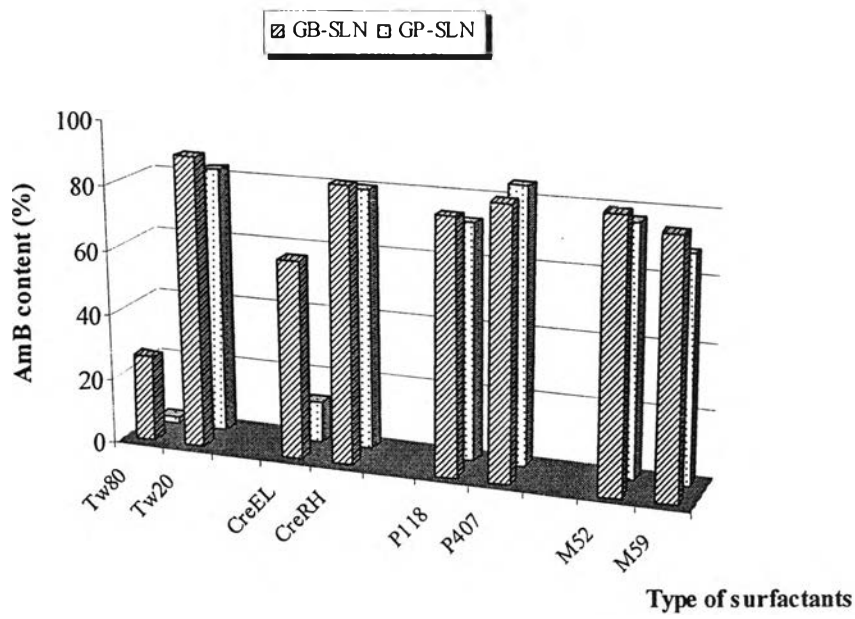

Figure 13 The percentage of AmB content in various GB-SLN and GP-SLN formulations prepared by HPH method

content of GB-SLN showed mostly equally and higher than those of GP-SLN. It was possibly proposed that the long chain length of the former could protect the drug during process preparation despite the high temperature was employed. Types of surfactant also had an effect on the initial drug content. Within group comparison of the tween and cremophor, Tw80 and CreEL gave lower drug content than Tw20 and CreRH ($p<0.05$), respectively. The amount of drug recovery when using GB with Tw80, Tw20, CreEL and CreRH were 26.51%, 89.77%, 60.90% and 84.78% whereas the content of AmB in the formulations consisted of GP with these surfactants were 2.46%, 82.71%, 12.85% and 80.43%, respectively. It could be concluded that Tw20, CreRH, P407 and M52 could protect the drug degradation during preparation which showed the drug content higher their within group. Therefore, these formulations would be further studied.

3.2 AmB content in lyophilized SLN products

The comparison of AmB content solubilized by 0.1N NaOH and DMSO in SLN dispersions prepared by WME method to lyophilized form, determined by HPLC, is shown in Figure 14. All lyophilized preparations showed the drug content slightly to moderately less than those of non-lyophilized ones; 3.78-15.78% when using 0.1N NaOH and 8.88-30.32% for using DMSO. The least decrease in drug content was from the formulations contained CreRH and either Gly or PG indicating that these two formulations could stabilize the drug during the lyophilization process.

Again, the comparison of the drug content in SLN dispersions to their lyophilized form prepared by HPH method is shown in Figure 15. Decrease in drug content was observed and similar to that described above. The decrease of drug contents were in the range of 0.10-15.67% and 2.00-18.30% for GB-SLN and GP-SLN, respectively.

Because the obtained results were not correlated, it could not be clearly concluded that the type of solubilizing agents which were used in WME method and the type of lipids in case of HPH method had an effect on the decrease in drug content

of the lyophilized forms. This was probably due to many critical process parameters involved in lyophilization process.

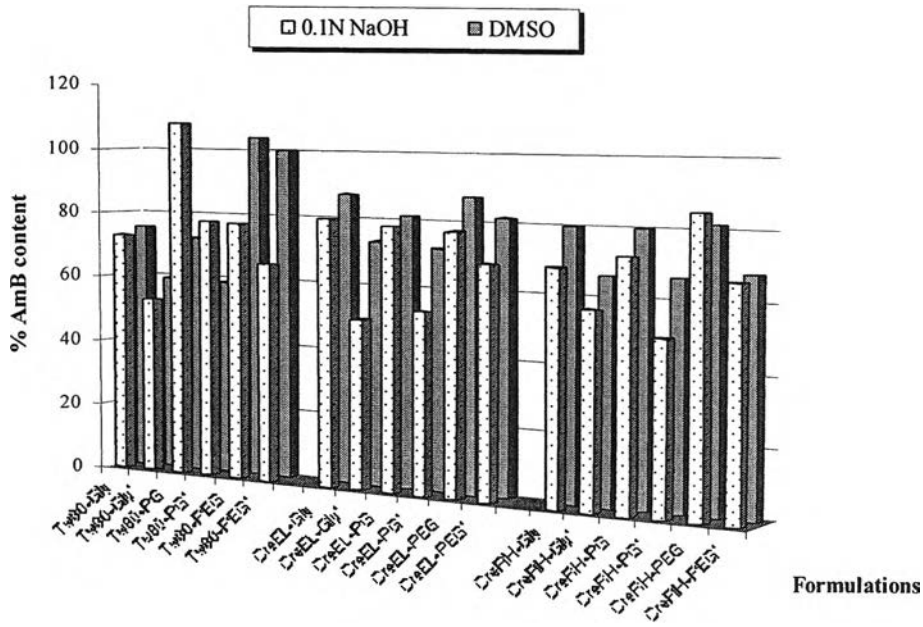

Figure 14 Comparison of the AmB content solubilized by 0.1N NaOH and DMSO in various GP-SLN dispersions to lyophilized form prepared by WME method; *:AmB freeze-dried products.

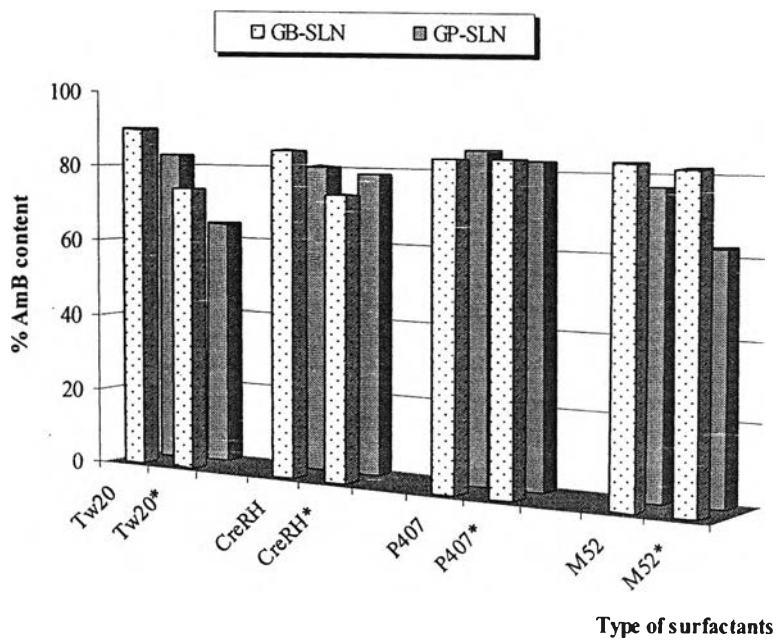

Figure 15 Comparison of the AmB content in various GB-SLN and GP-SLN dispersions to lyophilized form prepared by HPH method. Key: *: AmB freez-dried products.

3.3 AmB content in NLC formulations

The AmB contents of NLC formulations when using GB or GP as solid lipid and various surfactants are shown in Figure 16. With regarding to type of solid lipid, AmB content in GB-NLC was higher than GP-NLC formulations despite higher temperature employed during process preparation of 85°C and 70°C, respectively. The difference of drug content corresponding to type of lipid in NLC formulations had more potential effect than those of SLN formulations. It was concluded that oil played the important role to recover drug in preparation process which depended on the type of lipids. The initial drug content of GP-NLC formulations were in the range of 51.77%-69.21% whereas the drug content of GB-NLC formulations were more than 80%. It probably might be that the longer chain length of GB than GP, the faster recrystallized occurred which could form solid matrix. The solid characteristic could protect the drug from hydrolysis after preparation. In addition, report on the degradation of AmB during heat exposure at 60°C, 80°C, 100°C for 120 minutes showed similar content of 85%-87% whereas exposure to 120°C led to pronounced degradation within 20 minutes (Buttle and Müller, 2004).

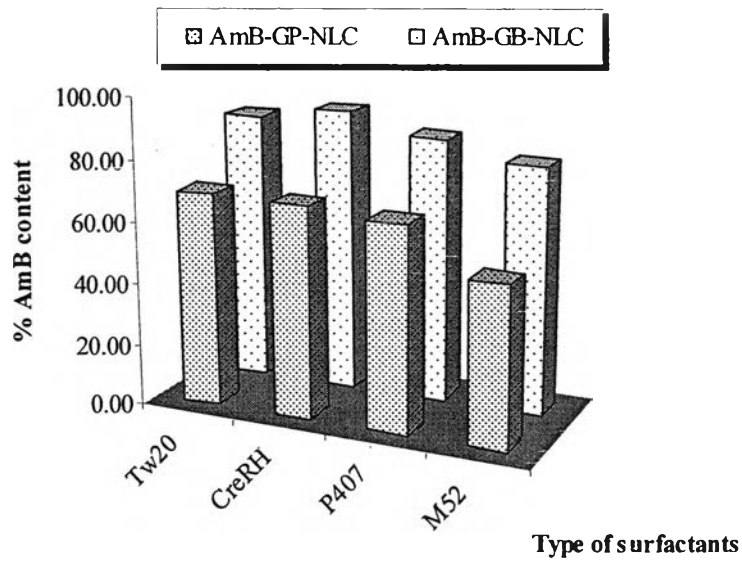

Figure 16 The percentage of AmB content in various GB-NLC and GP-NLC formulations prepared by HPH method.

4. Determination of entrapment efficiency (%EE)

4.1 Entrapment efficiency of AmB-SLN formulations

The AmB-SLN dispersions prepared by both WME and HPH method which had good physical stability were selected to study the entrapment efficiency as shown in Table 28. It was shown that AmB, an amphiphilic nature, could be successfully entrapped. The percentage of entrapment was higher than 95% as detected in all preparations. The entrapment efficiencies of AmB-SLN prepared by HPH were depended on the type of surfactants. The highest percentage of entrapment was AmB-SLN using Tw20 as surfactant while the lowest was AmB-SLN using P407 as surfactant. A possible explanation was the localization of AmB molecule onto the backbone of poloxamer which presented as polymeric micelle in the continuous phase. This was in agreement with the observations regarding the incorporation of prednisolone in GB nanoparticles and tetracaine in Dynasan 112 (zur Mühlen and Mehnert, 1995; Schwarz and Mehnert, 1999).

Table 28 Entrapment efficiency of AmB in various GP-SLN dispersions prepared by WME and HPH method

Formulation	Percentage drug entrapment of AmB loaded SLN (Mean ± SD)
WME method	
AmB:GP:(CreRH+Gly):W	98.22 ± 0.18
AmB:GP:(CreRH+PG):W	96.29 ± 0.17
AmB:GP:(CreRH+PEG):W	97.80 ± 0.10
HPH method	
AmB+3GP+2Tw20	96.38 ± 0.08
AmB+3GP+2CreRH	93.38 ± 0.76
AmB+3GP+2P407	52.77 ± 0.12
AmB+3GP+2M52	89.28 ± 1.17

4.2 Entrapment efficiency of AmB-NLC formulations

Entrapment efficiency of AmB was improved by blending small amounts of liquid oils with solid lipids in which crystal lattice insufficiently taken up

of AmB. Table 29 shows the entrapment efficiency of AmB in various types of NLC. It was noted that there was a slightly increase in the encapsulation efficacy of NLC containing Tw20 or CreRH while NLC containing P407 showed a significant increase ($p<0.05$). In contrast, NLC which used M52 as surfactant displayed no encapsulation improvement. A possible explanation could be that these particles differed in their size and, thus, surface area. The higher entrapment of NLC containing P407 might be the result of smaller particles which provided a higher surface area and higher accommodation probability for host molecules due to lower degree of crystallinity when compared with the corresponding SLN formulation; thus resulting in higher loading capacity. A marked improvement in encapsulation efficiency of retinol as a result of the presence of the MCT in solid lipid was reported by Jennings and Gohla (2001). This result was due to the binary mixture of liquid and solid lipids, resulting in only a very weak crystallization. Similar results on higher encapsulation efficiency were also reported by other investigations (Souto et al., 2004b; Hu et al., 2005)

Table 29 Entrapment efficiency of AmB in various GP-NLC dispersions prepared by HPH method

Formulation	Percentage drug entrapment of AmB loaded NLC (Mean ± SD)
1AmB+2.1GP+0.9MCT+2Tw20	98.21 ± 0.09
1AmB+2.1GP+0.9MCT+2CreRH	96.42 ± 0.74
1AmB+2.1GP+0.9MCT+2P407	75.33 ± 1.94
1AmB+2.1GP+0.9MCT+2M52	89.46 ± 0.74

5. Morphology of AmB formulations

5.1 Morphology of AmB loaded SLN prepared by WME

The morphology of two preparations containing AmB loaded GP-SLN containing CreRH with Gly and PEG detected by TEM are shown in Figure 17A and 17B, respectively. The particle sizes of particles were mostly smaller than 100 nm. The nanoparticles likely to be spherical and had irregular shape due to the particles were aggregated.

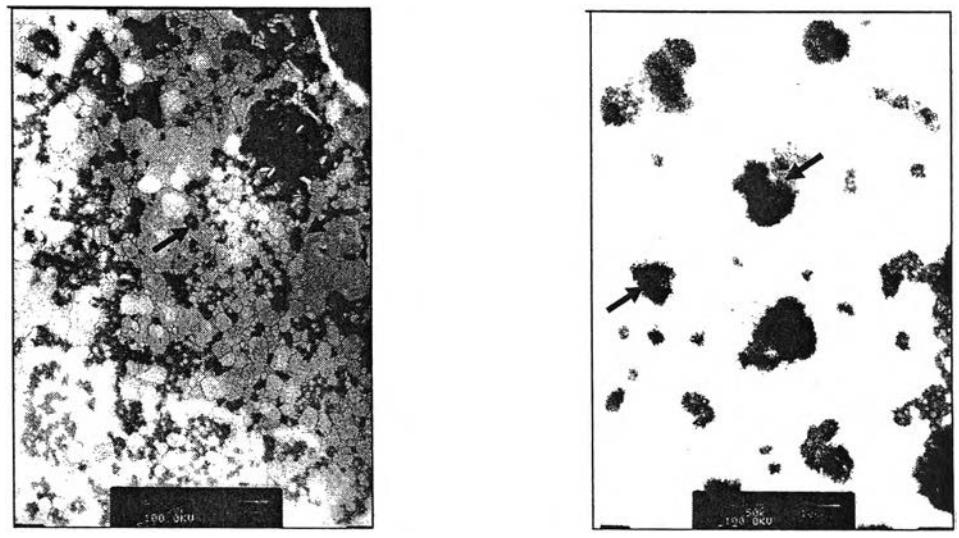

(A) (B)

Figure 17 The TEM micrographs of AmB loaded GP-SLN prepared by WME method; AmB: GP:(CreRH+Gly) (A); AmB: GP:(CreRH+PEG) (B)

5.2 Morphology of AmB loaded SLN prepared by HPH

The preparations containing AmB loaded GP-SLN containing Tw20, CreRH, P407 and M52 are shown in Figure 18A-18D, respectively. The TEM micrographs of SLN with Tw20 (18A) and with M52 (18D) displayed the irregular, elongated structure of particles and broad size distribution while those with CreRH (18B) exhibited small particles with round shape. Indeed, SLN with P407 (18C) showed regular, spherical and uniform nanospheres with no agglomeration. With respect to the particle size determination, the TEM studies supported the basic conclusion drawn from PCS measurements that the dispersions consisted predominantly of particles with dimensions below 100 nm for AmB loaded SLN with either Tw20 or CreRH, and over 100 nm for AmB loaded SLN with either P407 or M52.

From the Cryo-SEM shown in Figure 19A and 19B, the morphology of formulations of AmB containing 2% P407 with 3% GP or GB displayed the particles approximately 200-250 nm similarly to the particle analysis by PCS. In addition, the nanoparticles were discrete in disagreement with the result from TEM micrograph. This might be due to the method of sample preparation in TEM study.

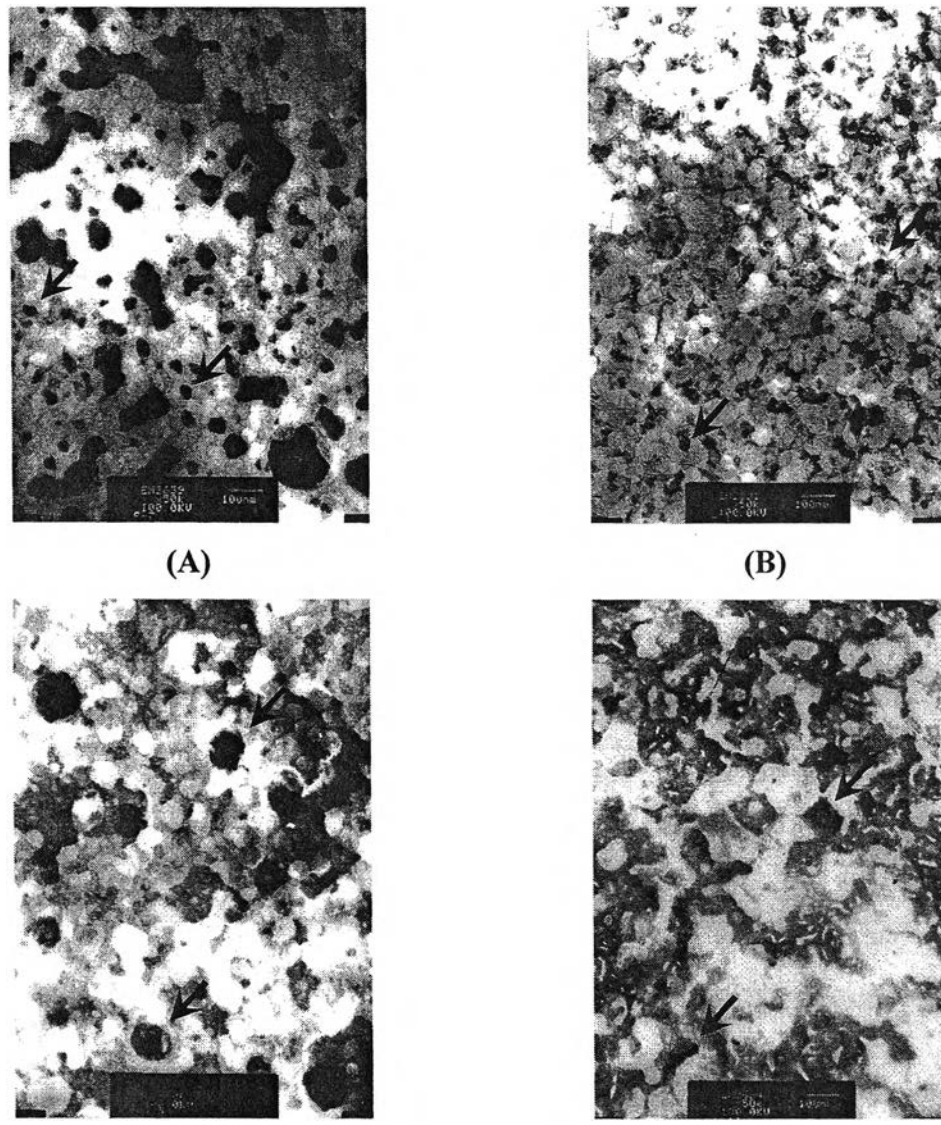

(A) (B)

(C) (D)

Figure 18 The TEM micrographs of AmB loaded GP-SLN dispersions prepared by HPH method: Tw20 (A), CreRH (B), P407 (C), M52 (D).

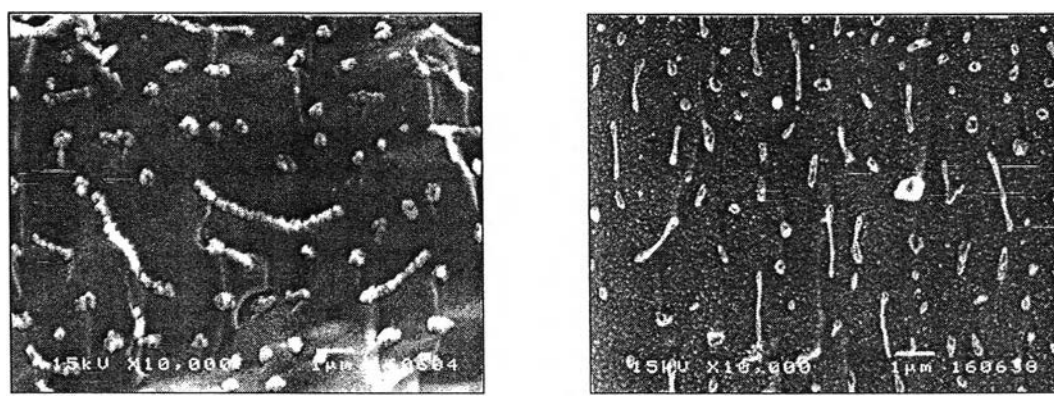

(A) (B)

Figure 19 The Cryo-SEM micrographs of AmB loaded GP-SLN dispersion with 2% P407 (A) and GB-SLN dispersion with 2% P407 (B).

5.3 Morphology of AmB loaded NLC

The structure of AmB loaded NLC were examined by TEM and Cryo-SEM. TEM of AmB loaded GP-NLC containing Tw20, CreRH, P407 and M52 are shown in Figure 20. The irregular shape of particles was observed in NLC with Tw20, CreRH and M52 while the micrograph of NLC stabilized by P407 showed spherical shape and homogenous in size distribution. The particles obtained by NLC were different from the corresponding SLN. There were spots located on the spherical structure of particles. These spots could be attributed to the presence of liquid oil on the surface of GP particles. In AmB-GP-NLC4 particles, the oil fraction stayed around the crystalline lipid. Similar results of Cryo-TEM investigation were also reported (Jores et al., 2004).

Cryo-SEM of AmB loaded GB-SLN and GP-SLN stabilizd by P407 are shown in Figure 21. There were tiny droplets sticked on the surface of particles which confirmed to the information obtained by TEM images.

6. Physical and chemical stability studies

6.1 Physical stability of AmB-SLN formulaitons

Particle sizes of AmB-SLN dispersions were evaluated by PCS at initial and after storage 4°C protected from light for 3 months in order to determine the physical stability of preparations. SLN formulations stored under this condition could be stable over the storage period of 3 years (Freitas et al., 1998b). Table 30 shows the particle size measured after 1-day production and 3 months storage of AmB solubilized by 0.1N NaOH and DMSO loaded SLN dispersions prepared by WME method, respectively. The particle sizes on 3-month storage of these preparations were slightly changed when compared with the initial.

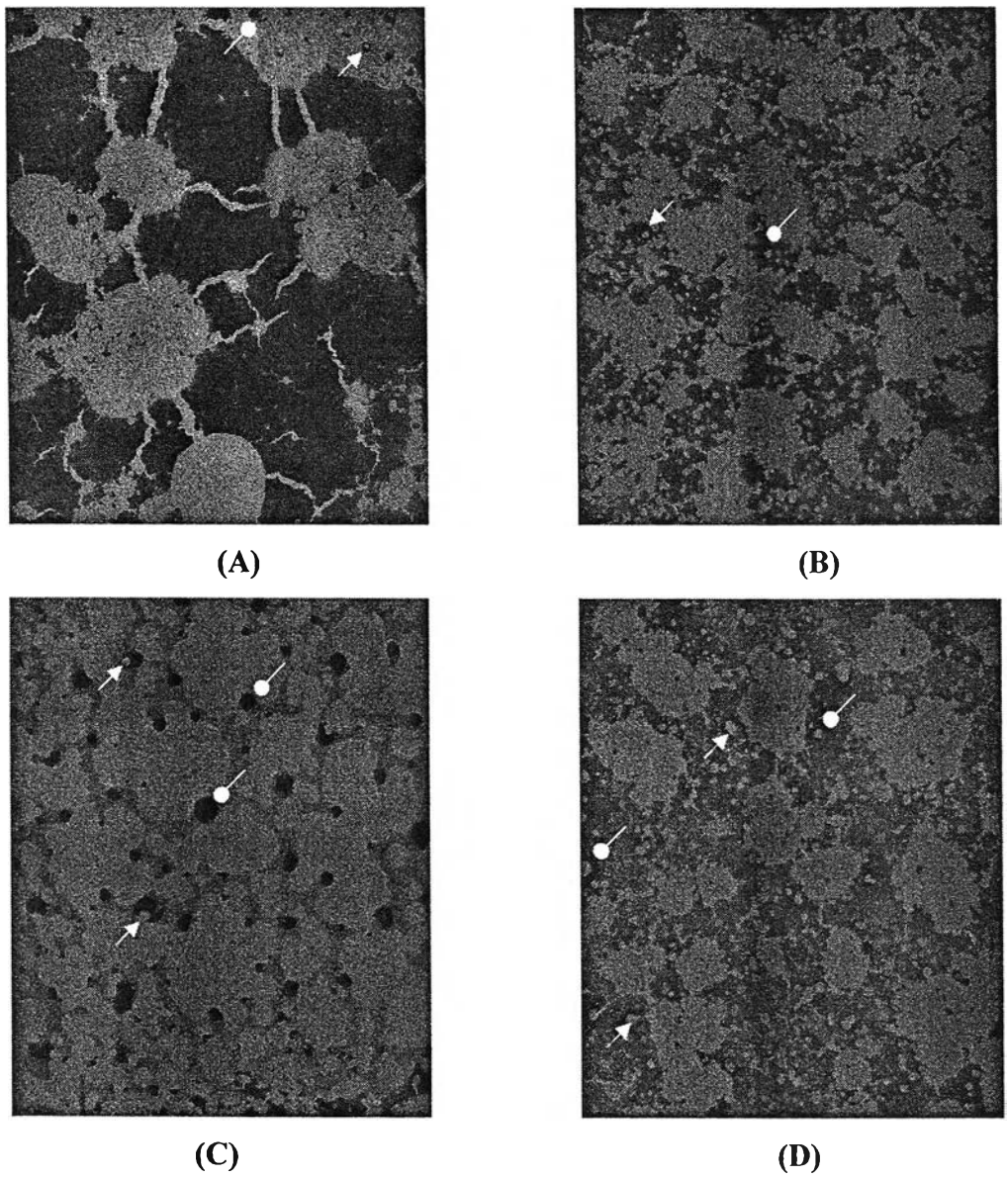

(A) (B)

(C) (D)

Figure 20 The TEM micrographs of AmB loaded GP-NLC dispersions prepared by HPH method; Tw20 (A), CreRH (B), P407 (C) and M52 (D); circle head, triangle head arrow: solid particles, oil spots

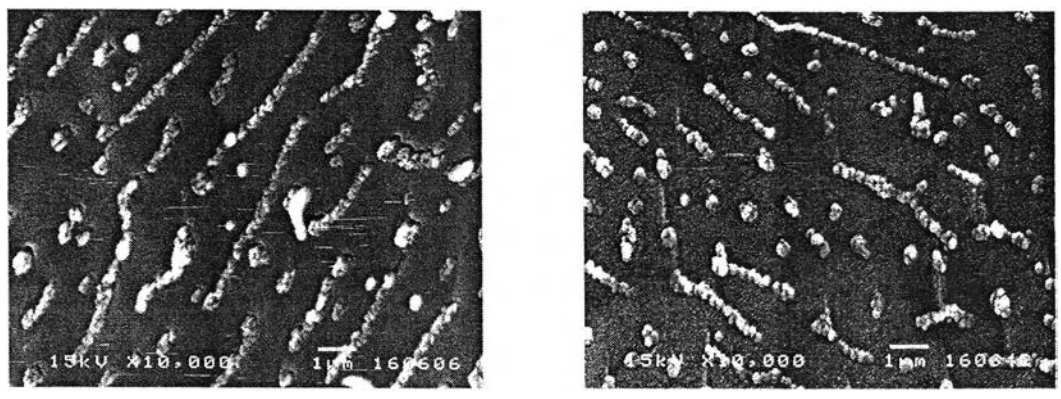

(A) (B)

Figure 21 The Cryo-SEM micrographs of AmB loaded GP-NLC dispersion with 2% P407 (A) and GB-NLC dispersion with 2% P407 (B).

Table 30 Particle sizes of AmB solubilized by 0.1N NaOH and DMSO loaded GP-SLN dispersions prepared by WME method at initial and after 3-months storage at 4°C.

Formulations	Particle size of various preparations on 4°C storage			
	Initial		3 months	
	Mean particle size (nm)		Mean particle size (nm)	
	Z value	PI	Z value	PI
AmB:GP:(CreRH+Gly)*	124.4 ± 7.8	0.347	169.1 ± 6.0	0.291
AmB:GP:(CreRH+PG)*	609.2 ± 40.5	0.248	ND	ND
AmB:GP:(CreRH+PEG)*	69.1 ± 0.5	0.253	74.3 ± 1.4	0.260
AmB:GP:(CreRH+Gly)**	51.2 ± 0.4	0.208	50.8 ± 0.2	0.246
AmB:GP:(CreRH+PG)**	46.6 ± 3.2	0.288	42.9 ± 1.2	0.211
AmB:GP:(CreRH+PEG)**	97.9 ± 1.1	0.248	95.9 ± 0.6	0.261

*: **: AmB solubilized by 0.1 NaOH, DMSO; ND: Not determined

The particle sizes of SLN preparations prepared by HPH method upon storing at 4°C for 3 months are shown in Table 31. With regarding to type of lipid, the particle sizes of SLN dispersions containing GB were significantly increased after storage ($p<0.05$) except that using poloxamer as stabilizer. Similar result was also investigated on SLN composed of 2%GB with 1.2% P188 that showed the particle size remained unchanged (Freitas and Müller, 1999). However, the PI of all cases did not increase after storage indicating of none or minimum aggregation upon the storage time, and remained centered in the 0.2-0.3 range. Therefore, the colloidal system retained their distinct distribution shape throughout the time interval studied. Surprisingly, the GP-SLN dispersions gave the opposite results. The particle sizes of these formulations were significantly reduced while the PIs were increased after storage for 3 months. It might be described in term of polymorphic transitions after recrystallization of triglyceride nanoparticles which were faster for shorter chain triglycerides than for long chain triglycerides (Venkateswarlu and Manjunath, 2004). Therefore, the recrystallization of GP was faster than that of GB leading to the smaller particles and broader PI value after storage. The nanosphere size distribution increase might be explained by the tendency of solubilized fatty acid to be adsorbed on the surface of the already formed solid nanoparticles (Laine et al., 1988).

Table 31 Particle sizes of AmB loaded GB-SLN and GP-SLN dispersions prepared by HPH method at initial and after 3-months storage at 4°C.

Formulations	Particle size of various preparations on 4°C storage			
	Initial		3 months	
	Mean particle size (nm)		Mean particle size (nm)	
	Z value	PI	Z value	PI
AmB+3GB+2Tw20	142.8 ± 12.6	0.326	261.3 ± 13.0	0.294
AmB+3GB+2CreRH	137.6 ± 3.4	0.326	326.7 ± 4.30	0.342
AmB+3GB+2P407	250.2 ± 2.8	0.249	257.4 ± 16.5	0.253
AmB+3GB+2M52	253.7 ± 3.2	0.217	322.0 ± 14.9	0.236
AmB+3GP+2Tw20	92.4 ± 2.2	0.178	ND	ND
AmB+3GP+2CreRH	115.7 ± 5.0	0.274	83.1 ± 0.8	0.406
AmB+3GP+2P407	201.6 ± 3.5	0.145	119.2 ± 1.8	0.314
AmB+3GP+2M52	263.0 ± 9.2	0.279	146.0 ± 3.5	0.376

ND: Not determined

6.2 Chemical stability of AmB-SLN formulations

To study the effect of temperature on chemical stability of drug, the selected SLN dispersions prepared by both WME and HPH methods were kept separately at 4°C and 30°C, protected from light. The colloidal dispersion was withdrawn after storage for 3 months for subjecting to analysis by HPLC. The differences of drug content from two storage conditions are shown in Figure 22 and 23. The content of AmB significantly lost after storage at 30°C compared with 4°C storage condition ($p<0.05$). It was clearly concluded that the temperature had an effect on chemical stability of AmB.

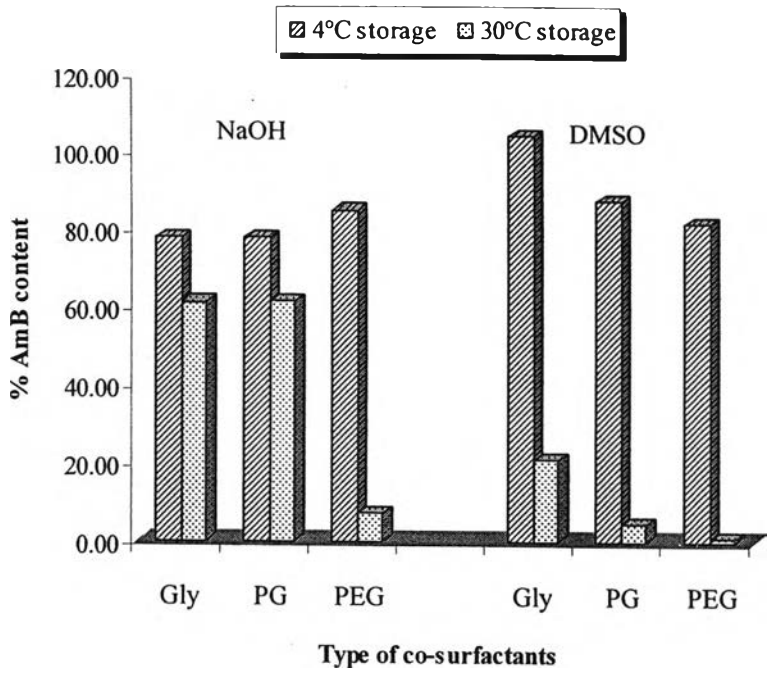

Figure 22 The percentage of AmB content in GP-SLN dispersions containing CreRH with various co-surfactants prepared by WME method after 3 months storage at 4°C and 30°C.

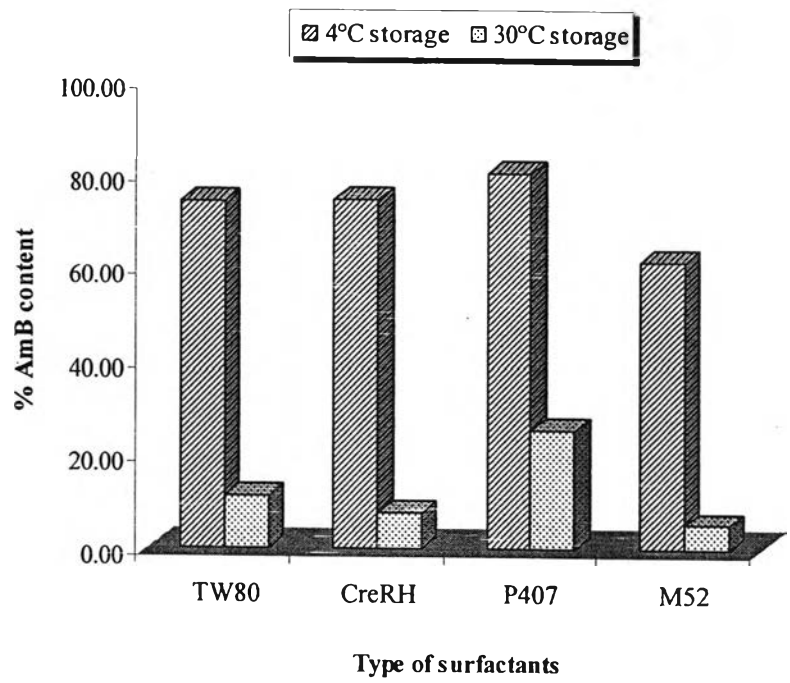

Figure 23 The percentage of AmB content in GP-SLN dispersions with various surfactants prepared by HPH method after 3 months storage at 4°C and 30°C.

From the result, storage condition at 4°C and protected from light was selected to further investigate the shelf life of AmB in all preparations. Under this condition, drug content was investigated in triplicate at 0, 1, 2 and 3 months. Table 32 and Figures 24-25 show the content and the stability profiles of AmB loaded SLN prepared by WME when using 0.1N NaOH and DMSO as solubilizing agent, respectively. It could be seen that Tw80 and CreEL could not protect the drug from degradation, particularly in the system which used 0.1N NaOH as solubilizing agent. The amount of the drug in all SLN consisted of Tw80 was nearly zero after storage for 3 months. Only SLN of CreRH with all co-surfactants had maintained the drug content during the time storage.

Drug content and stability profiles at 4°C of AmB in different SLN formulations prepared by HPH method are shown in Table 33 and Figures 26-27. Both GB-SLN and GP-SLN preparations with either Tw80 or CreEL revealed much faster degradation of the active ingredient than those with other surfactants. All drug in these preparations disappeared after storage for 1 month. The results were correlated to the chemical stability data of SLN dispersions prepared by WME method.

Tables 34 and 35 show the shelf-life of SLN preparations prepared by WME and HPH methods, respectively. Unlike the HPH process, the WME method employed elevated temperature for only as long as necessary to dissolve or disperse the drug and also there was no requirement for high shear power. It was observed that drug inactivation was highly influenced by temperature and degree of aeration (Tungjairukkandee, 1999; Müller et al., 2004). Therefore, the shelf-lives of CreRH with all co-surfactants were more than 6 months which were much higher than that of 4 months obtained from the same surfactant prepared by HPH method.

The shelf-lives when using M52 and M59 were less than 2 months whereas poloxamer could stabilize the AmB-SLN with longer shelf-lives especially the formulation containing GP and P407 which had the longest shelf-life of 6 months. This result was accordance to the review of Bummer (2004) who reported that SLN based on Pluronic F68 showed different stability when either GP, glyceryl

monostearate, or GB were employed as the matrix. Interestingly, these optimum AmB-SLN dispersions were more stable than that of AmB as nanosuspension examined by Kayser et al. (2003) which proved to be stable for 3 weeks. Moreno et al. (2000) also reported remarkable degradation phenomena after just 7 days of storage for non- lyophilized AmB microemulsion. The results might be described in terms of solid matrix of SLN which could protect the drug from continuous phase while the nanosuspension and microemulsion system as the liquid state led to degrade rapidly.

Table 32 The AmB content as a function of time at 4°C of GP-SLN dispersions prepared by WME method

Formulations	AmB content (%)	Residual AmB (%)		
	0 month	1 month	2 months	3 months
AmB:GP (Tw80+Gly)	72.84 ± 1.11*	31.70 ± 0.81*	0.50 ± 0.05*	0.43 ± 0.02*
	75.02 ± 0.61**	45.00 ± 0.53**	34.13 ± 1.81**	26.71 ± 0.49**
AmB:GP: (CreEL+Gly)	108.12 ± 1.32*	68.73 ± 1.36*	51.16 ± 0.76*	44.74 ± 0.31*
	72.02 ± 4.08**	58.71 ± 1.03**	26.89 ± 0.91**	22.73 ± 1.11**
AmB:GP: (CreRH+Gly)	77.49 ± 0.49*	73.70 ± 0.38*	73.51 ± 1.75*	73.47 ± 1.33*
	103.99 ± 3.42**	114.16 ± 1.23**	113.26 ± 1.26**	118.33 ± 0.25**
AmB:GP: (Tw80+PG)	79.85 ± 0.59*	34.17 ± 0.29*	9.23 ± 0.78*	0.16 ± 0.04*
	87.14 ± 0.23**	61.64 ± 0.44**	45.02 ± 0.66**	30.43 ± 0.49**
AmB:GP: (CreEL+PG)	78.21 ± 3.18*	41.77 ± 0.90*	19.39 ± 0.42*	9.63 ± 0.27*
	81.10 ± 2.14**	57.09 ± 0.13**	47.07 ± 0.34**	41.60 ± 1.00**
AmB:GP: (CreRH+PG)	77.47 ± 0.32*	77.60 ± 0.62*	75.33 ± 0.52*	78.67 ± 0.90*
	86.96 ± 0.27**	87.40 ± 0.12**	85.49 ± 0.28**	83.06 ± 0.24**
AmB:GP: (Tw80+PEG)	68.48 ± 1.66*	21.31 ± 0.63*	1.04 ± 0.02*	0.05 ± 0.03*
	79.53 ± 1.21**	60.97 ± 0.21**	42.37 ± 0.15**	33.23 ± 0.22**
AmB:GP: (CreEL+PEG)	72.24 ± 0.41*	37.95 ± 0.11*	20.98 ± 1.54*	18.91 ± 0.19*
	79.50 ± 0.55**	47.86 ± 0.40**	32.07 ± 0.19**	30.62 ± 0.18**
AmB:GP: (CreRH+PEG)	84.73 ± 1.49*	82.73 ± 0.66*	80.27 ± 0.99*	80.14 ± 0.80*
	81.15 ± 2.52**	79.62 ± 0.43**	80.49 ± 1.13**	80.20 ± 0.51**

*: AmB solubilized by 0.1N NaOH; **: AmB solubilized by DMSO

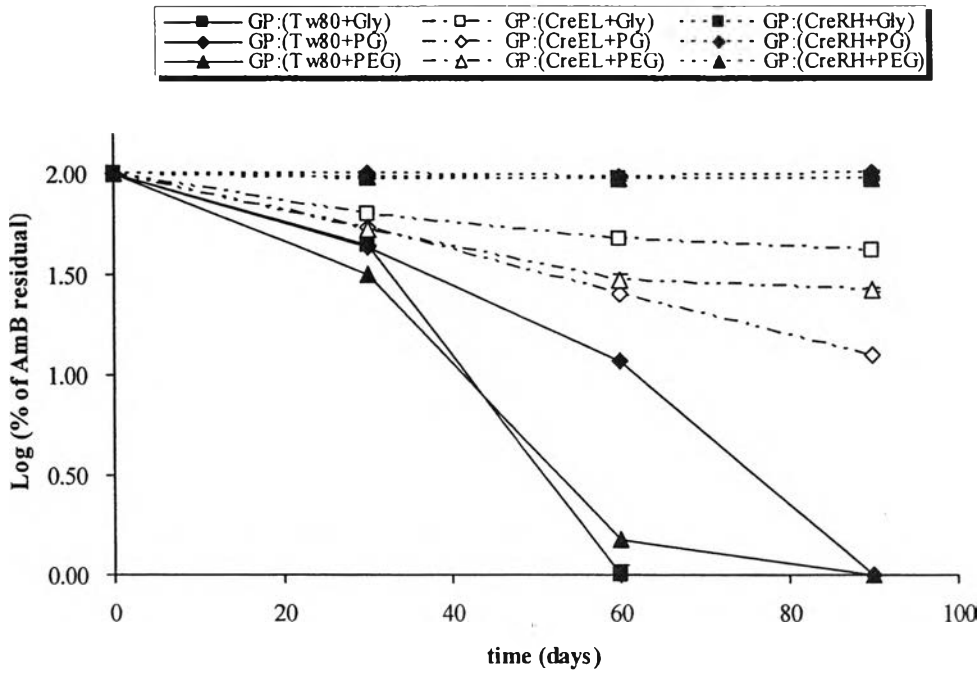

Figure 24 AmB residual content in various GP-SLN formulations prepared by WME method at 4°C as a function of time (AmB solubilized in 0.1N NaOH)

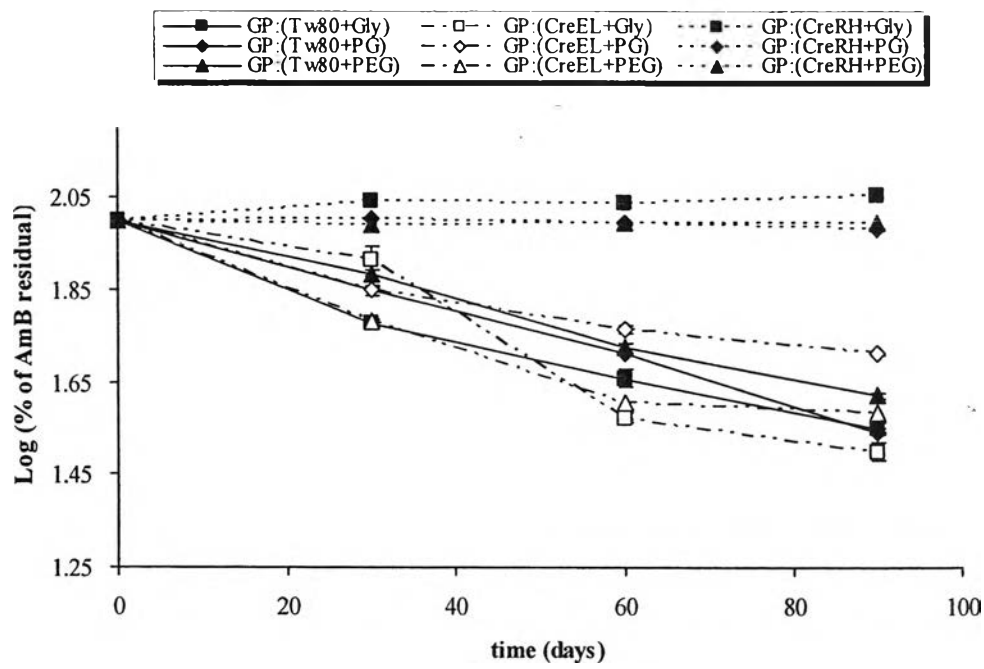

Figure 25 AmB residual content in various GP-SLN formulations prepared by WME method at 4°C as a function of time (AmB solubilized in DMSO)

Table 33 The AmB content as a function of time at 4°C of GB-SLN and GP-SLN dispersions prepared by HPH method

Formulations	AmB content (%)	Residual AmB (%)		
	0 month	1 month	2 months	3 months
AmB+3GB+2Tw80	26.51 ± 0.27	ND	ND	ND
AmB+3GB+2Tw20	89.77 ± 1.95	81.14 ± 0.53	81.99 ± 1.51	82.11 ± 1.29
AmB+3GB+2CreEL	60.90 ± 1.17	0.27 ± 0.01	ND	ND
AmB+3GB+2CreRH	84.78 ± 0.92	80.24 ± 0.11	77.14 ± 0.46	78.13 ± 0.28
AmB+3GB+2P118	78.07 ± 0.88	77.29 ± 1.51	73.17 ± 1.89	73.16 ± 0.07
AmB+3GB+2P407	83.30 ± 0.98	81.68 ± 3.55	74.82 ± 1.08	73.71 ± 0.27
AmB+3GB+2M52	82.98 ± 1.77	78.19 ± 0.45	73.50 ± 1.32	71.26 ± 0.55
AmB+3GB+2M59	78.52 ± 0.87	53.54 ± 0.19	46.43 ± 0.14	42.98 ± 0.47
AmB+3GP+2Tw80	2.46 ± 0.18	0.20 ± 0.00	ND	ND
AmB+3GP+2Tw20	82.71 ± 1.00	81.60 ± 1.47	80.49 ± 3.44	74.33 ± 1.57
AmB+3GP+2CreEL	12.85 ± 0.17	0.24 ± 0.01	ND	ND
AmB+3GP+2CreRH	80.43 ± 1.39	77.60 ± 0.30	75.12 ± 0.16	74.87 ± 1.00
AmB+3GP+2P118	72.97 ± 0.41	71.55 ± 0.39	69.61 ± 0.77	67.50 ± 0.61
AmB+3GP+2P407	85.11 ± 0.49	80.23 ± 0.91	79.70 ± 1.20	80.51 ± 1.45
AmB+3GP+2M52	76.97 ± 1.49	71.56 ± 0.62	67.76 ± 3.09	61.40 ± 0.53
AmB+3GP+2M59	68.95 ± 0.67	43.07 ± 0.11	31.08 ± 0.24	25.90 ± 0.43

ND = Not determined

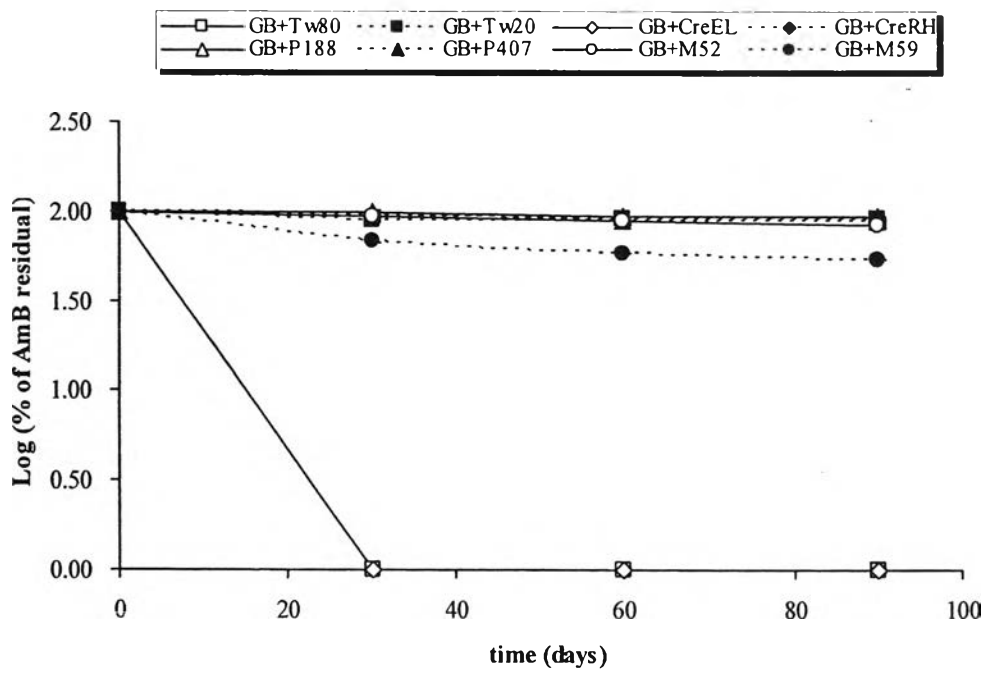

Figure 26 AmB residual content in various GB-SLN formulations prepared by HPH method at 4°C as a function of time

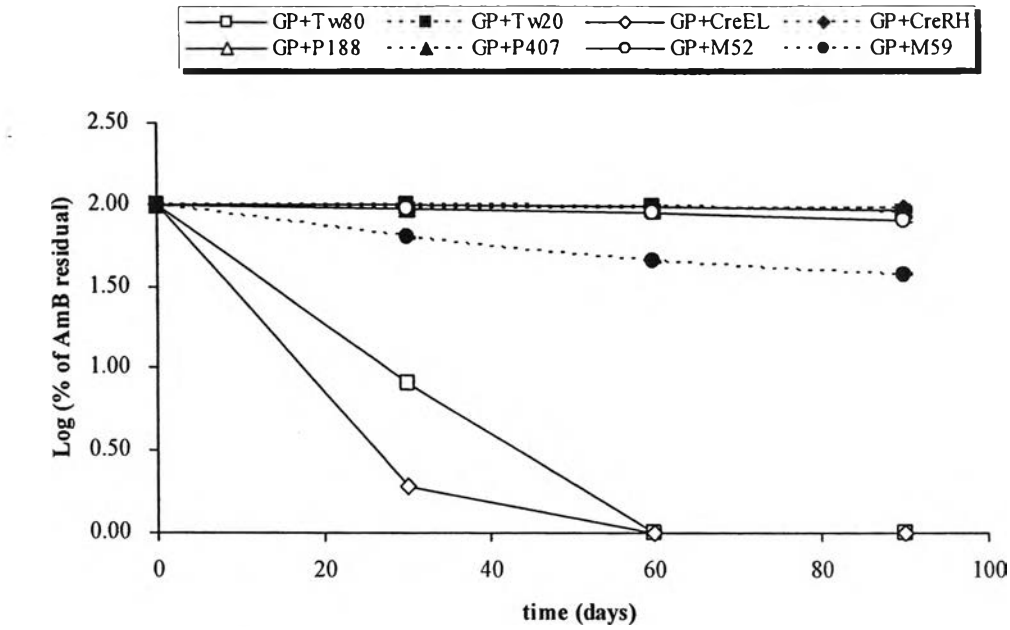

Figure 27 AmB residual content in various GP-SLN formulations prepared by HPH method at 4°C as a function of time

Table 34 Predicted shelf lives at 4°C of AmB in GP-SLN preparations prepared by WME method

Formulations	AmB Solubilized by			
	0.1 N NaOH		DMSO	
	K	t_{90} (days)	K	t_{90} (days)
Tw80+Gly	-	-	1.13×10^{-2}	9.33
CreEL+Gly	9.81×10^{-3}	10.70	1.41×10^{-2}	7.43
CreRH+Gly	0.54×10^{-3}	194.01	1.26×10^{-3}	82.75
Tw80+PG	-	-	1.16×10^{-2}	9.07
CreEL+PG	2.35×10^{-2}	4.47	7.32×10^{-3}	14.35
CreRH+PG	Θ	Θ	0.53×10^{-3}	197.37
Tw80+PEG	-	-	1.00×10^{-2}	10.45
CreEL+PEG	1.54×10^{-2}	6.82	1.09×10^{-2}	9.65
CreRH+PEG	0.66×10^{-3}	159.97	Θ	Θ

Θ: Could not be calculated

Table 35 Predicted shelf lives at 4°C of AmB in GB-SLN and GP-SLN preparations with various surfactants prepared by HPH method

Formulations	K	t_{90} (days)
3GB+2Tw80	-	-
3GB+2Tw20	0.86×10^{-3}	122.56
3GB+2CreEL	-	-
3GB+2CreRH	0.95×10^{-3}	110.66
3GB+2P118	0.83×10^{-3}	126.30
3GB+2P407	1.52×10^{-3}	69.29
3GB+2M52	1.73×10^{-3}	60.71
3GB+2M59	6.50×10^{-3}	16.14
3GP+2Tw80	-	-
3GP+2Tw20	1.12×10^{-3}	94.20
3GP+2CreEL	-	-
3GP+2CreRH	0.82×10^{-3}	127.35
3GP+2P118	0.86×10^{-3}	121.58
3GP+2P407	0.58×10^{-3}	182.37
3GP+2M52	2.44×10^{-3}	42.97
3GP+2M59	1.09×10^{-2}	9.65

6.3 Chemical stability of AmB lyophilized SLN products

The chemical stability after for 3 months storage at 4°C of lyophilized SLN prepared by WME and HPH method are shown in Table 36, 38, Figure 28-29 and Table 37, 39, Figure 30, respectively. As expected, the drug remaining in the lyophilized preparations was markedly higher than that from the colloidal dispersions, particularly in lyophilized formulations using Tw80 or CreEL with co-surfactants which could stabilize the drug for 3-5 months. The results were corresponding to the investigation of non-lyophilized and lyophilized AmB microemulsions by Moreno et al (2001). Surprisingly, in this investigation, the lyophilized preparations obtained from SLN dispersions prepared by HPH method showed the opposite results. The shelf-lives of AmB freeze-dried formulations containing GP with Tw20, CreRH and P407 were less than 2 months while those of the non-lyophilized ones were 3-6 months. The chemical stability of AmB freeze-dried product used M52 as stabilizer was not different from those of colloidal dispersions. However, in the HPH method,

the drug content of lyophilized form was lower than the corresponding dispersions. It might be due to the incompletion of lyophilization process which described in term of mass and heat transfer. AmB-SLN prepared by WME gave both lower particle size and solid content than AmB-SLN prepared by HPH method. The higher product resistance of the latter was from the thicker drying layer which affected the product quality on primary drying process (Pikel, 1992).

Table 36 The AmB content as a function of time at 4°C of lyophilized GP-SLN products prepared by WME method

Formulations	AmB content (%)	Residual AmB (%)		
	0 month	1 month	2 months	3 months
AmB:GP (Tw80+Gly)	53.14 ± 0.22*	50.83 ± 0.84*	50.90 ± 0.08*	48.87 ± 0.40*
	59.23 ± 0.40**	57.44 ± 0.52**	58.23 ± 1.78**	56.04 ± 0.55**
AmB:GP: (CreEL+Gly)	77.79 ± 2.38*	74.01 ± 0.34*	75.17 ± 0.47*	71.10 ± 0.82*
	58.65 ± 0.36**	57.34 ± 0.53**	55.64 ± 0.60**	56.21 + 0.74**
AmB:GP: (CreRH+Gly)	65.46 ± 0.54*	60.29 ± 0.25*	61.96 ± 0.03*	60.80 ± 0.49*
	100.20 ± 0.95**	99.68 ± 0.94**	99.55 ± 0.99**	96.59 ± 0.45**
AmB:GP: (Tw80+PG)	50.54 ± 3.27*	63.49 ± 0.14*	63.44 ± 0.25*	64.60 ± 0.23*
	73.13 ± 0.96**	71.81 ± 0.75**	70.12 ± 0.53**	67.69 ± 0.46**
AmB:GP: (CreEL+PG)	53.89 ± 0.09*	53.04 ± 0.63*	53.68 ± 0.42*	52.42 ± 0.27*
	71.75 ± 1.69**	69.50 ± 0.22**	68.52 + 0.90**	64.19 ± 0.62**
AmB:GP: (CreRH+PG)	68.59 ± 1.18*	67.20 ± 0.37*	63.65 ± 0.54*	61.83 ± 0.20*
	81.34 ± 1.79**	79.98 ± 0.46**	77.27 ± 0.21**	71.11 ± 1.29**
AmB:GP: (Tw80+PEG)	57.19 ± 0.41*	52.85 ± 0.04*	52.97 ± 0.50*	52.25 ± 0.80*
	65.89 ± 0.44**	64.20 ± 0.24**	62.98 ± 0.63**	61.91 ± 0.49**
AmB:GP: (CreEL+PEG)	50.50 ± 1.13*	49.91 ± 0.33*	48.34 ± 0.18*	45.95 ± 0.06*
	66.05 ± 0.97**	63.29 ± 0.19**	60.69 ± 0.34**	55.75 ± 1.90**
AmB:GP: (CreRH+PEG)	66.27 ± 1.37*	65.58 ± 0.19*	65.18 ± 0.54*	62.69 ± 0.25*
	67.81 ± 0.43**	66.41 ± 0.35**	65.32 ± 0.18**	62.70 ± 1.13**

*, **: AmB solubilized by 0.1N NaOH, DMSO, respectively.

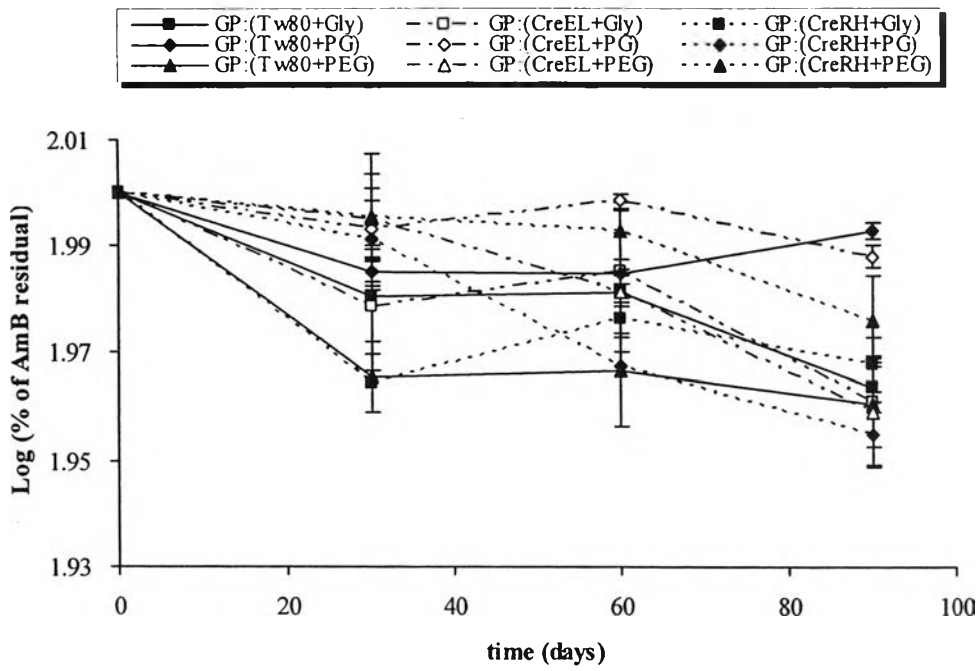

Figure 28 AmB residual content at 4°C in various lyophilized GP-SLN formulations as a function of time (AmB solubilized by 0.1N NaOH, prepared by WME method)

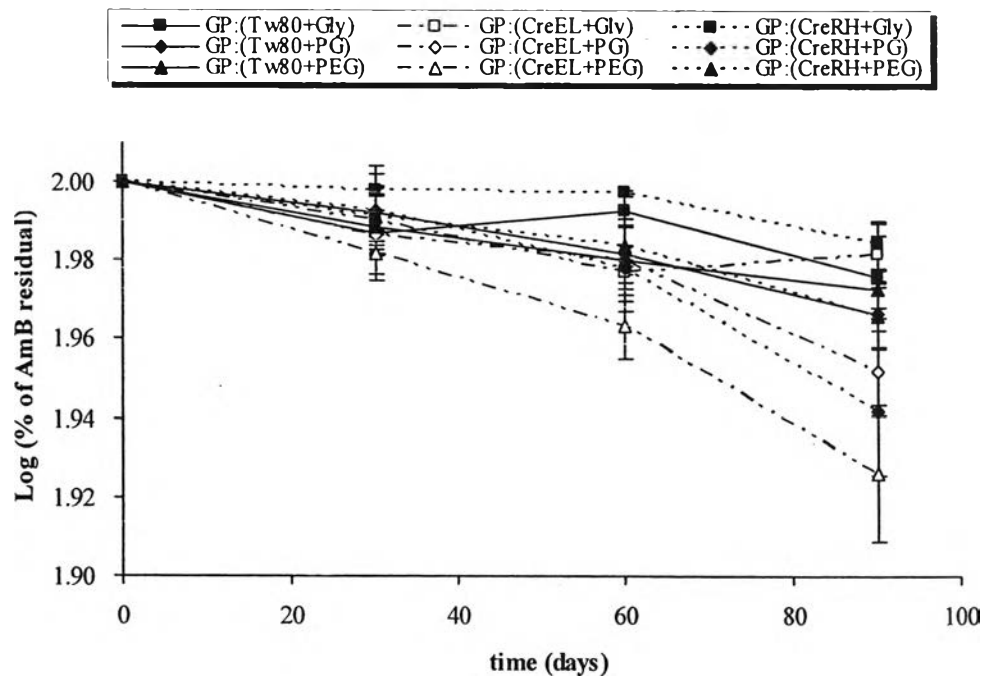

Figure 29 AmB residual content at 4°C in various lyophilized GP-SLN formulations as a function of time (AmB solubilized by DMSO, prepared by WME method)

Table 37 The AmB content as a function of time at 4°C of lyophilized GB-SLN and GP-SLN products prepared by HPH method

Formulations	AmB content (%)	Residual AmB (%)		
	0 month	1 month	2 months	3 months
AmB+GB+Tw20	74.10 ± 0.98	68.63 ± 1.98	60.08 ± 1.83	50.30 ± 0.79
AmB+GB+CreRH	73.57 ± 0.88	62.54 ± 1.77	58.49 ± 0.62	50.60 ± 0.15
AmB+GB+P407	82.33 ± 1.54	67.81 ± 0.25	68.90 ± 0.43	52.25 ± 0.80
AmB+GB+M52	80.47 ± 1.45	71.54 ± 0.70	70.80 ± 0.26	45.95 ± 0.06
AmB+GP+Tw20	64.42 ± 0.68	66.85 ± 0.37	68.97 ± 0.81	62.88 ± 0.72-
AmB+GP+CreRH	78.43 ± 0.67	73.25 ± 1.08	66.77 ± 0.26	56.96 ± 0.98
AmB+GP+P407	82.61 ± 1.55	70.49 ± 0.70	66.91 ± 0.80	60.80 ± 0.49-
AmB+GP+M52	62.50 ± 0.20	57.51 ± 2.03	53.39 ± 0.92	53.77 ± 0.77

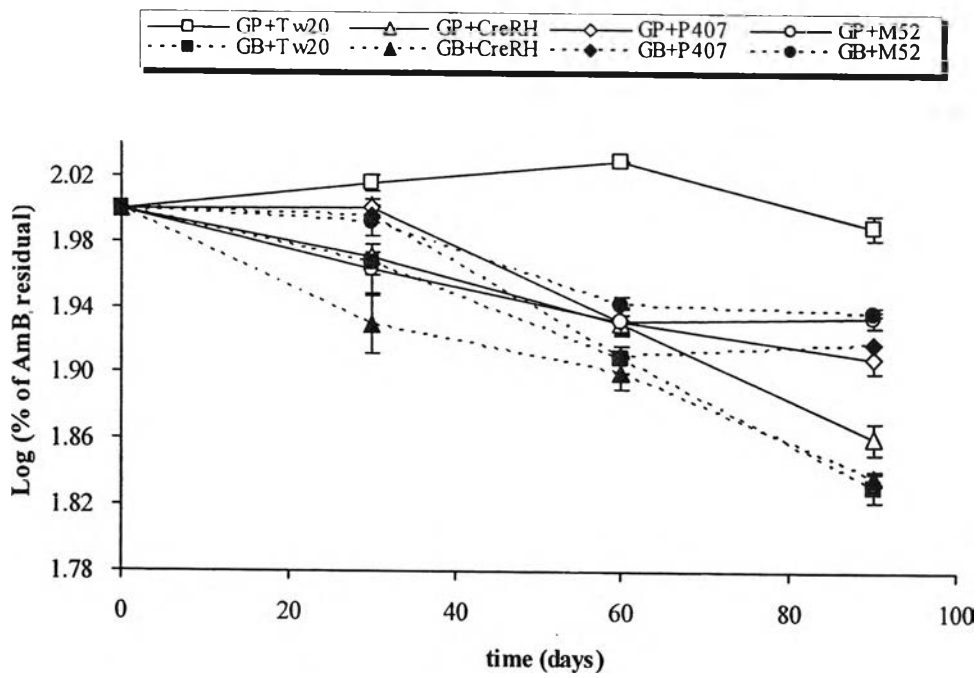

Figure 30 AmB residual content at 4°C in various lyophilized GB-SLN and GP-SLN formulations as a function of time (Prepared by HPH method)

Table 38 Predicted shelf lives at 4°C of AmB in lyophilized GP-SLN preparations prepared by WME method

Formulations	AmB Solubilized by 0.1 N NaOH		AmB Solubilized by DMSO	
	K	t_{90} (days)	K	t_{90} (days)
Tw80+Gly	0.83×10^{-3}	125.95	0.51×10^{-3}	206.30
CreEL+Gly	0.85×10^{-3}	124.23	0.53×10^{-3}	199.97
CreRH+Gly	0.65×10^{-3}	162.25	0.37×10^{-3}	283.18
Tw80+PG	Θ	Θ	0.85×10^{-3}	123.22
CreEL+PG	Θ	Θ	1.16×10^{-3}	90.46
CreRH+PG	1.22×10^{-3}	86.35	1.46×10^{-3}	72.03
Tw80+PEG	0.90×10^{-3}	117.20	0.69×10^{-3}	153.00
CreEL+PEG	1.05×10^{-3}	99.98	1.84×10^{-3}	57.06
CreRH+PEG	0.57×10^{-3}	183.10	0.84×10^{-3}	125.25

Θ: could not be calculated

Table 39 Predicted shelf lives at 4°C of AmB in lyophilized GB-SLN and GP-SLN preparations prepared by HPH method

Formulations	K	t_{90} (days)
GB+Tw20	4.32×10^{-3}	24.30
GB+CreRH	3.97×10^{-3}	26.48
GB+P407	2.53×10^{-3}	41.45
GB+M52	1.84×10^{-3}	57.13
GP+Tw20	Θ	Θ
GP+CreRH	3.51×10^{-3}	29.94
GP+P407	2.63×10^{-3}	39.99
GP+M52	1.75×10^{-2}	59.91

Θ: could not be calculated

6.4 Physical stability of AmB-NLC formulations

Table 40 displays the particle sizes of AmB loaded GB-NLC and GP-NLC with various types of surfactants at initial and after 3-months storage. The abbreviations in the figure were AmB-GP-NLC1, AmB-GP-NLC2, AmB-GP-NLC3 and AmB-GP-NLC4 and AmB-GB-NLC1, AmB-GB-NLC2, AmB-GB-NLC3 and AmB-GB-NLC4 which were designated the NLC formulations containing 1% AmB,

GP and GB with either Tw20, CreRH, P407 or M52, respectively. The result of particle sizes of GP-NLC was similar to the physical stability of AmB-SLN formulations. The particle sizes of these preparations after storage for 3 months were slightly decreased. On the contrary, the oil addition in GB-NLC resulted in improvement in physical stability by maintaining the particle sizes while the corresponding SLN formulation showed the particle size growth during storage. It could be envisaged that the oil incorporated in the system could retard the recrystallization of lipid which leading to the unchanged particle size during the storage. Similar result was also reported (Jores et al., 2004).

Table 40 Particle sizes of AmB loaded GB-NLC and GP-NLC with various surfactants prepared by HPH method at initial and after 3 months storage

Formulations	Particle size of various preparations on 4°C storage			
	Initial		3 months	
	Mean particle size (nm)		Mean particle size (nm)	
	Z value	PI	Z value	PI
AmB-GB-NLC1	191.1 ± 0.7	0.278	189.5 ± 3.9	0.303
AmB-GB-NLC2	173.2 ± 2.4	0.357	181.5 ± 2.1	0.368
AmB-GB-NLC3	247.7 ± 1.7	0.336	220.5 ± 2.8	0.331
AmB-GB-NLC4	202.7 ± 4.8	0.323	192.6 ± 6.8	0.324
AmB-GP-NLC1	112.4 ± 0.7	1.317	106.5 ± 1.6	0.337
AmB-GP-NLC2	108.8 ± 3.7	0.145	87.3 ± 0.2	0.338
AmB-GP-NLC3	127.6 ± 3.7	0.346	145.6 ± 1.1	0.225
AmB-GP-NLC4	156.1 ± 0.6	0.320	124.0 ± 2.6	0.324

6.5 Chemical stability of AmB-NLC formulations

Chemical stability studies at 4°C were performed on selected AmB loaded in GB-NLC and GP-NLC formulations. Table 41 and Figure 31 report the AmB content in the different formulations as a function of time and express as percentage of initial drug content. Stability data predicted shelf lives are shown in Table 42. It was found that NLC formulations could maintain 90% of AmB content for 1-4 months depended on its composition. The type of lipid affected the chemical stability of AmB. AmB-NLC formulation containing GP with Tw20 showed more drug remaining than corresponding AmB-SLN formulation. It was assumed that

during the storage, the GP matrix of SLN formulation with Tw20 transformed from high energy modifications to β-modification, forming a perfect crystal with no room for the drug. In addition, there was low physical stability that white precipitate appeared after storage for 3 months. Therefore, AmB expulsion from SLN could occur and led to low chemical stability. For NLC formulation, the lipids and liquid lipids, which could be mixed in such a combination that particles solidified upon cooling but did not recrystallize and remained in the amorphous state. AmB might stay as guest molecule which showed long shelf-life (Souto et al., 2004b). In contrast, the AmB-NLC formulations containing GP with P407 gave shorter shelf-life of the drug than the corresponding AmB-SLN formulation. It was suggested that AmB was located in the interfacial region of the emulsion and was presented partly in the oil phase of the emulsion (Washinton et al., 1988). However, this was highly unlikely due to the strongly hydroxylic nature of the AmB molecule correlating with the TEM micrograph of AmB loaded NLC formulation which used P407 as stabilizer which showed the adherence of MCT droplet on the surface. This might be due to the influence of large molecules and the relative high HLB of P407; thus, drug repulsion to the outer phase could occur after the lipid recrystallization. The shelf-lives of most AmB loaded NLC formulations were lower in some formulations than those of AmB-SLN formulations. It was might be that MCT oil did not distribute within solid lipid as nanocompartment. Therefore, the drug might lead to interact with continuous compartment during the storage time.

Table 41 The AmB content as a function of time at 4°C of GB-NLC and GP-NLC formulations with various surfactants prepared by HPH method.

Formulations	AmB content (%)	Residual AmB (%)		
	0 month	1 month	2 months	3 months
AmB-GB-NLC1	88.18 ± 0.10	84.34 ± 0.32	80.10 ± 0.21	57.95 ± 0.19
AmB-GB-NLC2	92.22 ± 1.49	86.41 ± 0.81	81.68 ± 1.31	80.50 ± 0.11
AmB-GB-NLC3	85.97 ± 0.13	86.41 ± 0.89	80.61 ± 0.92	77.67 ± 0.65
AmB-GB-NLC4	80.26 ± 0.09	77.67 ± 0.61	70.94 ± 3.72	71.74 ± 0.33
AmB-GP-NLC1	75.06 ± 0.10	73.56 ± 0.95	69.58 ± 0.05	69.21 ± 0.89
AmB-GP-NLC2	76.26 ± 0.27	75.24 ± 0.43	69.26 ± 0.43	68.64 ± 0.51
AmB-GP-NLC3	80.41 ± 2.59	70.43 ± 1.05	66.71 ± 0.50	66.41 ± 0.27
AmB-GP-NLC4	72.59 ± 1.79	64.77 ± 1.60	54.46 ± 0.33	51.77 ± 0.10

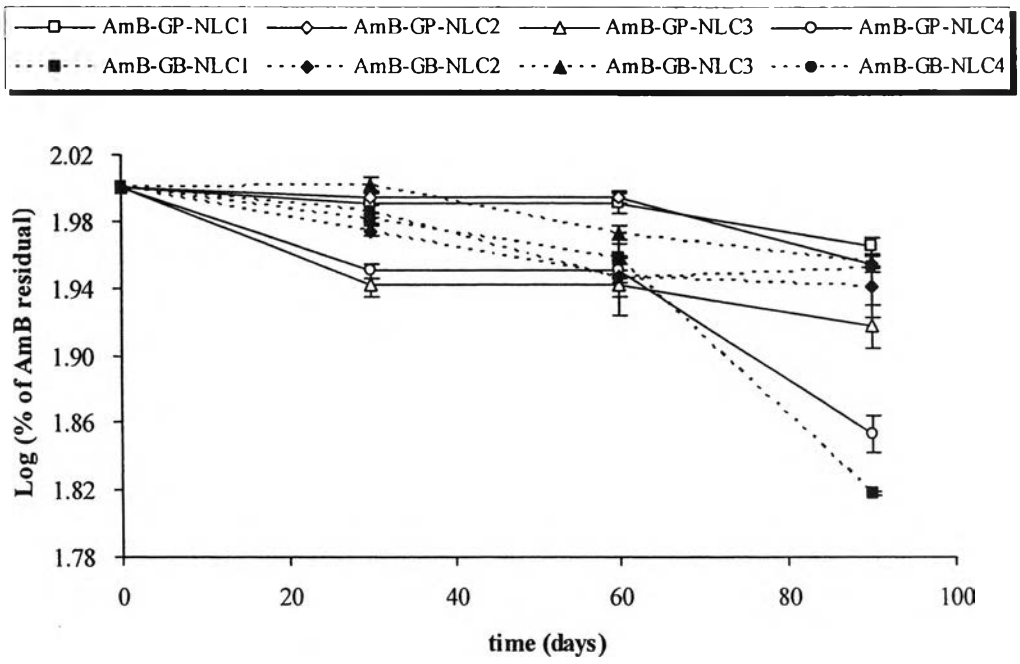

Figure 31 AmB residual content at 4°C in various GB-NLC and GP-NLC formulations prepared by HPH method as a function of time

Table 42 Predicted shelf lives at 4°C of AmB in GB-NLC and GP-NLC preparations prepared by HPH method

Formulations	K	t_{90} (days)
AmB-GB-NLC1	4.37×10^{-3}	24.02
AmB-GB-NLC2	1.56×10^{-3}	67.15
AmB-GB-NLC3	1.25×10^{-3}	84.12
AmB-GB-NLC4	1.43×10^{-2}	73.54
AmB-GP-NLC1	0.81×10^{-3}	129.16
AmB-GP-NLC2	1.05×10^{-3}	99.77
AmB-GP-NLC3	1.91×10^{-3}	55.00
AmB-GP-NLC4	3.38×10^{-3}	31.06

7. Effect of lecithin incorporated with AmB loaded SLN and NLC

Theoretically, AmB could be located either in the oily core of the emulsion droplets or at the interface. However, because AmB is not soluble either in soybean oil or in medium-chain fatty acids, it was assumed that it would be located in the phospholipids monolayer, as previously suggested by Washington et al (1988).

On preliminary study, aqueous dispersions of both GB and GP as solid lipid comprised of lecithin mixture were prepard by HPH method. Neither Epikuron® 200 nor Phospholipon® 90H (PL) could stabilize solid lipid nanoparticles resulting in semi-solid products after 2 hours upon cooling down to room temperature. Insufficient steric or electrostatic stabilization of phospholipon® 80 on the formation of GB-SLN had also been reported by Viriyaroj (2001).

Transformation of the lecithin stabilized SLN dispersions into semi-solid preparations was obviously retarded but not prevented. Gel formation was generally not observed with phospholipid stabilized tripalmitate dispersion stored at temperatures above the melting temperature of the triglyceride indicating that gel formation did not occur as long as the systems existed in the emulsion state. In general, the SLN dispersions could not be stored on this condition, particularly the drug, AmB was sensible to temperature. Another way to prevent gel formation of lecithin stabilized SLN dispersion was the subsequent adsorption of polyoxyethylene-polyoxypropylene block copolymers of poloxamer and poloxamine type (Westesen and Siekmann, 1997).

The particle size and size distribution of GP-SLN dispersions was less than and those of GB-SLN dispersion and showed the monomodal distribution. In addition, the particle sizes of GP-SLN formulations were significantly reduced while increased particle size was obtained from GB-SLN formulations after storage. Therefore, GP-SLN and GP-NLC were selected to study the effect of lecithin incorporation which designated AmB-SLN-L and AmB-NLC-L, respectively.

Physical appearance

The visual observations of AmB loaded SLN-L and NLC-L with various type of stabilizers are shown in Table 43. The AmB-SLN-L formulation consisted of 3% GP, 2% of various 2:1 surfactant:PL while the AmB-NLC-L consisted of the same composition but replacing 30% MCT oil to the total solid lipid. The abbreviations of AmB-SLN-L1 to AmB-SLN-L4 were AmB-SLN-L stabilized by Tw20, CreRH, P407 and M52, respectively. The AmB-NLC-L1 to AmB-NLC-L4 were designated the same as AmB-SLN-L formulations. AmB-SLN-L preparations

were yellowish colloidal dispersions which derived from the color of AmB and PL. AmB-NLC-L formulations displayed light yellowish colloidal dispersions due to the effect of oil incorporated. They could maintain the color without precipitation on storage for 3 months, except those stabilized by P407 and Tw20 which formed gel and precipitation, respectively after storage for 2 months. In contrast, all AmB-SLN-L formulation maintained the colloidal state during the time study. This might be possibly that some parts of oil in NLC-L formulations were localized on the surface of particles which subsequently tended to spontaneous gel formation and small molecules of Tw20 had insufficient steric stabilization in this system.

Table 43 The physical appearances of AmB loaded SLN-L and NLC-L formulations prepared by HPH method

Formulation	Macroscopic observation	
	a	b
AmB-SLN-L1	+	+
AmB-SLN-L2	+	+
AmB-SLN-L3	+	+
AmB-SLN-L4	+	+
AmB-NLC-L1	+*	P3M
AmB-NLC-L2	+*	+*
AmB-NLC-L3	+*	G2M
AmB-NLC-L4	+*	+*

a, b: initial and after storage at 4°C for 3 months; +, +*: yellowish colloidal dispersions, light yellowish colloidal dispersions; P3M, G2M: prepicitate appeared within 3 months, gel formation within 2 months

Particle size

The particle sizes of AmB-SLN-L and AmB-NLC-L using various surfactants are shown in Table 44. All AmB-SLN-L formulations had larger particle sizes than AmB-SLN due to the presence of phospholipid in the system. According to Heiati et al (1996), basically, phospholipid energetically favor the oil/water interface. Thus, to accommodate the additional phospholipid, additional interfacial area was produced, leading to smaller particle sizes. However when the radius of curvature reached a particular low value, the phospholipid may no longer energetically favor further decreases in particle size. At this point the phospholipid formed other structures,

possibly including multilayers. The phospholipid: triglyceride ratio in preparation greater than 0.15 which indicated of excess of phospholipid did not result in the formation of liposomes but formed multiple bilayer structures around the lipid core of the SLN. In this study, the ratio of phospholipid:triglyceride was 0.22; therefore, the excess phospholipid might be crucial factor on the increased particle size.

In contrast, AmB-NLC-L formulations showed smaller particles than their oil-free formulations indicating that the oil could be incorporated inside the particles except those stabilized by poloxamer formulation. The oil was possibly located on the surface of particles or distributed to the side chain of poloxamer which displayed larger particle size than oil-free formulations.

Table 44 Particle sizes of AmB loaded SLN-L and NLC-L formulations with various stabilizers prepared by HPH method

Formulation	Mean particle size by PCS (nm)	
	Z value ± SD	PI
AmB-SLN-L1	166.1 ± 5.2	0.335
AmB-SLN-L2	128.2 ± 0.3	0.382
AmB-SLN-L3	171.0 ± 3.2	0.325
AmB-SLN-L4	241.6 ± 4.3	0.333
AmB-NLC-L1	110.1 ± 0.7	0.323
AmB-NLC-L2	94.1 ± 0.9	0.303
AmB-NLC-L3	203.4 ± 6.4	0.294
AmB-NLC-L4	130.6 ± 4.4	0.305

pH , osmolality, and zeta potential

The pH, osmolality, and zeta potential of AmB-SLN-L and AmB-NLC-L formulations were examined and are shown in Table 45. The pH and osmolality values of these preparations were the same as of the AmB-SLN and AmB-NLC formulations which displayed optimum pH of 6-7 for chemical stability and obviously low in osmolality. In contrast, the presence of oil in the system obviously could reduce the zeta potential which promoted particle attraction and led to physical instability (Freitas et al., 1998).

Table 45 The pH, osmolality and zeta potential of AmB loaded SLN-L and NLC-L formulations with various stabilizers prepared by HPH method.

Formulation	pH	Osmolality (mosmol/kg)	Zeta potential (mV)
AmB-SLN-L1	6.88±0.02	11.3±0.6	-28.73
AmB-SLN-L2	6.87±0.02	8.7±0.6	-13.70
AmB-SLN-L3	7.00±0.01	9.0±0.0	-26.57
AmB-SLN-L4	7.22±0.02	7.7±1.2	-20.80
AmB-NLC-L1	6.94±0.02	11.0±0.0	-15.83
AmB-NLC-L2	6.99±0.02	7.3±0.6	-13.75
AmB-NLC-L3	6.69±0.02	5.3±0.6	-15.16
AmB-NLC-L4	7.12±0.01	6.3±0.6	-12.66

AmB content in SLN-L and NLC-L formulations

The AmB content in SLN-L and NLC-L formulations using various surfactants determined by HPLC are shown in Figure 32. Under the same process condition, the initial drug content of SLN-L formulations exhibited slightly lower than those of NLC-L formulations at the ranges of 76.32%-89.06% and 83.60%-92.21%, respectively. Incorporation of oil in the system did not change the drug content when compared to the corresponding SLN-L formulations.

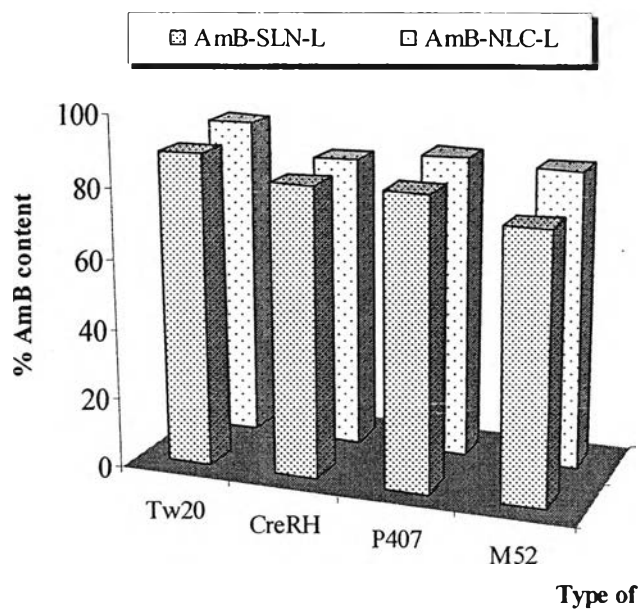

Figure 32 The percentage of AmB content in various SLN-L and NLC-L formulations prepared by HPH method

Entrapment efficiency of AmB-SLN-L and NLC-L formulations

The entrapment efficiencies of AmB-SLN-L and AmB-NLC-L formulations are shown in Table 46. The application of lecithin in the SLN dispersions could increase the drug incorporation into the particles. This finding agreed with a previous investigation by Wang et al (2002). They characterized the loading capacity of 3',5'-dioctanoyl-5-fluoro-2'-deoxyuridine SLN dispersion containing glyceryl tristearate, Pluronic F-68, and lecithin. Satisfactorily high entrapment efficiency of 95-97% was found. Nevertheless, adding oil into the system showed less degree in entrapment. The nanoparticles dispersions stabilized by P407 displayed the lowest value (44.50%) possibly due to the localization of the drug between oil and lecithin formed mixed micelle or liposome which expelled to the aqueous phase and was unable to be detected in the lipid pellet after ultracentrifugation.

Table 46 Entrapment efficiency of AmB in various SLN-L and NLC-L dispersions prepared by HPH method

Formulation	Percentage drug entrapment (Mean ± SD)
AmB-SLN-L1	98.81 ± 0.42
AmB-SLN-L2	93.76 ± 0.62
AmB-SLN-L3	81.17 ± 0.36
AmB-SLN-L4	90.40 ± 1.28
AmB-NLC-L1	89.19 ± 0.75
AmB-NLC-L2	95.58 ± 0.82
AmB-NLC-L3	44.50 ± 0.67
AmB-NLC-L4	82.39 ± 0.23

Morphology of AmB loaded SLN-L and NLC-L

Figure 33A and 33B show TEM micrographs of SLN-L and NLC-L containing 1% AmB and P407 as stabilizer, respectively. TEM examination of SLN-L formulation revealed the existence of irregular shapes. They appeared rod or spherical shapes with the particle size approximately 150-200 nm which was in agreement with the particle size obtained by PCS measurement. Within the particles, tiny particles of lecithin were observed. Although phospholipids was incorporated intended to be

between the lipid and liquid interface. Due to lecithin leakage during SLN preparation, some could form lamellar interfaces indicating liposome formation as well as the formation of spherical bilayers surrounding a triglyceride core (Schubert and Müller-Goymann, 2005). The occurrence of small unilamellar vesicles representing the excess of phospholipids in the system exhibited a high electron density resulting in a high contrast against the aqueous phase has been reported by Westesen and Siekmann (1997).

The TEM micrograph of NLC-L containing 1% AmB shows irregular shape with no definite edge whereas that from corresponding SLN-L showed lecithin in the lipid particles with the coexistence of other lipid structures. The oil droplets were predominantly shown on the surface of particles and formed spots or even incomplete films which sticked on the particle surface. The difference in the structures of these formulations might affect the entrapment efficiency, *in vitro* release and also chemical stability.

Cryo-SEM micrographs of AmB-SLN-L and AmB-NLC-L containing P407 as stabilizer are shown in Figure 34. The particle sizes of both cases were in the range of 100-200 nm with broad size distribution due to the co-existence of additional colloidal structures such as mix-micelles, liposomes etc. However, AmB-SLN-L and AmB-NLC-L images could not be differentiated under this technique.

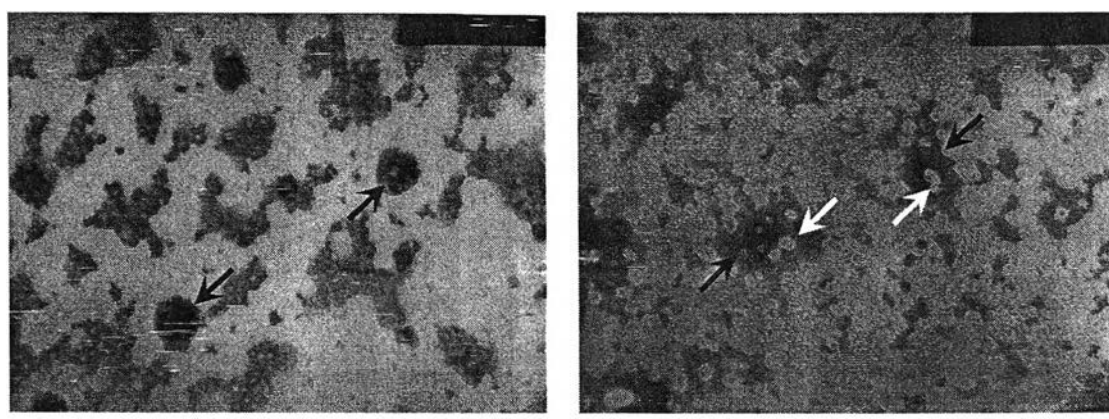

A B

Figure 33 The TEM micrographs of AmB-SLN-L (A) and AmB-NLC-L (B) formulation stabilized by P407 prepared by HPH method; black arrow: phospholipid; white arrow: oil spots

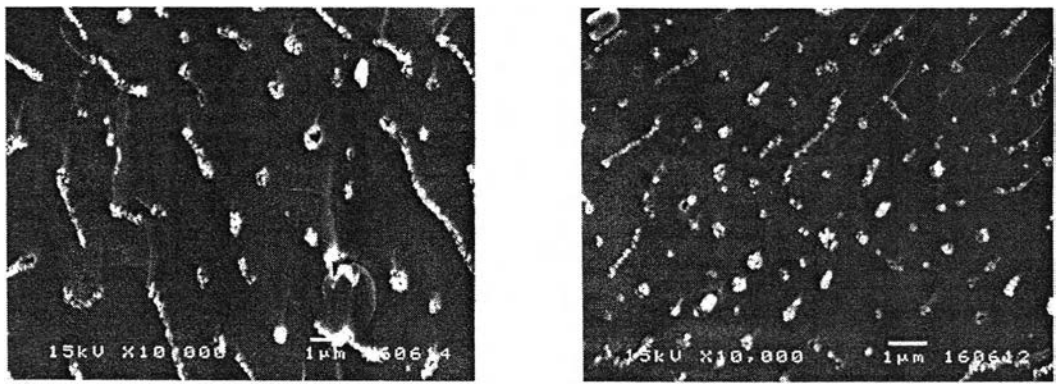

(A) (B)

Figure 34 The Cryo-SEM micrographs of AmB-SLN-L (A) and AmB-NLC-L (B) formulations stabilized by P407 prepared by HPH method

Physical stability of AmB-SLN-L and AmB-NLC-L formulations

The particle sizes of AmB-SLN-L and AmB-NLC-L at initial and after storage for 3 months are shown in Table 47. The results showed the particle size slightly decreased after storage. However, not all formulations could be stable for 3 months. AmB-NLC-L containing Tw20 showed sedimentation and the particle size could not be measured under PCS technique. The result from macroscopic observations revealed that AmB-NLC-L stabilized by P407 had physical instability with particle size growth after storage ($p<0.05$). The possible mechanism of the particle growth was due to the gel formation which leading to zeta potential reduction. Large lipid particles could approach each other due to the loss of electrostatic repulsion and formed a network. The reduction in zeta potential indicated the structural changes. Therefore further investigations concerning especially the structural properties of the lipid phase were performed to confirm the suggested mechanism of gel formation (Freitas et al., 1998).

Table 47 Particle sizes of AmB loaded SLN-L and NLC-L formulations at initial and 3 months storage

Formulations	Particle size of various preparations on 4°C storage			
	Initial		3 months	
	Mean particle size (nm)		Mean particle size (nm)	
	Z value	PI	Z value	PI
AmB-SLN-L1	166.1 + 5.2	0.335	150.2 + 2.0	0.291
AmB-SLN-L2	128.2 ± 0.3	0.382	107.4 ± 0.9	0.311
AmB-SLN-L3	171.0 ± 3.2	0.325	119.8 ± 0.8	0.223
AmB-SLN-L4	241.6 ± 4.3	0.333	216.1 ± 4.3	0.443
AmB-NLC-L1	110.1 ± 0.7	0.323	ND	ND
AmB-NLC-L2	94.1 ± 0.9	0.303	87.6 ± 0.7	0.245
AmB-NLC-L3	203.4 ± 6.4	0.294	702.2 ± 25.8	0.157
AmB-NLC-L4	130.6 ± 4.4	0.305	128.9 ± 2.8	0.289

Chemical stability of AmB-SLN-L and AmB-NLC-L formulations

The chemical stability of AmB-SLN-L and AmB-NLC-L formulations are shown in Tables 48-49 and Figure 35. Again, the drug content of both AmB-SLN-L and AmB-NLC-L formulations containing M52 were declined rapidly especially the latter formulation. About 40.61% and 5.17% of AmB were could be detected when the dispersions were stored for 3 months. It could be clearly concluded that M52 was inappropriate to stabilize the drug from degradation. With regarding to the data of shelf-life and the drug content after storage for 3 months of AmB-SLN-L formulation, the ranking order of stability was AmB-SLN-L1> AmB-SLN-L2> AmB-SLN-L3> AmB-SLN-L4. Similar rank order was also shown in the AmB-NLC-L formulations.

However, both AmB-SLN-L and AmB-NLC-L formulations exhibited shorter shelf-life than AmB-SLN and AmB-NLC formulations. Comparison among formulations stabilized by P407, the maximum shelf-life of AmB-SLN formulation was 6 months whereas NLC formulation had the shelf-life below 2 months. Furthermore, the shelf-lives of AmB-SLN-L and AmB-NLC-L were less than 1 month. This meant the phospholipid or phospholipid with oil incorporated could not protect the drug degragation despite the drug prefered to intercalate or form complex with lecithin. This was possibly due to the distribution of drug in lecithin which was deposited on the surface of particles. Thus, the drug closely contacted to the

environment leading to drug decomposition. And, also another data derived from the morphology by TEM and the entrapment efficiency explained the formation of liposome or mixed micelles. These structures were in the liquid state in which the drug activity would loss faster than in the solid matrix; especially, the presence of both phospholipid and oil in the AmB-NLC-L formulation.

Table 48 The AmB content as a function of time at 4°C of SLN-L and NLC-L formulations prepared by HPH method

Formulations	AmB content (%)	Residual AmB (%)		
	0 month	1 month	2 months	3 months
AmB-SLN-L1	89.06 ± 0.24	89.69 ± 0.27	89.42 ± 1.45	87.02 ± 1.77
AmB-SLN-L2	82.70 ± 0.27	83.58 ± 0.62	79.17 ± 1.55	78.84 ± 0.89
AmB-SLN-L3	83.06 ± 0.79	73.79 ± 0.34	60.37 ± 4.02	57.50 ± 2.52
AmB-SLN-L4	76.32 ± 1.26	60.67 ± 0.52	50.29 ± 0.66	40.61 ± 0.17
AmB-NLC-L1	92.21 ± 0.64	91.41 ± 0.82	89.22 ± 2.03	82.80 ± 0.60
AmB-NLC-L2	83.60 ± 0.20	85.89 ± 0.77	81.59 ± 0.87	71.63 ± 3.18
AmB-NLC-L3	86.50 ± 0.09	87.65 ± 0.80	70.96 ± 0.90	68.78 ± 0.43
AmB-NLC-L4	84.96 ± 0.12	33.44 ± 0.02	11.68 ± 0.11	5.17 ± 0.43

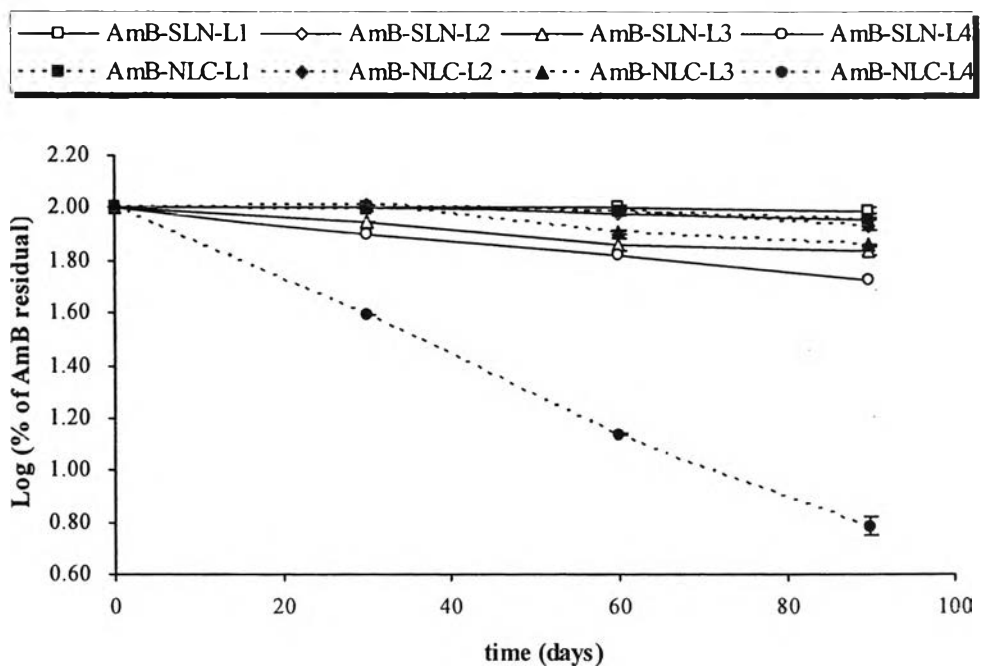

Figure 35 AmB residual content at 4°C in various SLN-L and NLC-L formulations as a function of time

Table 49 Predicted shelf lives at 4°C of AmB in SLN-L and NLC-L formulations with various surfactants prepared by HPH method

Formulations	K	t_{90} (days)
AmB-SLN-L1	Θ	Θ
AmB-SLN-L2	1.18×10^{-3}	89.05
AmB-SLN-L3	4.35×10^{-3}	24.15
AmB-SLN-L4	6.94×10^{-3}	15.14
AmB-NLC-L1	1.16×10^{-3}	90.64
AmB-NLC-L2	1.72×10^{-3}	61.17
AmB-NLC-L3	3.98×10^{-3}	26.40
AmB-NLC-L4	3.15×10^{-2}	3.33

Θ: Could not be calculated

8. Physical evaluations of various formulations

8.1 Fourier Transform infrared Spectroscopy

FT-IR analysis was used to ensure that no chemical interactions between the drug and the ingredients in the preparations. The infrared of spectra of GP, CreRH, AmB and solid lipid pellet prepared by ultracentrifugation at 60,000 rpm, 4°C for 6 hours of three SLN formulations of WME1, WME2 and WME3 which were represented SLN formulations containing CreRH with either Gly, PG and PEG, respectively are shown in Figure 36.

The principal peaks of GP were observed at the wavenumbers of 3440, 2919, 2851, 1739, 1471, 1181, 722 cm^{-1}. The peak at 3440 cm^{-1} was O-H stretching. The sharp peaks at 2919 cm^{-1} and 2851 cm^{-1} were CH_2 symmetric and CH_2 asymmetric of aliphatic C-H stretching, respectively. The distinguished peak at 1739 cm^{-1} was the C=O stretching. The peaks of 1471 and 722 cm^{-1} were CH_2 bending and CH_2 rocking, respectively. The peak of 1181 cm^{-1} was C-O stretching (Bugay and Findlay, 1999).

The infrared spectrum of CreRH had shown the board peak at 3452 cm^{-1}, the strong peaks at 3452, 2925, 2861, 1734, 1463, 1110 $cm^{-1}$and also a small peak at 724 cm^{-1}. The peak at 3452 cm^{-1} was O-H stretching. The sharp peaks at 2925 cm^{-1} and

2861 cm^{-1} were CH_2 symmetric and CH_2 asymmetric of aliphatic C-H stretching, respectively. The distinguished peak at 1734 cm^{-1} was the C=O stretching. The peaks of 1463 and 724 cm^{-1} were CH_2 bending and CH_2 rocking, respectively. The sharp peak of O-C-O stretching was at 1110 cm^{-1}.

The infrared spectrum of AmB had no bands of high intensity. It was characterized by a sharp C=O stretching band at 1695 cm^{-1}, C=C stretching band at 1562 cm^{-1} and a poorly resolved substructure at 800-950 cm^{-1} which was similar to previous reports (Schwartzman et al., 1978; Espuelas et al., 1997)).

It was found that the infrared spectra of WME1, WME2 and WME3 which using CreRH as surfactant with either Gly, PG or PEG as co-surfactant did not display any change or appearance of new bands. This seemed to indicate the absence of chemical interaction among solid lipid, stabilizer and the drug in AmB-SLN preparations. These spectra did not show the characteristic bands of the drug because of its low intensity and they were hidden by the bands produced by the solid lipid and stabilizer.

Figure 37 exhibits the intact materials and solid lipid pellet of AmB-SLN and AmB-NLC formulations prepared by using P407 as stabilizer. The IR spectrum of P407 showed the sharp peak of O-C-O stretching at 1112 cm^{-1} and the CH_2 symmetric stretching at 2890 cm^{-1}. In addition, the small peaks at 1244 cm^{-1}-1470 cm^{-1} displayed CH_2 bending vibrations. The IR spectrum of SLN dispersions containing 1% AmB, 3% GP and 2% P407 showed the peak of both GP and P407. The sharp peaks at 2918, 2851, 1737, 1471, 1106, and 719 cm^{-1} were observed from the combination of both spectra. No new peak was detected from its mixture.

For MCT oil, the IR spectrum exhibited the principle peaks similar to the pattern from GP. They was observed at the wavenumber of 2928, 2857, 1745, 1463, 1160 and 725 cm^{-1} while the IR spectrum of AmB-NLC showed the basic peaks similar to intact GP which was the majority of the formulation. The sharp peaks corresponding to those of GP were 2918, 2852, 1740, 1471 and 719 cm^{-1}. And also, it was accordance with the peaks of P407 which were the sharp peak at 1114 cm^{-1} and

the small peaks at 964, and 844 cm^{-1}. This indicated that there was no interaction between the GP, drug and other components in both formulations.

Figure 38 showed the spectra of pure components used in formulations and lipid matrices of AmB-SLN-L and AmB-NLC-L. The IR spectrum of PL showed peaks of 3383, 2924, 2854, 1736, 1464, 1238, 1089, and 721 cm^{-1}. The peak at 3383 cm^{-1} was O-H stretching. The sharp peaks at 2924 cm^{-1} and 2854 cm^{-1} were CH_2 symmetric and CH_2 asymmetric of aliphatic C-H stretching, respectively. The distinguished peak at 1736 cm^{-1} was the C=O stretching. The peaks of 1464 and 721 cm^{-1} were CH_2 bending and CH_2 rocking, respectively. The sharp peak of P=O stretching was at 1238 cm^{-1} (Pretsch et al., 2000) and the peak of 1089 cm^{-1} was the C-N stretching. The infrared spectrum of AmB-SLN-L showed spectra corresponding to the superimposition of their parent substances. The sharp peaks were at 2918, 2851, 1737, 1471, 1107, 719 cm^{-1}. In case of AmB-NLC-L which consisted of the materials as AmB-SLN-L but replacing 30% MCT oil to the solid lipid, the spectrum displayed the peaks at 2918, 2851, 1737, 1471 and 1095 cm^{-1} observed from the combination of its components. No new peak was detected from its ingredients. The data indicated that no strong interaction among the compositions. It was assumed that there was no incompatibility occurred in all formulations.

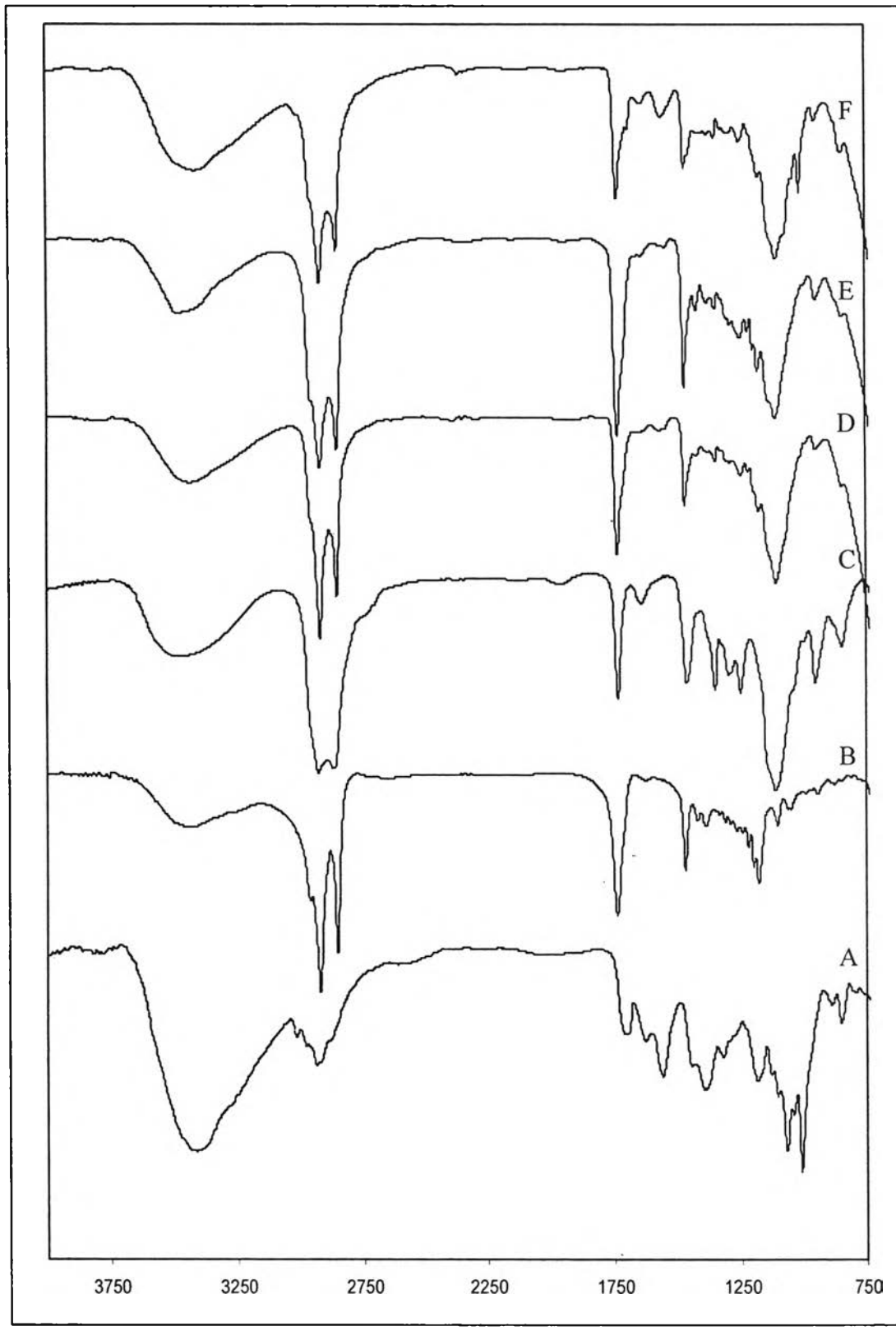

Figure 36 IR spectra of AmB(A); GP(B); CreRH (C);and lipid pellets of preparations AmB-WME1 (D); AmB-WME2 (E); AmB-WME3 (F)

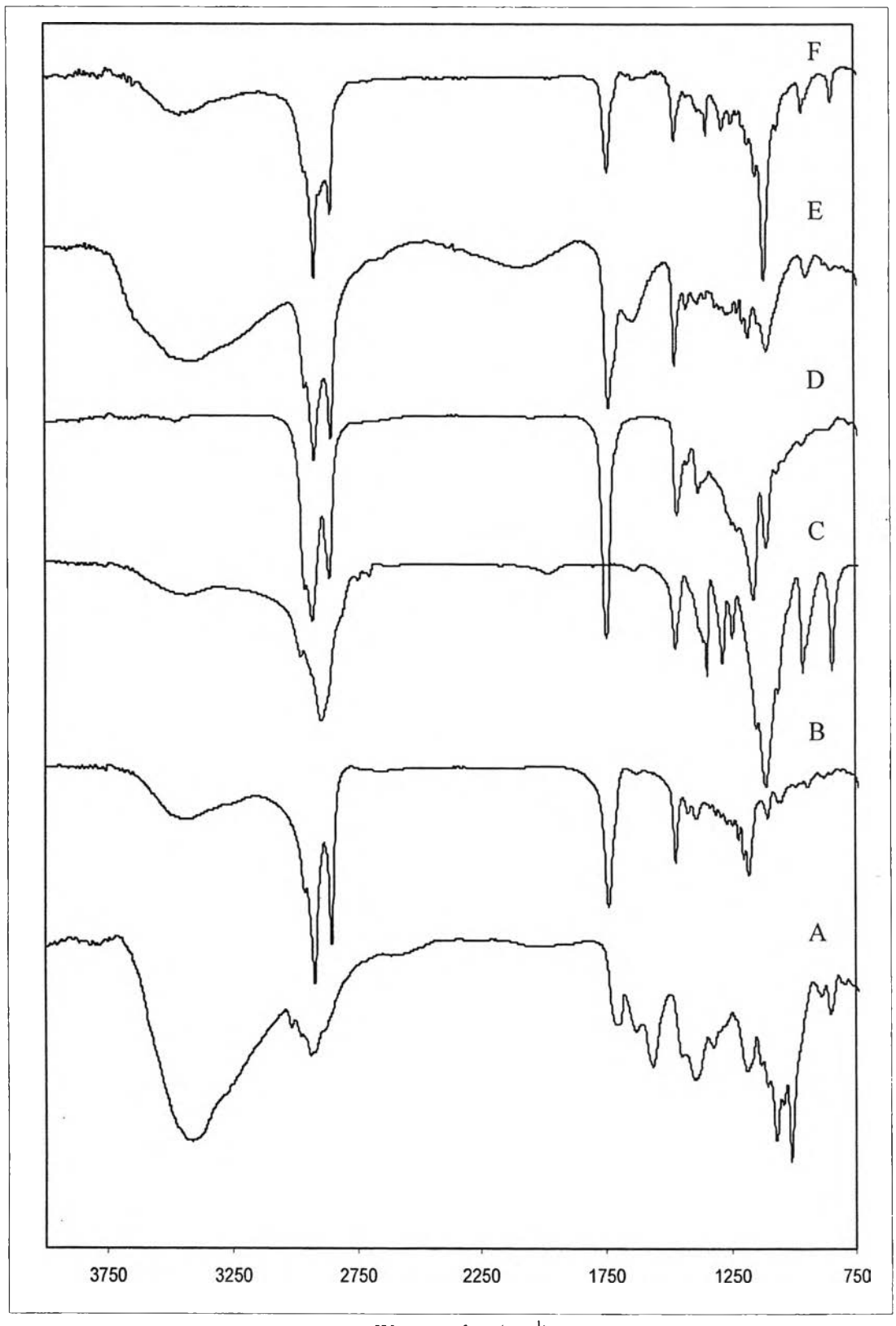

Figure 37 IR spectra of AmB(A); GP (B); P407(C); MCT oil(D) and lipid pellets of preparations AmB-SLN (E); AmB-NLC (F) stabilized by P407.

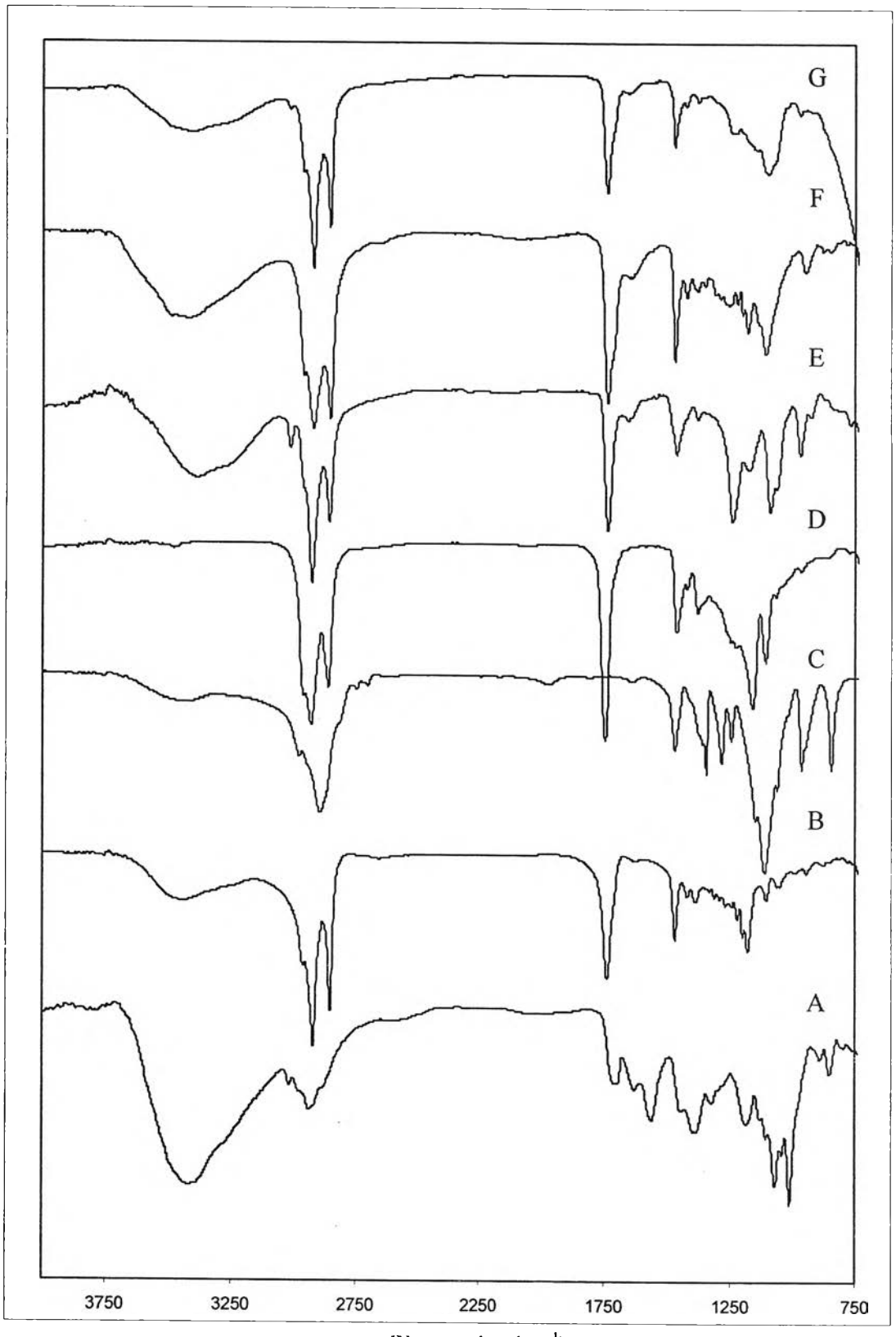

Figure 38 IR spectra of AmB(A); GP(B); P407(C); MCT oil(D); PL(E) and lipid pellets of preparations AmB-SLN-L (F); AmB-NLC-L (G) stabilized by P407.

8.2 Thermal analysis

8.2.1 Differential Scanning Calorimetry

DSC gives an insight into the melting and recrystallization behavior of crystalline material like lipid nanoparticles. The break down of the crystal lacttice by heating the sample yields inside information on, e.g. polymorphism, crystal ordering, eutectic mixtures or glass transition processes. DSC experiments are useful to understand solid dispersions like solid solutions, simple eutectic mixtures or, as in this case drug and lipid interactions and mixture behaviour of GP/GB and medium chain triglyceride.

Recrystallization of the melted lipid does not take place immediately after production. The recrystallization speed after high pressure homogenization is a function of SLN size, nature (melting point) and concentration of lipid and surfactant. A large difference between melting point and room temperature seems to promote recrystallization, which take place within minutes or hours (Müller et al., 1995).

The DSC thermograms of GB, GP, P407 and AmB are displayed in Figure 39. The thermogram of GB showed endothermic peaks at 73.49°C which began from 70.34°C to 76.88°C while the thermogram of GP exhibited the melting range 51.13°C -62.57°C with the melting peak at 58.33°C. The thermogram of P407 showed endotherm between 54.27°C and 60.46°C which had the peak at 56.83°C whereas the thermogram of AmB displayed an endothermic transition which began around 137°C with the maximum slope near 205°C which was corresponding to the investigation of Espuelas et al (1997).

The samples prepared by lyophilization of SLN containing 3% GB, 2% P407 with or without 1% of drug are displayed in Figure 40. The GB thermograms of drug-free and 1% loaded lyophilized SLN showed the melting peaks at 72.36°C and 73.44°C, respectively. The melting peak of GB from drug-free SLN was lower than that of intact material whereas that from the drug loaded was sightly increased. From

the data, it was indicated that the depression of drug-free GB-SLN was due to the size of paricles and its composition.

To study the effect of oil adding to the SLN formulations, the DSC thermograms of drug-free and drug loaded NLC containing 30% of MCT oil incorporated to GB-SLN were also investigated as depicted to Figure 40. Both drug-free and drug loaded GB-NLC formulations displayed the melting peaks of lipid at 68.22°C and 69.78°C, respectively which were lower than those of GB-SLN formulations. The broadening of the heating peak and the reduction of the melting point indicated an increased number of lattice defects (Westesen et al., 1993). In addition, Jores et al (2003) presented the nearly linear of decreasing in GB melting point with the increasing medium-chain triglyceride loaded NLC (from 0-75%) which meant an interaction of oily molecules with the crystalline matrix.

Similarly, the drug-free and drug loaded SLN and NLC formulations which using GP as solid lipid showed the melting peak of lipid at 57.64°C, 58.14°C and 54.00°C, 54.37°C, respectively (Figure 41 and Table 50). As expected, the preparation process and the presence of drug in the formulation could disturb the thermal characteristics of lipid as previously described. Comparing to the formulation of GB, the melting range of GP-SLN and GP-NLC was significantly broader than those of GB-SLN and GB-NLC. This was due to the longer fatty acid chains and/or higher melting range of glycerides which was less sensitive to such physical modifications (Sutannanta et al., 1995). The results were also in accordance to the research of Hamdani et al (2003). In addition, the melting range of P407 was 54.27°C -60.46°C which overlapped to the melting range of GP.

The increasing melting range could be correlated with the impurities or less ordered crystals which could be characterized by the melting enthalpy. For the less ordered crystal or amorphous state, the melt of the substance did not require or just required less energy than perfect crystalline material which needed to overcome lattice force. From the data, the melting enthalpies of intact GB and its SLN were 162.15 and 80.91 J/g while the melting enthalpies of the physical mixture of GP and poloxamer and the bulk mixture turned into SLN were 155.48 and 132.25 J/g,

respectively. It was concluded that the lipid within nanoparticles was in a less ordered arrangement compared to the bulk material corresponding to the DSC analysis (Hou et al., 2003).

The effect of phospholipids incorporated to the following preparations: SLN-L and NLC-L formulations could be seen from the thermograms of drug-free and drug loaded SLN-L and NLC-L formulations as shown in Figure 42. The melting peaks of GP in SLN-L and NLC-L were lower than those in SLN and NLC, respectively. It was likely that the incorporation of phospholipid reduced the melting point of lipid by disturbing the crytal lacttice of glycerides. Indeed, in case of NLC-L formulation, the influence of combination of phospholipid and oil had shown a strong effect on the thermal behaviour.

Table 50 Thermal behaviours of intact materials, drug-free and drug-loaded in various formulations stabilized by P407

Compounds or Formulations	Melting temperature range (°C)		Melting temperature (°C)	
	1st peak	2nd peak	1st peak	2nd peak
GB	70.34-76.88	-	73.49	-
GP	51.13-62.57	-	58.33	-
P407	54.27-60.46	-	56.83	-
AmB	115.20-148.95	189.82-222.42	137.96	205.86
PL	47.92-58.78	232.63-239.49	54.94	235.45
GB-SLN	70.70-73.70	-	72.36	-
1%AmB-GB-SLN	69.97-75.01	-	73.44	-
GB-NLC	65.57-70.27	-	68.22	-
1%AmB-GB-NLC	66.28-72.30	-	69.78	-
GP-SLN	48.41-59.49	-	57.64	-
1%AmB-GP-SLN	48.50-60.58	-	58.14	-
GP-NLC	50.98-59.14	-	54.00	-
1%AmB-GP-NLC	49.39-56.28	-	54.37	-
SLN-L	47.54-58.21	-	55.28	-
1%AmB-SLN-L	43.05-58.13	-	55.64	-
NLC-L	45.57-55.01	-	50.54	-
1%AmB-NLC-L	47.28-54.19	-	51.72	-

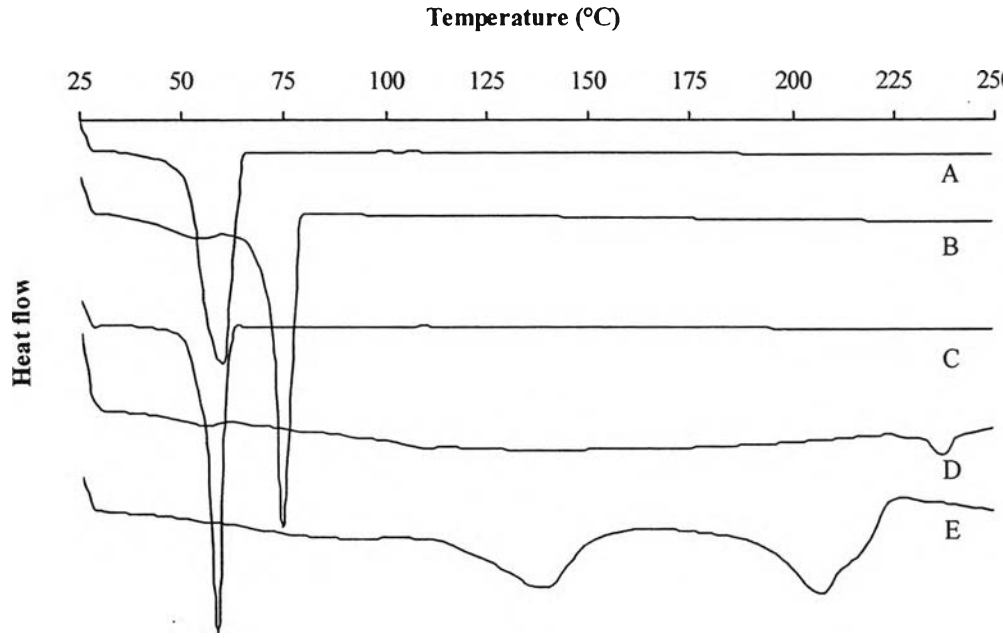

Figure 39 DSC thermograms of GP (A); GB (B); P407 (C); PL (D); and AmB (E)

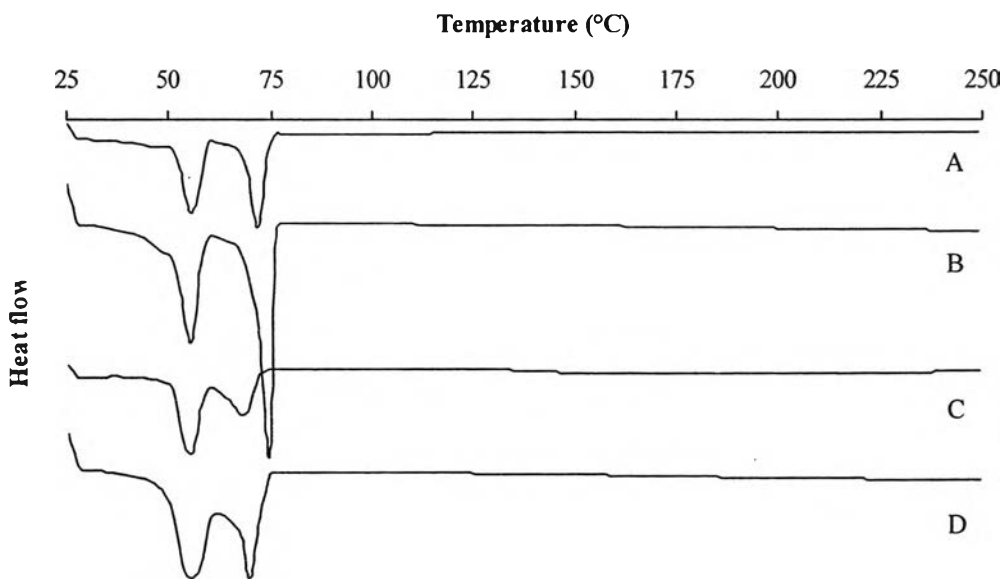

Figure 40 DSC thermograms of lipid matrices of preparations containing drug-free GB-SLN (A); 1%AmB loaded GB-SLN (B); drug-free GB-NLC (C); and 1%AmB loaded GB-NLC (D).

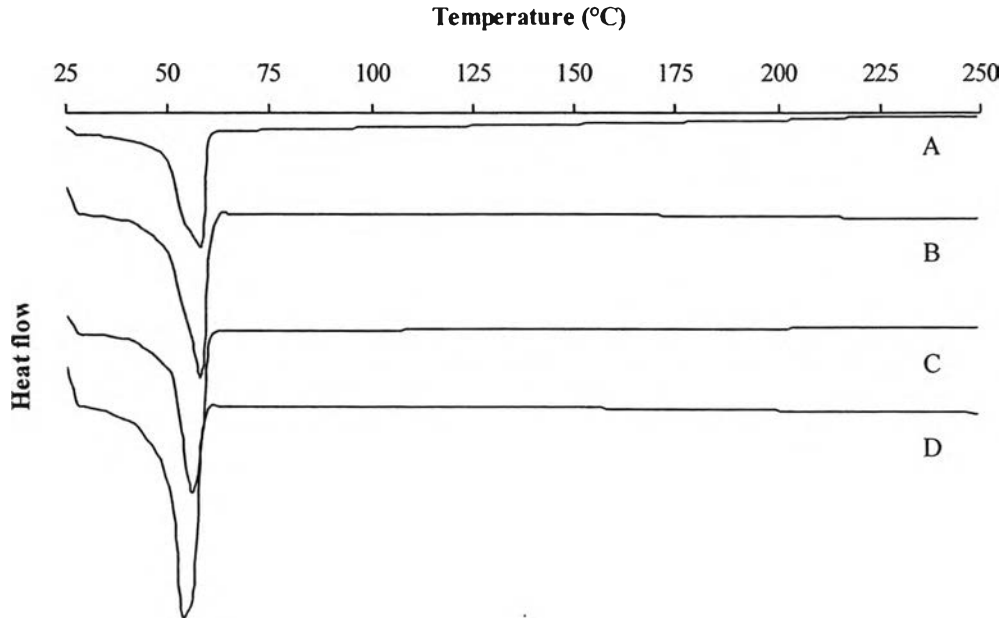

Figure 41 DSC thermograms of lipid matrices of preparations containing drug-free GP-SLN (A); 1%AmB loaded GP-SLN (B); drug-free GP-NLC (C); and 1%AmB loaded GP-NLC (D)

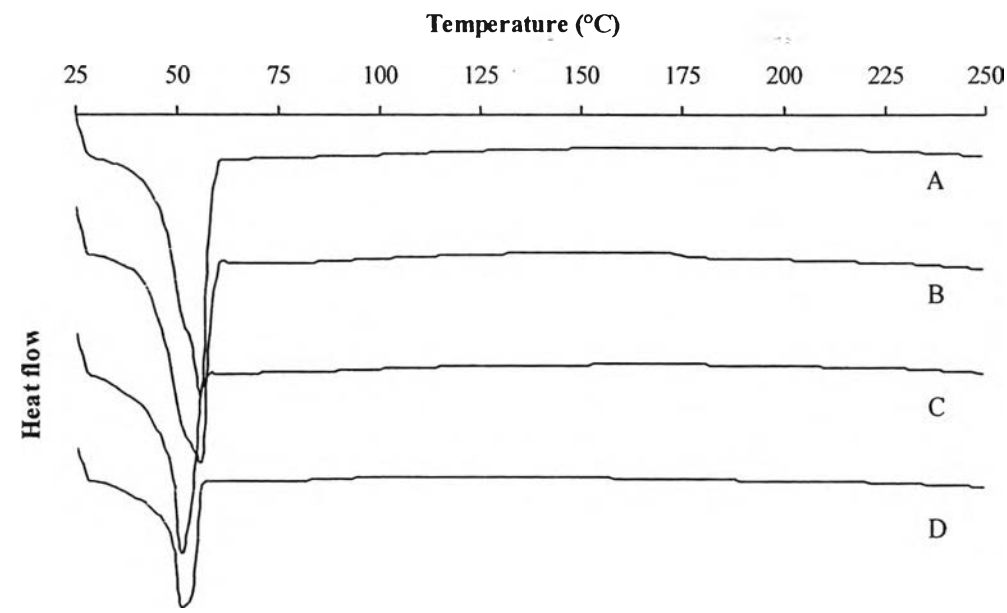

Figure 42 DSC thermograms of lipid matrices of preparations containing drug-free GP-SLN-L (A); 1%AmB loaded GP-SLN-L (B); drug-free GP-NLC-L (C); and 1%AmB loaded GP-NLC-L (D).

8.2.2 Hot stage microscopy

HSM technique is to understand the nature of the different physical events observed. This semi-quantitative method involves heating a sample on a hot stage and simultaneously observing the material under microscope.

Figure 43A and 44A show the HSM microphotographs obtained from SLN containing 1% AmB using GB or GP as solid lipid with the gradual melting ranges of these preparations were 70°C-74°C, 53°C-59°C, respectively. The HSM microphotographs observations correlated to the DSC results (Figure 40 and 41) which showed a narrower melting range for GB than GP. With regarding to the technique, DSC results showed the broader melting range of both GB and GP than HSM data. This indicated that DSC technique in which a property of the analyte was determined as a function of an externally applied temperature. At the melting point, all heat introduced into the system was used to convert the solid phase into the liquid phase, and no increase in system temperature could take place as long as solid and liquid remained in equilibrium with each other. In the equilibrium condition, the system effectively exhibited an infinite heat capacity. Thus, measurement of melting curves could be used to obtain very accurate evaluations of the melting point of a compound when slow heating rates were used. However, the phase transition could not be visually monitoring. Therefore, HSM method was most appropriate to perform in combination with DSC. HSM technique could be used to present both unmelted material and the totally melt one by visual observations.

The microphotographs of NLC containing GB and GP with the 30% MCT oil calculated by total solid lipid added are shown in Figure 43B and 44B, respectively. The melting ranges of these preparations from HSM were 66°C-71°C, 51°C-57°C, respectively. The melting point of both samples were lower than the unmodified ones which described in term of liquid oil adding into the system as shown in the DSC investigations.

The effect of phospholipids incorporated in SLN and NLC preparations on thermal characteristic was determined by observing AmB-SLN-L and AmB-NLC-L

under hot stage microscope as shown in Figure 44C and 44D, respectively. The melting ranges of these preparations from HSM were 53°C-58°C, 49°C-54°C, respectively. It could be seen that their melting ranges were lower than AmB-SLN and AmB-NLC preparations, respectively. The results were similar to the DSC result. Thus, it was concluded and confirmed that phospholipids could disturb the cystallinity of solid lipid as resulted in the lower melting point.

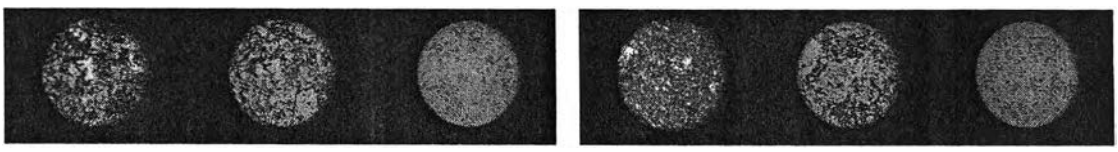

I (70°C) II (72°C) III (74°C) I (66°C) II (68°C) III (71°C)

A B

Figure 43 HSM microphotographs of (I)unmelt GB; (II)melting GB to (III)totally melt GB (magnification 40x) obtained from lyophilized 1%AmB-SLN (A), 1%AmB-NLC (B).

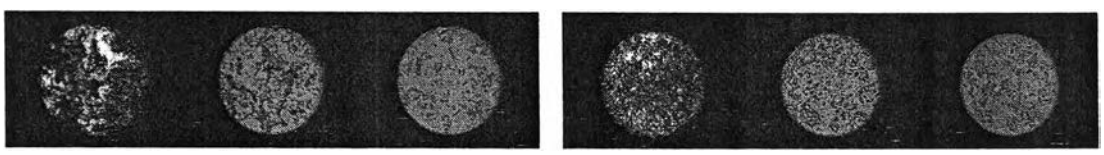

I (53°C) II (57°C) III (59°C) I (51°C) II (53°C) III (57°C)

A B

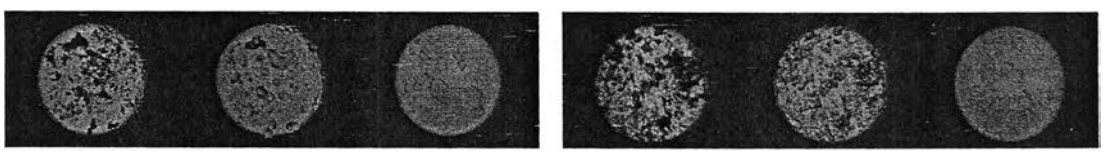

I (53°C) II (55°C) III (58°C) I (49°C) II (52°C) III (54°C)

C D

Figure 44 HSM microphotographs of (I)unmelt GP; (II)melting GP to (III)totally melt GP (magnification 40x) obtained from lyophilized 1%AmB-SLN3 (A), 1%AmB-NLC3 (B), 1%AmB-SLN3-L (C) and 1%AmB-NLC3-L (D).

8.3 Powder X-ray Diffractometry

Solids may be either crystalline or noncrystalline. The crystalline state is characterized by a perfectly ordered lattice, and the noncystalline (amorphous) state is characterized by a disordered lattice. These represent two extremes of lattice order, and intermediate states are possible. The term degree of cystallinity is useful in attempts to quantify these intermediate states of lattice order.

X-ray powder diffractometry is widely used to determine the degree of crystallinity of pharmaceuticals. X-ray diffractometric methods were originally developed for determining the degree of cystallinity of polymers. Many polymer exhibit properties associated with both crystalline (e.g., evolution of latent heat on cooling from the melt) and noncrystalline (e.g., diffuse x-ray pattern) materials (Suryanarayanan, 1995).

The X-ray diffractogram of AmB, GP, PL and P407 are shown in Figure 45a. GP was crystalline and showed the characteristic peaks at 19.40°, 21.28°, 23.36°, and small peak at 5.60° which were in accordance with the investigation by Hamdani et al. (2003). In addition, they examined the X-ray diffraction patterns obtained from different GP samples. It was observed that there was no superimposition between X-ray results obtained from the freshly solidified and aged samples. P407 displayed two high peaks at 19.08° and 23.20° whereas AmB had strong peaks at 13.88° and 21.52°.

Figure 45b shows the X-ray diffractogram of SLN, NLC, SLN-L and NLC-L formulations containing 1% AmB. The diffractogram of AmB-SLN prepared from lyophilization of SLN showed the characteristic similarly to the diffractogram of GP sharp peaks at 19.04° and 23.28°, intermediate peak at 21.24° and small peak at 5.40°; hence, the crystallinity of the preparation was not changed. However they displayed weaker diffractogram intensity than pure GP. Nevertheless, the intensities of those sharp peaks were higher than that of each component due to the reinforcement of each other. No new diffractogram pattern was detected from the mixture. The characteristic peak of AmB at 13.88° was disappeared that the drug might disperse in amorphous form.

The X-ray diffractograms of AmB-NLC had the characteristic peaks at 19.00°, 23.24° and small peak at 5.64° and 21.12°. The peak of AmB at 21.52° was superimposed to the peak of NLC while the distinguished peak of AmB at 13.88° was not found. This result was corresponded to that from the AmB-SLN. MCT oil had no effect on the diffractogram; therefore, the lipid crystal structure in X-ray measurements did not seem to be disturbed by the addition of oil (Jores et al, 2003). However, in comparison with the diffractogram of AmB-SLN, the peak intensity at 21.12° obtained from AmB-NLC was lower than that of AmB-SLN indicating the decrease in crysallinity of lipid by the addition of oil. It was assumed that the drug in NLC may disperse in molecular level or amorphous form more than in SLN. Thus, MCT oil not only improved the solubility of drug but also avoided the crystallization. The lower lipid crystallinity in NLC formulation was in agreement with the obtained DSC data. These X-ray crystallization studies confirmed that transition rates of liquid oils are lower than those of solid lipids due to the more ordered structure of the latter (Souto et al., 2004a).

The diffractogram of AmB-SLN-L formulation had the same the characteristic peaks as GP combined with P407 whereas the diffractogram of characteristic peaks of PL at 6.28°, 8.04°, 16.24°, 19.52° and 21.20° were not shown. This investigation was agreed with the report of Friedrich and Müller-Goymann (2003) who showed no additional interferences with the adding of Phospholipon®90 concentrations up to 50% in hard fat mixtures indicating a dissolution of the lecithin.

For NLC-L preparation, the diffractogram pattern displayed the strongly characteristic peaks at 19.20° and 23.16°, and also a small peak at 5.60°similarly to that of AmB-NLC. However the peak of GP at 21.28° was not found thus some lipid structure might be changed. For AmB, the peak at 21.52° might be reinforced by strong peak of GP whereas the disappearance of peak at 13.88° might due to the drug dispersed in molecular level.

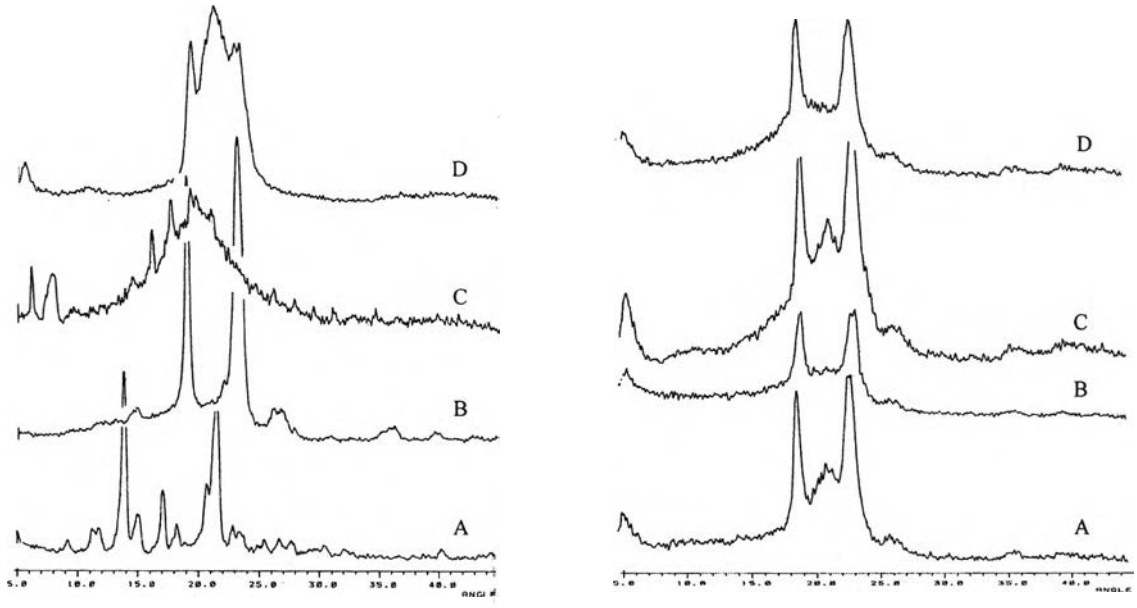

(a) (b)

Figure 45: (a)X-ray diffractogram of AmB(A); P407(B); PL(C) and GP(D); (b)1%AmB-SLN(A); 1%AmB-NLC(B); 1%AmB-SLN-L(C) and 1%AmB-NLC-L (D)

8.4 Proton Nuclear Magnetic Resonance (^{1}H-NMR)

^{1}H-NMR is a non-invasive, non-destructive and fast method with simple preparation of samples. There is no need to dilute the sample or separate the compounds, permitting serial measurements of the same sample (Zimmermann et al., 1999a). Because of its better resolution and the possibility of using techniques for molecular dynamics determination, liquid-state NMR is more useful as a structural determination tool than solid-state NMR. In addition, liquid-state NMR can also be very informative in the case of solid materials containing liquid cavities inside. Therefore, liquid-state NMR is potentially able to identify the presence of liquid reservoirs within colloidal systems (Garcia-Fuentes et al., 2005) and, hence, in this study, the difference in the inner structure of SLN, NLC, SLN-L and NLC-L were investigated.

In order to facilitate the peak assignment of the ingredients in the SLN and NLC dispersions, ^{1}H-NMR spectra of GP and MCT oil in $CDCl_3$, and P407 and PL in deuterated water were recorded and are shown in Figures 46 and 47a. From the spectra of GP and MCT oil, the signal of the terminal methyl groups appeared as triplet at δ = 0.9 ppm whereas the strong peak at δ = 1.3 ppm and two smaller peaks at δ = 1.6 and 2.4 ppm represented the methylene protons. The spectrum of P407 exhibited the peaks at chemical shift of 1.2 ppm for methylene protons, and at 3.7 ppm which indicated the proportion of the protons of the ethylenoxide groups (-CH_2-O-CH_2-). The data agreed with the report by Jores et al. (2003). The chemical shift values for methyl and methylene groups of poloxamer can easily be distinguished from those of MCT, since they are downfield due to the presence of oxygen in the polymer backbone.

Figure 46 show ^{1}H-NMR spectrum of AmB-SLN which display a signal at around 1.2 ppm attributed to methylene protons of the alkyl chains. The huge signal at δ = 4.7 ppm corresponds to water. The peak at δ = 3.7 ppm showed protons of the ethyleneoxide group (-CH_2-O-CH_2-) of P407. Since GP contains no fractions of liquid lipids at room temperature, only very weak and broad signals corresponding to the lipid were detected (Jenning, 2000). The result agreed with Jores et al. (2003) which reported the absence of methyl and methylene NMR signals in glyceryl behenate-water mixture because solid ingredients were not detected under the experimental conditions due to very short relaxation times.

The ^{1}H-NMR spectrum of AmB-NLC in Figure 46 exhibits the peaks at δ = 1.2 and 3.7 ppm representing the protons of methylene and ethylenoxide groups of P407, respectively. The chemical shifts of 0.9, 1.3, 1.6, and 2.25 ppm showed different types of the protons of MCT oil. For the CH_2 protons next to the glycerol moiety (α-CH_2) the chemical shift was 2.25 ppm. This indicates that the oil molecules in NLC formulation might be incorporated in the solid particles, while the glyceryl palmitostearate molecules remain in the solid state since no lipid proton was detected.

The ^{1}H-NMR spectrum of PL exhibits the peaks at δ = 0.9 ppm (-CH_3-), 1.3 ppm (-CH_2- of bulk aliphatic chain), 1.6, 2.0, 2.3 and 2.8 ppm (methylene protons), 3.4 ppm (trimethyl ammonium (-N^+-$(CH_3)_3$) protons), 3.7-4.0 ppm (methylene protons adjacent to phosphate group), 4.0-4.3 ppm (methylene protons adjacent to oxygen of ester group) and 5.1-5.4 ppm (CH_2- protons attached to ester bond near phosphate group which are similar to those reported by Garcia-Fuentes et al. (2005) and Schubert et al. (2005).

Figures 47b and 47c show ^{1}H-NMR spectra of AmB-SLN-L and AmB-NLC-L formulations, respectively. Sharp peaks at δ = 1.2 and 3.7 ppm, attributed to protons of methylene and ethylenoxide groups of P407, were shown while the biggest peak at 4.7 ppm represented water protons. Other signals of AmB-SLN-L can be observed at δ = 0.9, 1.3, 1.8 and 3.0-3.5 ppm. AmB-NLC-L exhibited proton signals at the chemical shifts of 0.9, 1.3, 1.6, 1.8, 2.25 and 3.0-3.5 ppm with slightly broader peaks and higher amplitude than AmB-SLN-L. Surprisingly, the line widths of the lipid methylene protons in AmB-SLN-L were found despite of without liquid oil. It was likely that phospholipid could disturb the crystallinity of solid lipid and liquefied GP. For AmB-NLC-L, α-CH_2 at the chemical shift 2.25 ppm could be detected similarly as in the AmB-NLC formulations.

Similar report on two different chemical shifts observed for each lipid proton of low and high oil loaded solid lipid in which the oil molecules were surrounded by the matrix of GB molecules for the former and formed cluster inside the particles for the latter (Jenning et al, 2000). However, Jores and co-workers (2003) concluded that MCT molecules were not well fixed in the solid matrix of the particles. Whether they were inside the solid matrix or at the outer surface could not solely be investigasted by NMR. Additional information from ESR study had to be conducted.

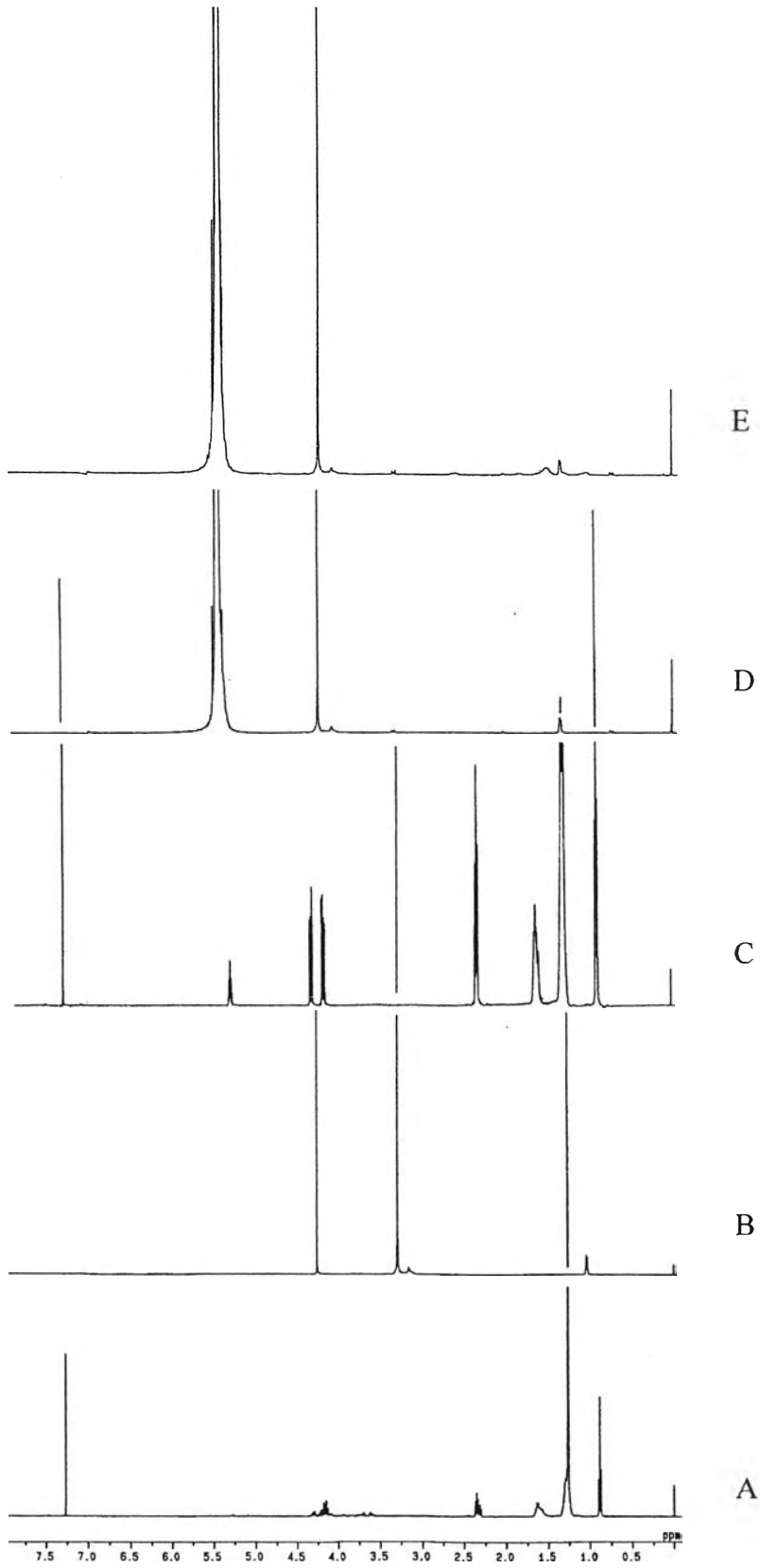

Figure 46 The 500 MHz ^{1}H-NMR spectrum of GP in $CDCL_3$(A); P407 in D_2O(B); MCT oil in $CDCL_3$(C); AmB-SLN in D_2O(D); AmB-NLC in D_2O(E).

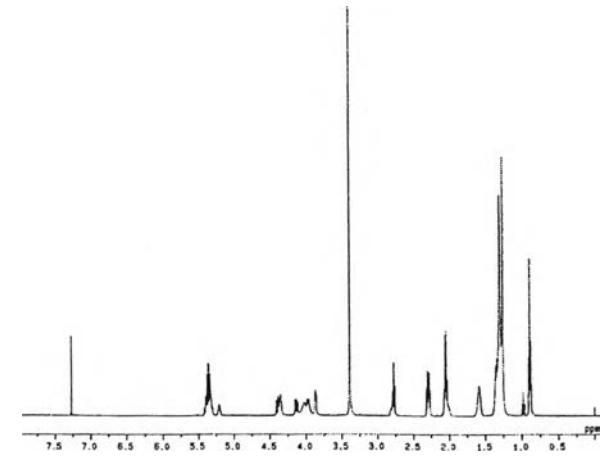

(a)

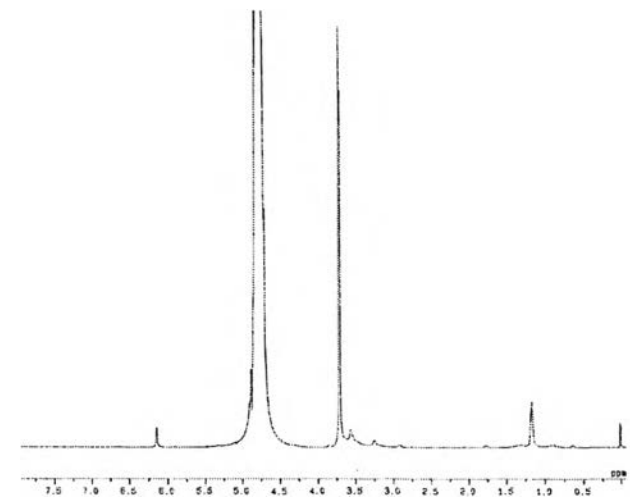

(b)

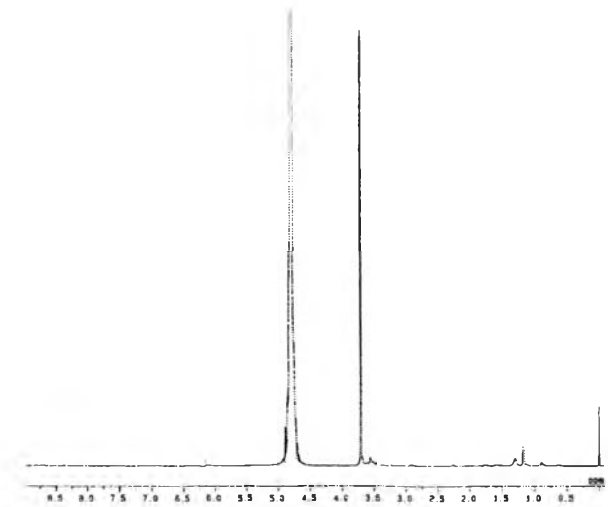

(c)

Figure 47 The 500 MHz ^{1}H-NMR spectrum of PL in D_2O(a); AmB-SLN-L in D_2O(b); AmB-NLC-L in D_2O(c).

8.5 Spectroscopic studies – aggregate state of AmB

Due to the amphiphilic nature and limited solubility of AmB, it poses a formulation challenge, particularly with respect to controlling the aggregation behavior of the drug. Aggregates are the forms responsible for drug toxicity while monomers are sufficient for the activity. In this study, the aggregation state of AmB was determined by absorption spectroscopy. The shape of the spectra depended on the state of aggregation of the molecules. In water, AmB is poorly soluble and shows several forms: monomeric, oligomeric, water-soluble and aggregates non-water insoluble. As a control, the aggregation state of AmB in the absence of the ingredients used in formulations was also monitored. Thus, The absorption spectra of AmB in DMSO:MeOH (1:999 %v/v) and PBS, pH 7.4 were recorded.

The absorption spectra of AmB stock solutions in DMSO:MeOH (1:999 %v/v), AmB and Fungizone® in PBS, pH 7.4 are shown in Figure 48a. With DMSO:MeOH (1:999 %v/v), the absorption spectrum of AmB contained four bands, exhibiting maxima at 403 and 380 nm and a shoulder around 360 and 343 nm which meant the drug existed in an unaggregated, or monomeric state while AmB solubilized by a small amount of DMSO:MeOH (1:999 %v/v) and finally diluted with PBS, pH=7.4 in the range of 2-12 μg/ml displayed a broad band centered at 331 nm and other lower intensity bands at 362, 385 and 408 nm which was characteristic of AmB in a highly aggregated state (Shervani et al., 1996; Espuelas et al., 1997; Aramwit et al., 2000). This result was corresponding to the obtained spectrum of Fungizone®. For confirming this data, the degree of aggregation of AmB was plotted by the proportional ratio of peak I (at 323-348) to peak IV (at 403-414). This ratio was < 0.25 when the drug was monomeric, and as high as 2.0 was highly aggregated species. From the data in Figure 49a, AmB dissolved in DMSO:MeOH (1:999 %v/v) showed the degree of aggregation in the range of 0.22-0.29 while AmB and Fungizone® dissolved in PBS displayed 1.73-2.93 and 1.51-3.40, respectively indicating the drug was in monomeric state for the former whereas the drug was in highly aggregated state in the two latter solutions.

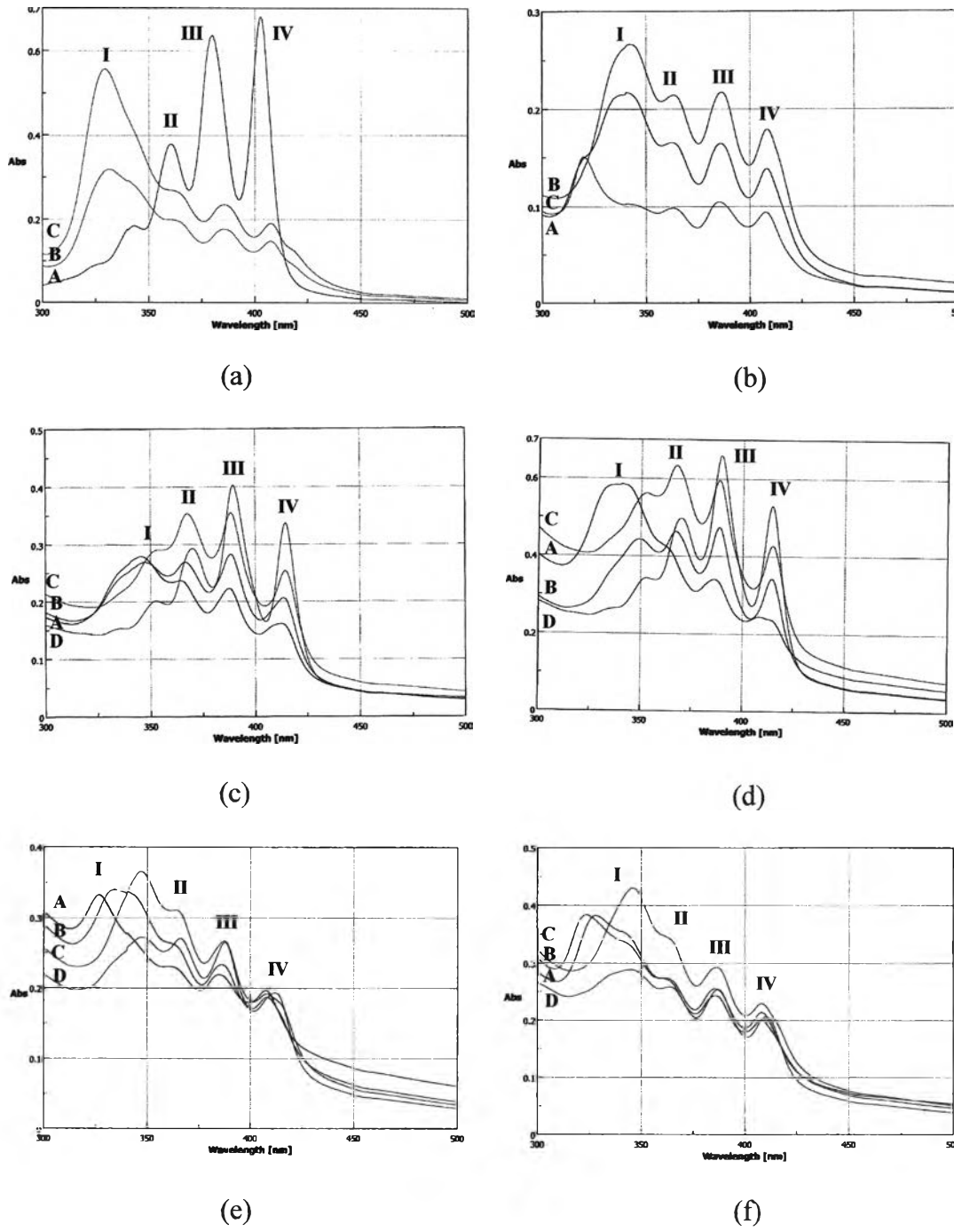

Figure 48 (a):UV-Visible absorption spectra of AmB solubilized in DMSO:MeOH (1:999 %v/v) (A);AmB in PBS, pH 7.4 (B) and Fungizone® in PBS, pH 7.4 (C); (b): various AmB-SLN prepared by WME method. AmB-WME1 (A), AmB-WME2 (B) and AmB-WME3 (C); (c,d,e,f):various AmB-SLN, AmB-NLC, AmB-SLN-L, AmB-NLC-L formulation in PBS, pH 7.4 prepared by HPH method, stabilized by Tw20(A), CreRH(B), P407(C), M52(D).

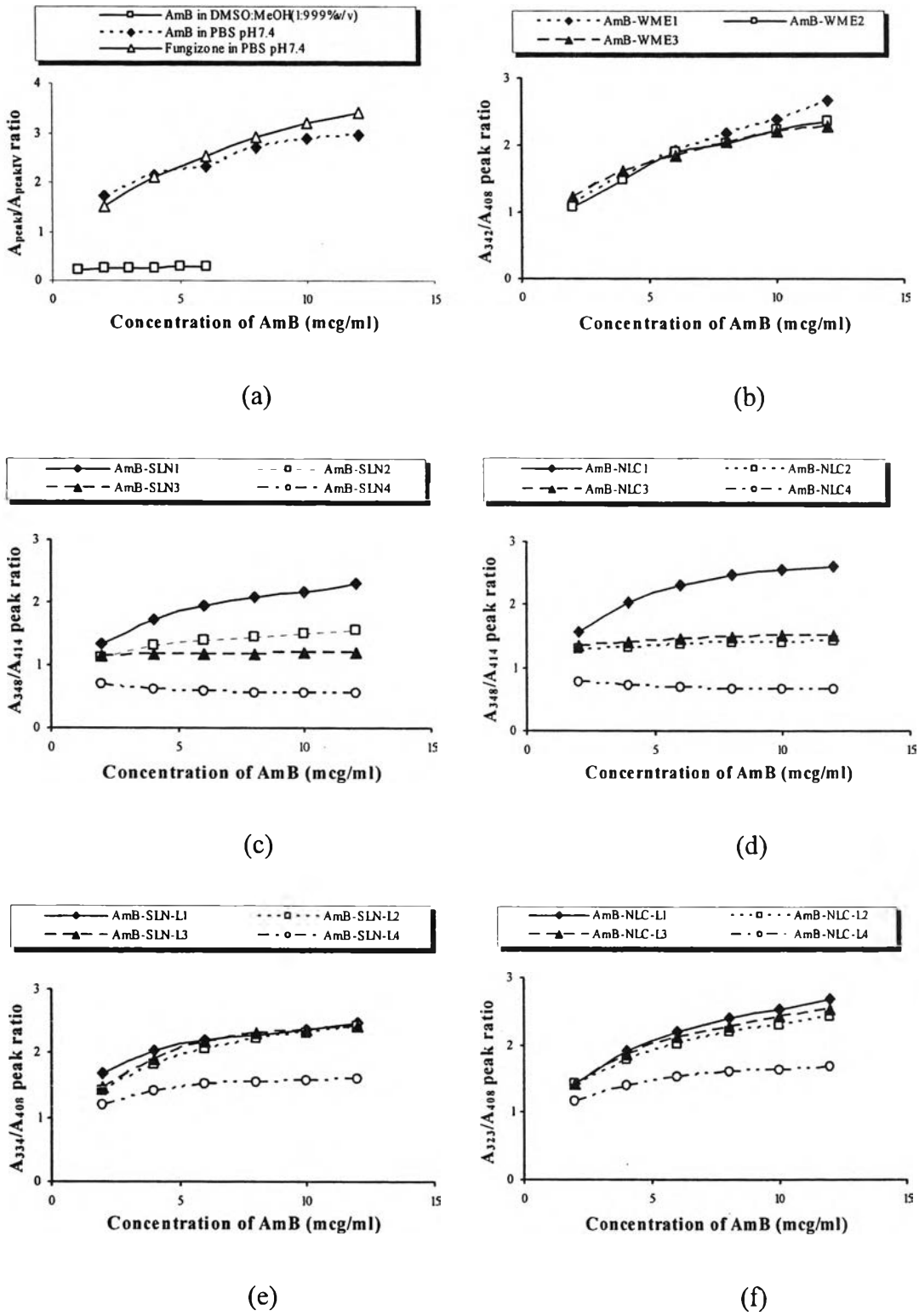

Figure 49 The absorbances peakI/peakIV ratio of AmB in various formulations as function of concentrations; (a): AmB in DMSO:MeOH (1:999%v/v); AmB and Fungizone in isotonic PBS, pH 7.4; (b): AmB-SLN formulations prepared by WME method; (c, d, e, f): AmB-SLN, AmB-NLC, AmB-SLN-L and AmB-NLC-L formulations prepared by HPH method.

Figure 48b shows the absorption spectra of various formulations of AmB-SLN prepared by WME method. The AmB-WME1 and AmB-WME2 had the absorption spectra similar with a broad intense single band at 340 nm, along with smaller peaks at higher wavelengths. The absorption spectrum of AmB-WME3 showed the position of the centered band, characteristic of self-associated AmB at 320 nm which was different with the others.

The assessment of aggregate species of AmB loaded SLN prepared by WME method is shown in Figure 49b. Although there was a difference in the centered band, the degrees of aggregation were slightly different. The proportional ratio of peak I to peak IV was between 1.07 and 2.07 which displayed the aggregate state of AmB.

The absorption spectra of various formulations of AmB-SLN prepared by HPH method are shown in Figure 48c. The AmB-SLN1, AmB-SLN2, AmB-SLN3 and AmB-SLN4 formulations represented the AmB-SLN stabilized by Tw20, CreRH, P407 and M52, respectively. In comparison with AmB-WME, there was a bathochromic shift to 414 nm for AmB loaded in SLN prepared by HPH method. The absorption spectra of AmB-SLN1 and AmB-SLN2 showed the flattened band centered at 346 and 348 nm, respectively. The spectra of AmB-SLN3 and AmB-SLN4 showed the shoulder bands at 354 and 352 nm, respectively. AmB loaded SLN3 exhibited a similar spectrum to AmB encapsulated in PEO-b-PHSA micelles at 70% stearic acid substitution which was reported by Lavasanifar et al. (2002b). They discussed that the obtained spectrum looked like the spectrum of drug binding to serum lipiproteins, which had cores rich in triglycerides, or that binding to sterols. The AmB-SLN4 spectrum showed the pattern similar to that of AmB dissolved in DMSO:MeOH (1:999 %v/v) which indicated the monomer state of AmB.

The degree of aggregate state of AmB by observing the ratio of peak I to peak IV is shown in Figure 49c. The higher AmB concentrations, the more aggregation species of AmB occurred with poorly concentration-dependent manner, since the same bands were observed at low and high AmB concentrations. The ranking order of aggregate state was: AmB-SLN1 > AmB-SLN2 > AmB-SLN3 > AmB-SLN4. Indeed, the AmB loaded SLN containing M52 showed the least degree of aggregation

with the ratio of 0.5. It was accordance to the reported on AmB loaded in a nearly monomeric state into PEO-b-p(HASA) micelles was due to hydrophobic interaction with the stearate side chains (Adams and Kwon, 2004). And also, it was considered as a reservoir of the monomeric form of AmB that released only limited amount of free AmB in the aqueous media like AmB-Lipofundin™ (Tabosa do Egito et al., 2002).

Figure 48d shows the absorption spectra of various formulations of AmB-NLC. Although replacing of oil to a portion of solid lipid, the spectra pattern of these formulations did not significantly change. However, the result of degree of aggregation calculated as the ratio and plotted in Figure 49d showed little difference. The order of aggregate state was as followed: AmB-NLC1 > AmB-NLC2 ≈ AmB-NLC3 > AmB-NLC4. In addition, their peak ratios were slightly higher than those of SLN series. This indicated the moderate degree of aggregate form.

The absorption spectra of various formulations of AmB-SLN-L1 - AmB-SLN-L4 are shown in Figure 48e. The spectra of these formulations were nearly similar. Strong absorption was shown in the 330-340 nm region indicating the self-aggregation or oligomers (Adams and Kwon, 2004; Moreno et al., 2001) It was therefore highly probable that the drug was at the interface of the disperse system as an AmB-lecithin complex. For the spectra of AmB-SLN-L2, AmB-SLN-L3, and AmB-SLN-L4, at high concentrations, the band at 408 nm was replaced by a 414 nm band. The band shift of AmB-lecithin complex was corresponding to the examination of Moribe (1998) when increasing the amount of DSPE-PEG which indicated that the polyene moiety of AmB contributes to the interaction leading to the complex formation.

The result of the correlation of the ratio of peak I to peak IV is shown in Figure 49e. The degree of aggregation of AmB loaded SLN containing M52 and PL was lower than that of the others. In comparison, the former two formulations showed no significant difference in degree of aggregation. However, the degrees of aggregation of SLN-L in all formulations were higher than those of SLN formulations.

Figure 48f shows the absorption spectra of various formulations of AmB-NLC-L. The spectra pattern of these formulations did not significantly changed when compared to the SLN-L formulations. This indicated and comfirmed that the presence oil in the formulations had no affect on the absorption spectra. Nevertheless, at high concentrations, the band at 408 nm was not replaced by 414 nm even if the phospholipid was presented which differed from the AmB-SLN-L formulations. This might be due to weakly interaction of lecithin-drug complex.

The degree of aggregation from the plot between A_{323}/A_{408} peak ratio of AmB loaded NLC-L formulations against its concentration in Figure 49f showed a slightly higher degree of aggregation when compared with those of SLN-L formulations. Similarly, the AmB loaded NLC-L4 which used M52 and PL had less degree of aggregation when compared with the other formulations.

9. Model of four different AmB lipid particles

From the results of entrapment efficiency, physical evaluations, morphology, and physical and chemical stability studies, the proposed models of different AmB lipid particles which were AmB-SLN, AmB-NLC, AmB-SLN-L and AmB-NLC-L formulations are shown in Figure 50. Due to more perfect crystalline β-modifications could be formed during storage and the nature of AmB was insoluble in both oil and water, AmB-SLN was the formation of a perfect crystal liked "brick wall" with drug enriched shell (Müller et al., 2002b). AmB-NLC was solid but not crystalline by special mixtures of solid lipid and liquid lipid. This led to more imperfections in the crystal and higher drug loaded (Müller et al., 2002a). The highest entrapment efficiency of AmB loaded SLN-L due to it localized in the interfacial lecithin layer as report on SolEmuls® (Müller et al., 2004b). In contrast to AmB-NLC-L exhibited the lowest entrapment efficiency which probably might be the leakage of complex formation of drug with oil and lecithin to the aqueous phase. However, co-existence of additional colloidal structures were not excluded.

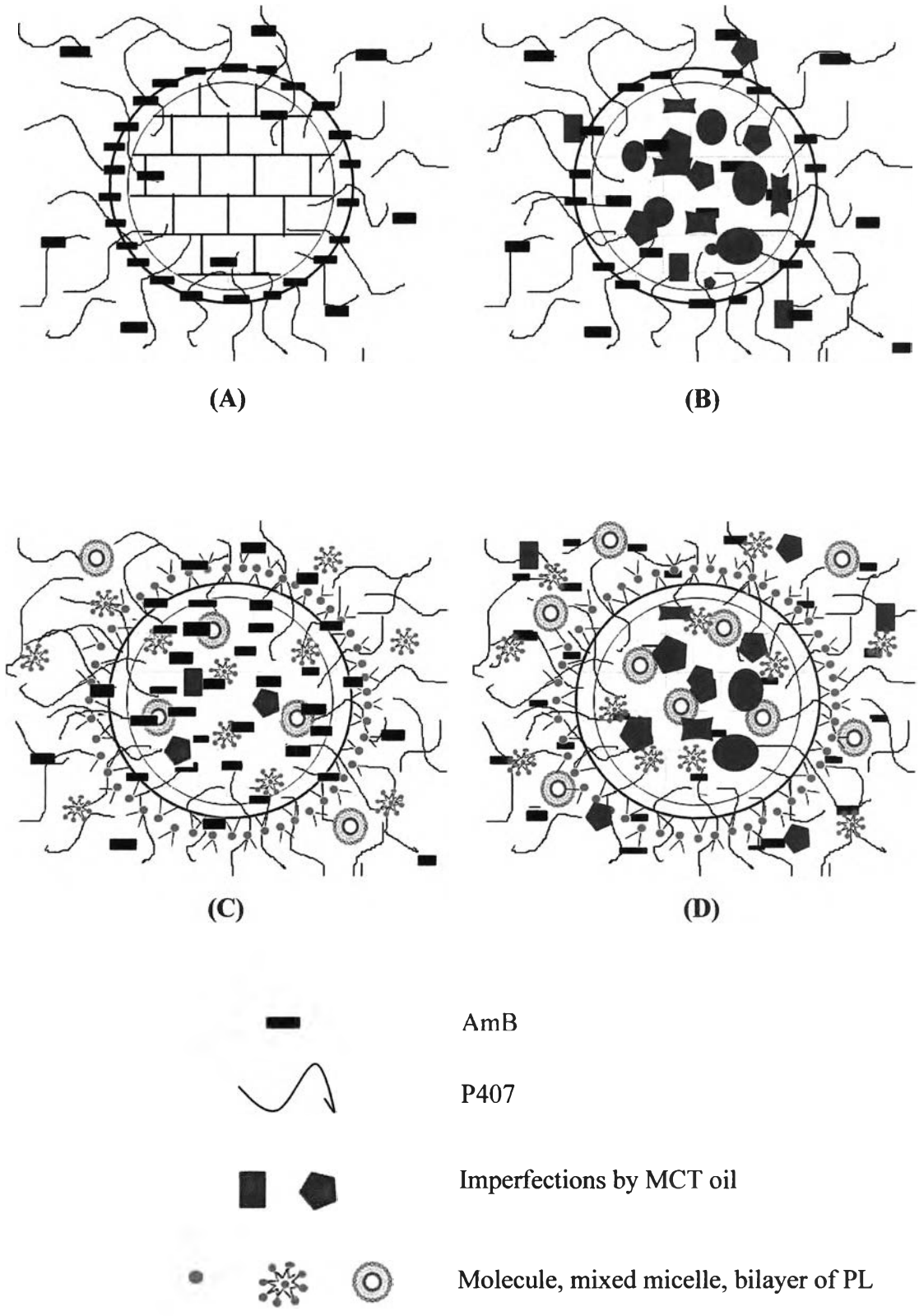

Figure 50 Models of AmB loaded different lipid nanoparticles: AmB-SLN (A); AmB-NLC (B); AmB-SLN-L (C); AmB-NLC-L (D)

10. Effect of drug loading in various formulations

For AmB-SLN prepared by WME method, precipitation appeared when higher amount of drug than 20 mg from the previous study was added. Thus, only various AmB formulations prepared by HPH method were investigated the effect of drug loading.

Physical appearances

The physical appearances of AmB loaded in different lipid nanoparticles formulations which stabilized by P407 are shown in Table 51. With regarding to macroscopic aspect, the SLN dispersions containing 1-5% AmB showed no alteration after storage for 3 months whereas other formulations displayed physical changes. The dispersions composed to 2.5-5% AmB loaded in both NLC and SLN-L were viscous gel-like after storage whereas the 1% AmB loaded did not change in appearance. This result indicated that the amount of drug affect on the physical stability. The higher amount of AmB in the preparations resulted in the increasing viscosity shown in Figure 51. The effect of phospholipid incorporated in the system was more viscous than the system using oil. The gel formation limited the maximum amount of drug to be incorporated in the investigated dispersions. However, gelation could be avoided by using binary (or ternary) surfactant mixtures (Schwarz and Mehnert, 1999). Westesen et al. (1993) could load coenzyme Q10 in SLN dispersion stabilized by phospholipids and sodium glycocholate up to 10%. Addition of the latter led to a reduction in particle size and yielded a stable product compared with the use of phospholipids alone that tended to gel. Semi-solid viscous gel was obtained to all AmB loaded in NLC-L formulations after storage. Moreover, The NLC-L containing AmB 5% showed phase separation after 2 months. Because the the nature of AmB is amphiphilic character which might behave like the phospholipids, the excess AmB possibly formed multilayers around the particles and/or leak into the aqueous phase leading to the formation of liposomes, mixed micelles or other aggregates which caused physical instability after storage.

Table 51 The physical appearances of different amount of AmB loaded in various formulations

Formulation type	Macroscopic observation					
	1%AmB		2.5%AmB		5%AmB	
	a	b	a	b	a	b
SLN	+	+	+	+	+	+
NLC	+	+	+	G3M	+	G3M
SLN-L	+	+	+	G3M	+	G3M
NLC-L	+	G2M	+	G2M	+	S2M

a, b: initial and stability on storage 4°C for 3 months; +: yellowish fluid dispersion; G2M, G3M: Gel formation within 2, 3 month; S2M: Phase separation within 2 months

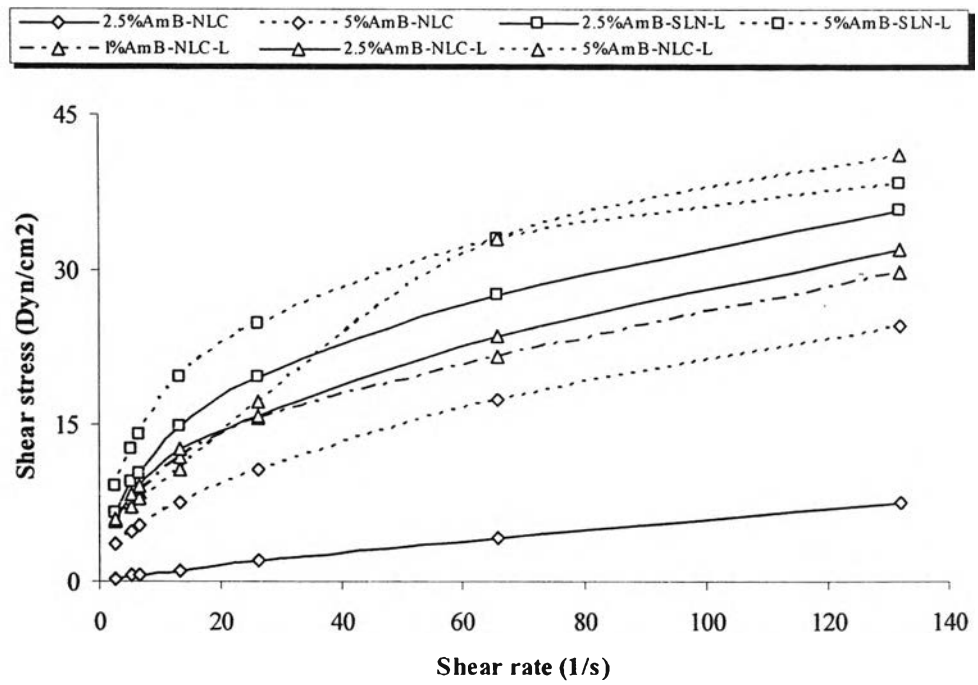

Figure 51 Shear stress vs. shear rate plots for various amount AmB loaded NLC, SLN-L and NLC-L formulations

Particle size

The incorporation of AmB had no or little effect on the mean particle size of SLN and NLC dispersions as shown in Table 52. This indicated that the optimum production parameters established for drug-free formulations could be employed for the drug loaded nanoparticles. In contrast, the SLN-L and NLC-L formulations showed the mean diameter decreased with the increasing amount of drug. It was assumed that AmB was of amphoteric structure which might intercalate into the phospholipid moiety and formed monolayer around the lipid particles.

Table 52 Particle sizes of different amount of AmB loaded in various formulations

Formulation type	AmB incorporated in lipid matrix					
	1.0%		2.5%		5.0%	
	Mean particle size (nm)		Mean particle size (nm)		Mean particle size (nm)	
	Z value	PI	Z value	PI	Z value	PI
SLN	201.6 ± 3.5	0.145	164.3 ± 1.0	0.334	224.7 ± 4.8	0.337
NLC	127.6 ± 3.7	0.346	143.4 ± 0.4	0.189	137.1 ± 2.3	0.260
SLN-L	171.0 ± 3.2	0.325	145.2 ± 4.0	0.298	106.3 ± 1.7	0.292
NLC-L	203.4 ± 6.4	0.294	108.2 ± 0.5	0.293	128.7 ± 0.4	0.222

pH , zeta potential and osmolality

Table 53 shows the pH of 1.0, 2.5 and 5.0% AmB loaded in various types of SLN dispersions. It could be seen that the type of preparations merely affect the pH. Increasing the amount of AmB resulted in the higher pH of preparations due to the amount of NaOH which was a strong base. However, the pH of 1.0 and 2.5% AmB loaded preparations was in the range of the optimum stability of the drug (pH 6-7). In case of 5% AmB loaded, the pH of 9 was optimum for processing parameter which was supported by the investigation of Santhi et al (1999) and Moreno et al (2001).

Table 53 The pH of different amount of AmB loaded in various formulations

Formulations	AmB incorporated in lipid matrix		
	1.0%	2.5%	5.0%
	pH		
SLN	7.07±0.01	7.77±0.03	9.05±0.01
NLC	6.74±0.01	7.90±0.01	9.12±0.01
SLN-L	7.00±0.01	7.86±0.01	9.00±0.01
NLC-L	6.69±0.02	7.47±0.01	9.25±0.01

The osmolality of drug incorporated in different types of SLN dispersions is shown in Table 54. The amount of drug added did not affect the obtained osmolality. However, the osmolality in all preparations was still too low to be used as intravenous parenteral formulations. Therefore, the use of isotonicity agent such as glycerol 2.25% was necessary in order to be compatible to physiological fluid.

Table 54 The osmolality of different amount of AmB loaded in various formulations

Formulations	AmB incorporated in lipid matrix		
	1.0%	2.5%	5.0%
	Osmolality (mosmol/kg)		
SLN	8.0±0.0	8.3±0.6	10.3±0.6
NLC	8.0±0.0	8.0±1.0	9.0±1.0
SLN-L	9.0±0.0	7.0±0.0	9.7±0.6
NLC-L	5.3±0.6	7.7±0.6	8.7±0.6

The zeta potentials of 1, 2.5 and 5.0% AmB loaded in various SLN dispersions shown in Table 55 were different with regarding to their compositions. The zeta potentials of drug-loaded SLN stabilized with P407 were between -14.74 and -21.55 which were too low for solely electrostatic stabilization. Nevertheless, the steric stabilization would additionally enhance the physical stability. Moreover, increasing the amount of drug loaded would increase zeta potentials. It might be resulted from the orientation of a flexible hydrophilic portion bearing seven hydroxyl group of AmB on the surface of SLN. The latter three formulations, NLC, SLN-L, NLC-L, had lower zeta potential when increasing the amount of drug. This indicated that oil loaded and/or presence of phospholipids which carrying positive charge interfered the negative characteristic of the drug in preparations. Particularly, the

formulation containing both oil and phospholipid tended to physical instability. In addition, the effect of recrystallization and polymorphic trasition rate of lipid was slower than SLN formulation. The result agreed with the aforementioned macroscopic observations.

Table 55 The zeta potential of different amount of AmB loaded in various formulations

	AmB incorporated in lipid matrix		
	1.0%	2.5%	5.0%
Formulations	Zeta potential (millivolt)		
SLN	-14.74	-14.85	-21.55
NLC	-27.17	-15.59	-13.14
SLN-L	-26.57	-15.31	-10.11
NLC-L	-15.16	-4.77	-3.34

AmB content in various AmB loading in formulations

The drug content of 2.5% and 5% AmB loaded in various system determined by HPLC is shown in Figure 52. The drug contents were in the range of 80.14%-85.53%. There was no significant difference in initial drug amount. This was due to the similarly critical process parameters of the systems.

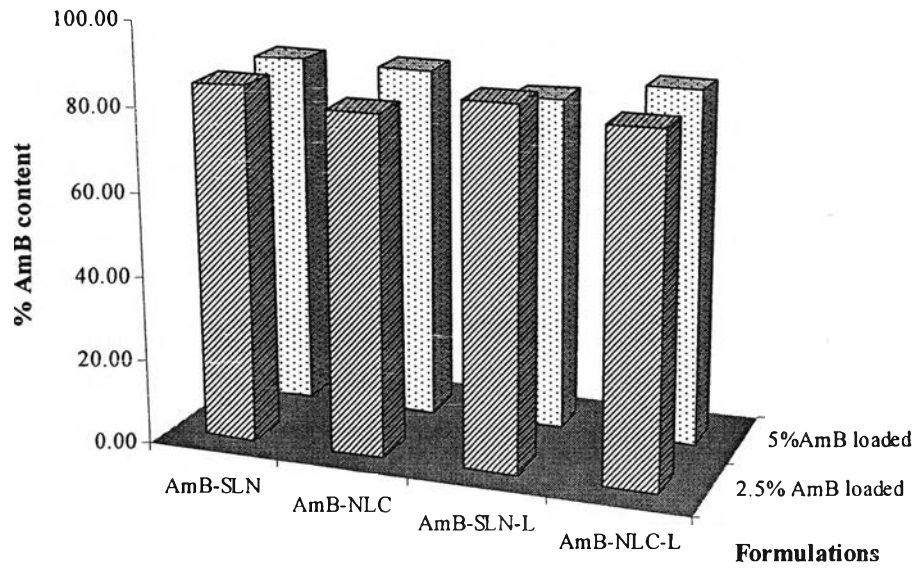

Figure 52 The percentage of AmB content of different amount loaded in various formulations.

Entrapment efficiency of various AmB loading in formulations

AmB was incorporated in different amounts of 1.0, 2.5 and 5% (calculated as weight percentage of the lipid matrix). The obtained entrapment efficiency ranged from 44.5 to 93.16% (Table 56). The highest entrapment was observed from AmB loaded in SLN-L which used P407 and PL as stabilizers (81.16-93.16%). However, the influence of oil loaded to the formulation of the corresponding NLC-L showed the lowest entrapment (44.50-78.11%). It was assumed that the AmB localized in the interfacial between the oil and phospholipid surrounded the shell of particles or dispersed as co-existence of colloidal dispersions in the continuous phase. Stabilization of these particles in SLN and NLC with the P407 without phospholipid also reduced the entrapment slightly to 52.77-88.61%. A possible explanation was that the solubilized AmB by poloxamer acted as polymeric micelles. This was agreed with the observations regarding the incorporation of tetracaine in cetylpalmitate SLN and prednisolone in Compritol nanoparticles (Schwarz and Mehnert, 1999; zur Mühlen and Mehnert, 1995). The entrapment efficacies of AmB incorporated in NLC were higher than of those in SLN. AmB might be located in the mixture of oil and solid lipid as nanocompartment. However, with regarding to amount of drug added, all 2.5% AmB loaded formulations showed the highest entrapment efficiency. It was noted that 2.5% of AmB calculated to solid lipid was the optimum drug loading.

Table 56 Entrapment efficiency of different amount of AmB loaded in various formulations.

	AmB incorporated in lipid matrix		
	1.0%	2.5%	5.0%
Formulations	Entrapment efficiency		
SLN	52.77 ± 0.12	88.61 ± 2.04	69.47 ± 3.29
NLC	75.33 ± 1.94	83.11 ± 2.69	73.90 ± 0.24
SLN-L	81.17 ± 0.36	93.16 ± 0.24	86.97 ± 1.59
NLC-L	44.50 ± 0.67	78.11 ± 0.53	59.54 ± 1.25

Morphology of 2.5% and 5%AmB loaded in various formulations

SEM images of 2.5, 5.0% of AmB-SLN, AmB-NLC and AmB-SLN-L are presented in Figure 53. It could be observed that the dispersions of 2.5% and 5%

AmB-SLN tended to be globule clusters. For AmB-NLC and AmB-SLN-L displayed the cluster chain. The mean diameter of 2.5% AmB in various formulations detected by both PCS and Cryo-SEM were not different. In contrast the particle sizes of 5% AmB loaded obtained by Cryo-SEM method were larger than those from PCS analysis. The possible explanation was that the sample of preparation method by Cryo-SEM had to be frozen by liquid nitrogen and evaporated under vacuum that might cause shrinkage so that they could be agglomerate on the surface; particularly, the 5.0% AmB loaded NLC and SLN-L preparations which had low mobility.

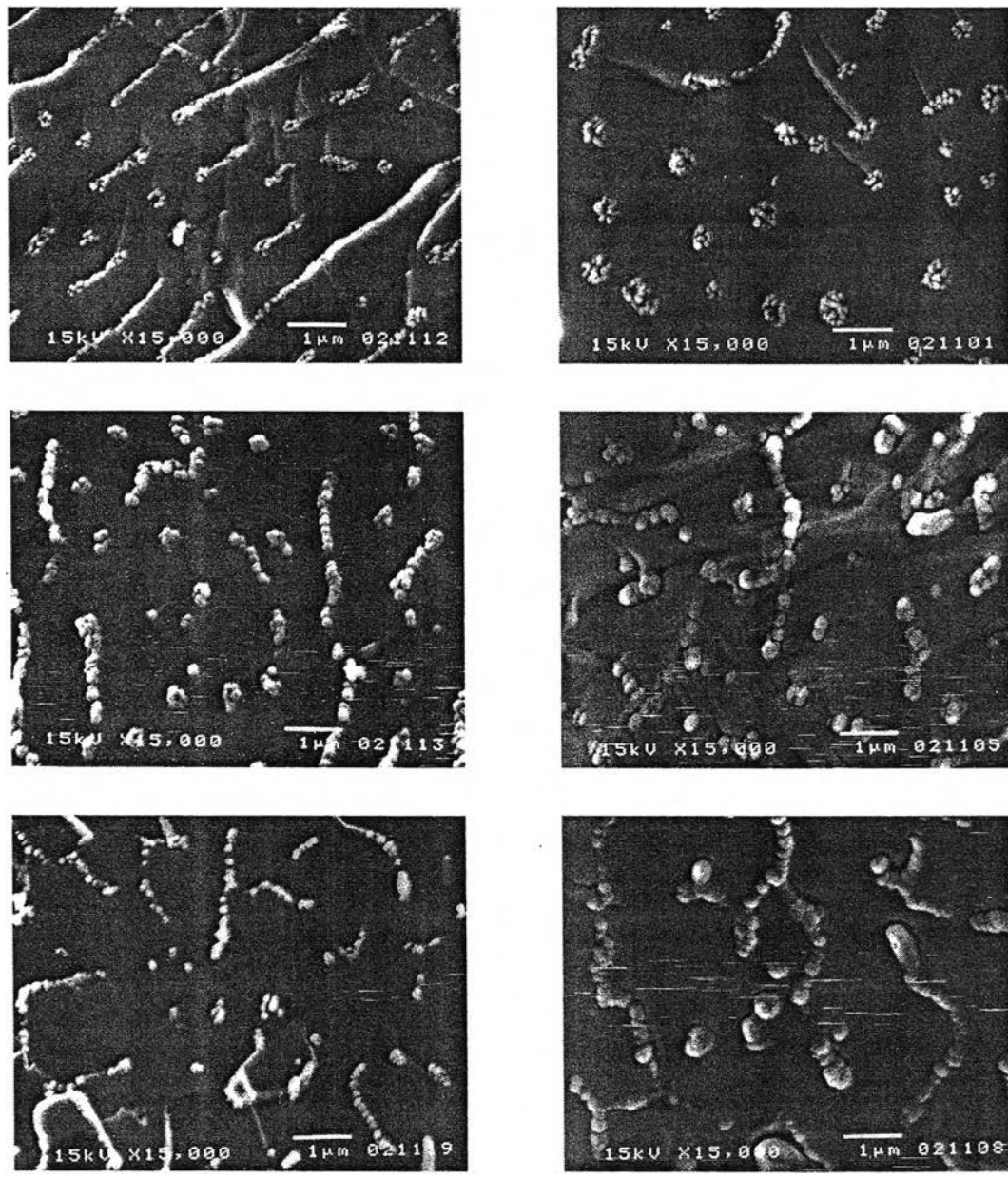

Figure 53 The Cryo-SEM micrographs of AmB-SLN (top), AmB-NLC (middle), AmB-SLN-L (bottom); 2.5, 5% AmB loaded (left, right)

Physical stability of 2.5% and 5% AmB loaded in various formulations

The stability of particle size plays an important role in optimizing colloidal carrier system. Incorporation of drugs might affect the physical long-term stability. Therefore, the stability of drug- loaded SLN dispersions was investigated. Table 57 shows the particle sizes of different drug loaded in SLN, NLC, SLN-L and NLC-L formulations. There was minute difference in the mean diameters of two drug-loaded SLN formulations. Therefore the amount of drug did not affect the physical stability of SLN dispersions for more than 3 months. The latter three formulations of NLC, SLN-L, and NLC-L of both 2.5% and 5% drug-loaded led to less stable preparations with markly increasing the mean diameter after 3 months storage.

Chemical stability of 2.5% and 5% AmB loaded in various formulations

Due to poor physical stability of AmB loaded NLC-L formulation, it was excluded from this study. Thus, chemical stability studies were performed on AmB loaded SLN, NLC and SLN-L formulations stored at 4°C. The percent content of AmB in different formulations as function of time are summarized in Table 58 and Figure 54. From the results, it was found that the amount of drug loading and type of system affected the chemical stability. This was due to AmB was very unstable in water, whereas in lipids a much improved stability could be observed. Investigating drug content of the lipid particles as a function of time could be used to determine the distribution of drug between the continuous phase and the lipid phase of solid lipid nanoparticles. High drug remaining rates after storage indicated that drug was in the lipid phase. If only small amounts of AmB were entrapped, the drug was mostly present in the water phase and, thus, subjected to degradation. However, because of the insolubility of the drugs in pure water, no direct measurement of the stability in water was possible (Jennings and Gohla, 2001).

The degradation rate constants and shelf-life values of 2.5 and 5% AmB in different types of lipid nanoparticles were calculated as shown in Table 59. The t_{90}% values of 2.5% and 5% in SLN and NLC showed significant differences whereas those of SLN-L formulations displayed the lowest values. This confirmed

Table 57 Particle sizes of different amount of AmB loaded in various formulations at initial and 3 months storage

Formulations	Particle size of various preparations on 4°C storage			
	Initial		3 months	
	Mean particle size (nm)		Mean particle size (nm)	
	Z value	PI	Z value	PI
2.5% AmB-SLN	164.3 + 1.0	0.334	136.6 + 3.1	0.310
2.5% AmB-NLC	143.4 ± 0.4	0.189	194.1 ± 1.7	0.291
2.5% AmB-SLN-L	145.2 ± 4.0	0.298	596.6 ± 7.4	0.355
2.5% AmB-NLC-L	108.2 ± 0.5	0.293	510.2 ± 28.5	0.183
5% AmB-SLN	224.7 ± 4.8	0.337	271.0 ± 7.4	0.289
5% AmB-NLC	137.1 ± 2.3	0.260	373.2 ± 36.5	0.246
5% AmB-SLN-L	106.3 ± 1.7	0.292	419.5 ± 34.6	0.256
5% AmB-NLC-L	128.7 ± 0.4	0.222	313.4 ± 33.8	0.195

Table 58 The AmB content as a function of time at 4°C of 2.5% and 5% AmB in various formulations

Formulation types	AmB content (%)	Residual AmB (%)		
	0 month	1 month	2 months	3 months
SLN*	85.04 ±1.06	84.72 ±1.27	80.70 ±4.05	77.77 ±0.08
NLC*	84.50 ±0.07	83.00 ±0.56	79.34 ±3.24	79.13 ±1.17
SLN-L*	80.14 ±1.40	73.48 ±0.24	70.09 ±2.23	63.47 ±1.13
SLN**	84.80 ±0.25	81.57 ±1.26	79.69 ±2.16	75.10 ±0.49
NLC**	80.82 ±1.71	75.09 ±0.54	77.61 ±3.09	70.73 ±1.22
SLN-L**	85.53 ±0.24	82.10 ±4.18	80.04 ±2.27	72.30 ±1.12

*,** : 2.5%, 5% AmB loaded

that the drug loaded in SLN-L formulations when using PL as stabilizing agent were not localized exclusively on the lipid surface, but also in the aqueous phase. From the previous result of entrapment efficiency in the lipid nanoparticles, the entrapment efficiencies of 2.5% drug loaded were higher than those of 5% drug loaded lipid dispersions which meant the 5% drug loaded was too high and might be expeled from the particles into the water phase where the degradation occurred and led to low chemical stability. It was noted that the SLN dispersions did not contain any chemical stabilizers (e.g. antioxidant) and were prepared with no special precautions such as

oxygen exclusion and de-gasing with argon. If desired, this could be performed, thus enhance further the stability of incorporated compound (Dingler et al., 1999).

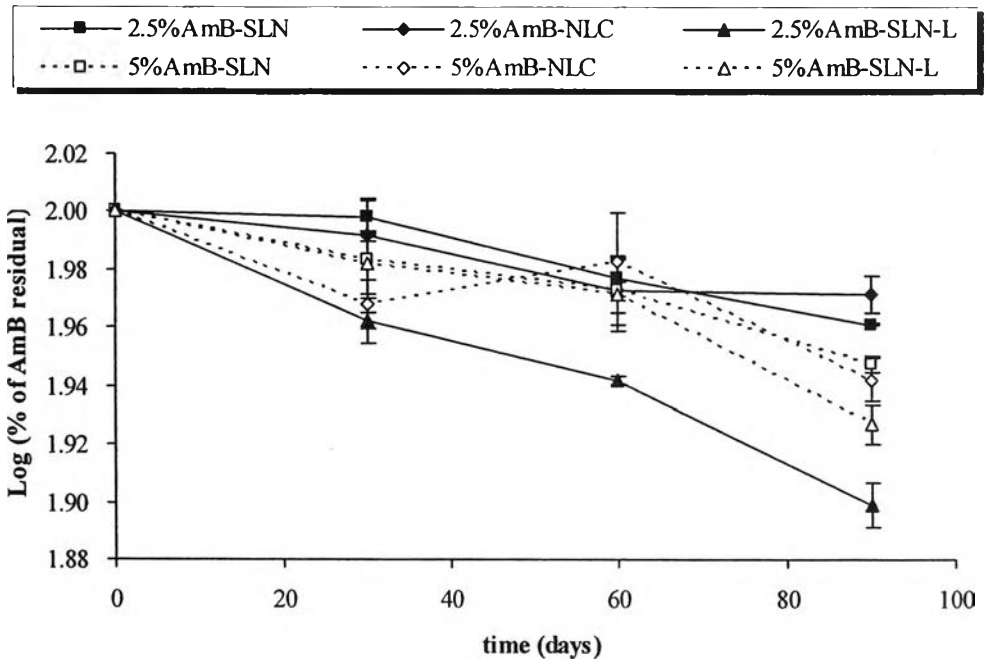

Figure 54 AmB residual contents at 4°C of 2.5% and 5% loaded in various formulations as a function of time

Table 59 Predicted shelf lives at 4°C of different amount AmB loaded in various preparations

Formulations	K	t_{90} (days)
2.5% AmB-SLN	1.06×10^{-3}	99.33
2.5% AmB-NLC	0.81×10^{-3}	130.26
2.5% AmB-SLN-L	2.49×10^{-3}	42.14
5% AmB-SLN	1.29×10^{-3}	81.27
5% AmB-NLC	1.22×10^{-3}	85.86
5% AmB-SLN-L	1.76×10^{-3}	59.52

Physical evaluations of loading in formulations loaded with various amount of AmB

Fourier Transform infrared Spectroscopy

Figure 55 shows the infrared spectra from top to the bottom of solid lipid pellet of SLN containing AmB 1%, 2.5%, 5%, and physical mixture of lyophilized SLN base and 5% of drug powder, respectively.

The IR spectra of SLN containing 3% GP, 2% P407 and incorporated with 1%, 2.5% and 5% AmB of total lipid showed spectra bands corresponding to the superimpositions of their parent materials. The sharp peaks at 3411, 2918, 2851, 1738, 1471, 1106, 719 cm^{-1} were observed from the combination spectra of its composition. No new peak was detected from its mixture. Therefore, the data indicated that no strong interaction and significant shift occurred among the ingredients. It was assumed that there was no incompatibility in AmB-SLN. These spectra did not display the bands characteristic of the drug because they were of low intensity and were hidden by the bands produced by the solid lipid and stabilizer. Nevertheless, The band of 1565 cm^{-1} C=C stretching band of AmB was observed when 5% of the drug calculated to total lipid was incorporated into the preparation.

The 1-5% AmB loaded NLC, SLN-L, and NLC-L obtained by ultracentrifugation presented the similar pattern with the physical mixture as shown in Figure 56, 57 and 58, respectively. The spectra did not show any new peak. They displayed spectra corresponding to superimposition of their intact materials and no significant shift of the major peaks of AmB. The intensity of the band at 1565 cm^{-1} which represented the functional group C=C stretching of AmB was higher when increasing the concentration of the drug in preparations. The data indicated that no strong chemical interaction between AmB and its mixture.

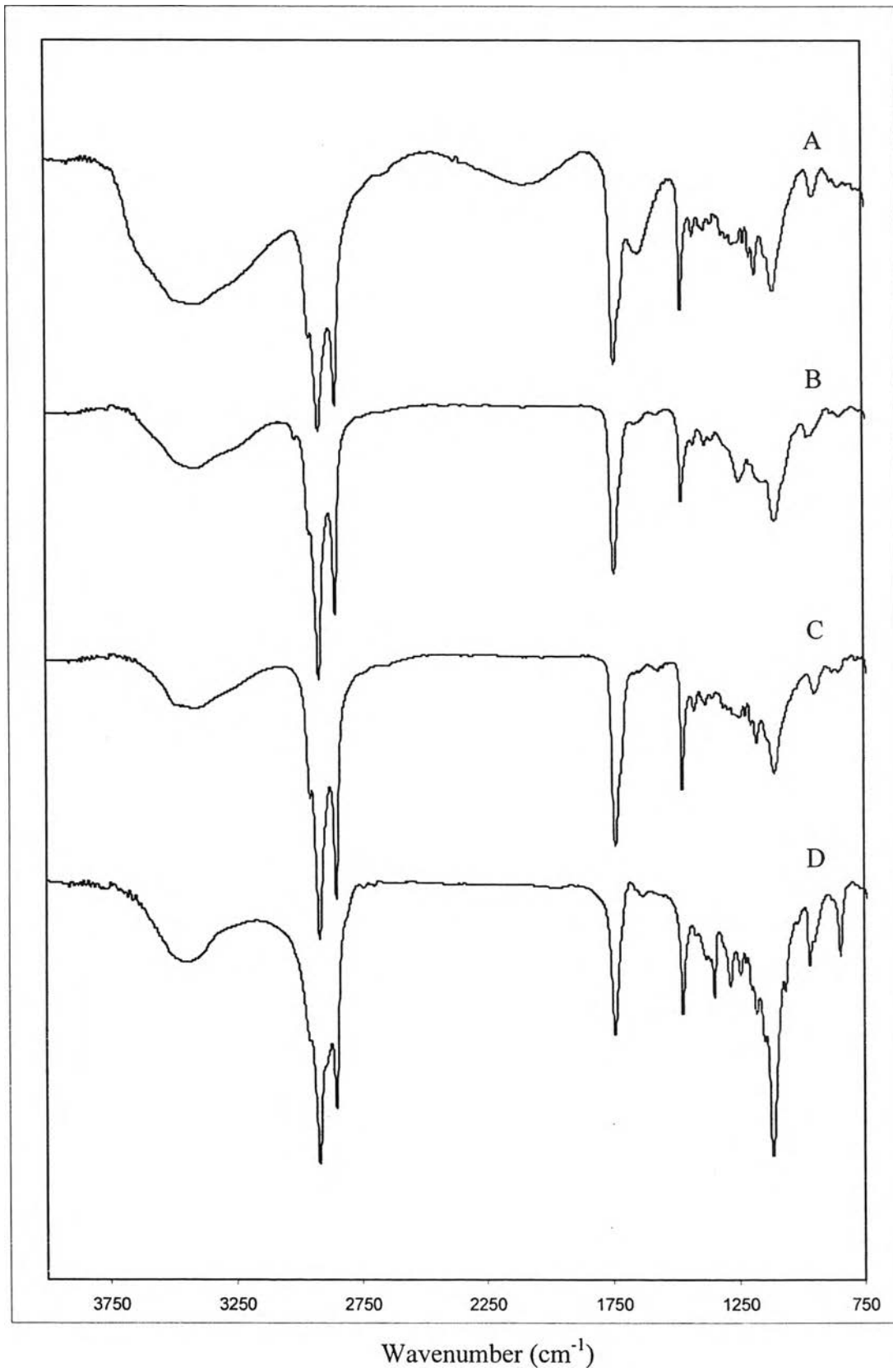

Figure 55 IR spectra of AmB-SLN containing 1% AmB(A); 2.5%AmB(B); 5%AmB(C) and physical mixture of lyophilized SLN base and 5% of AmB powder(D)

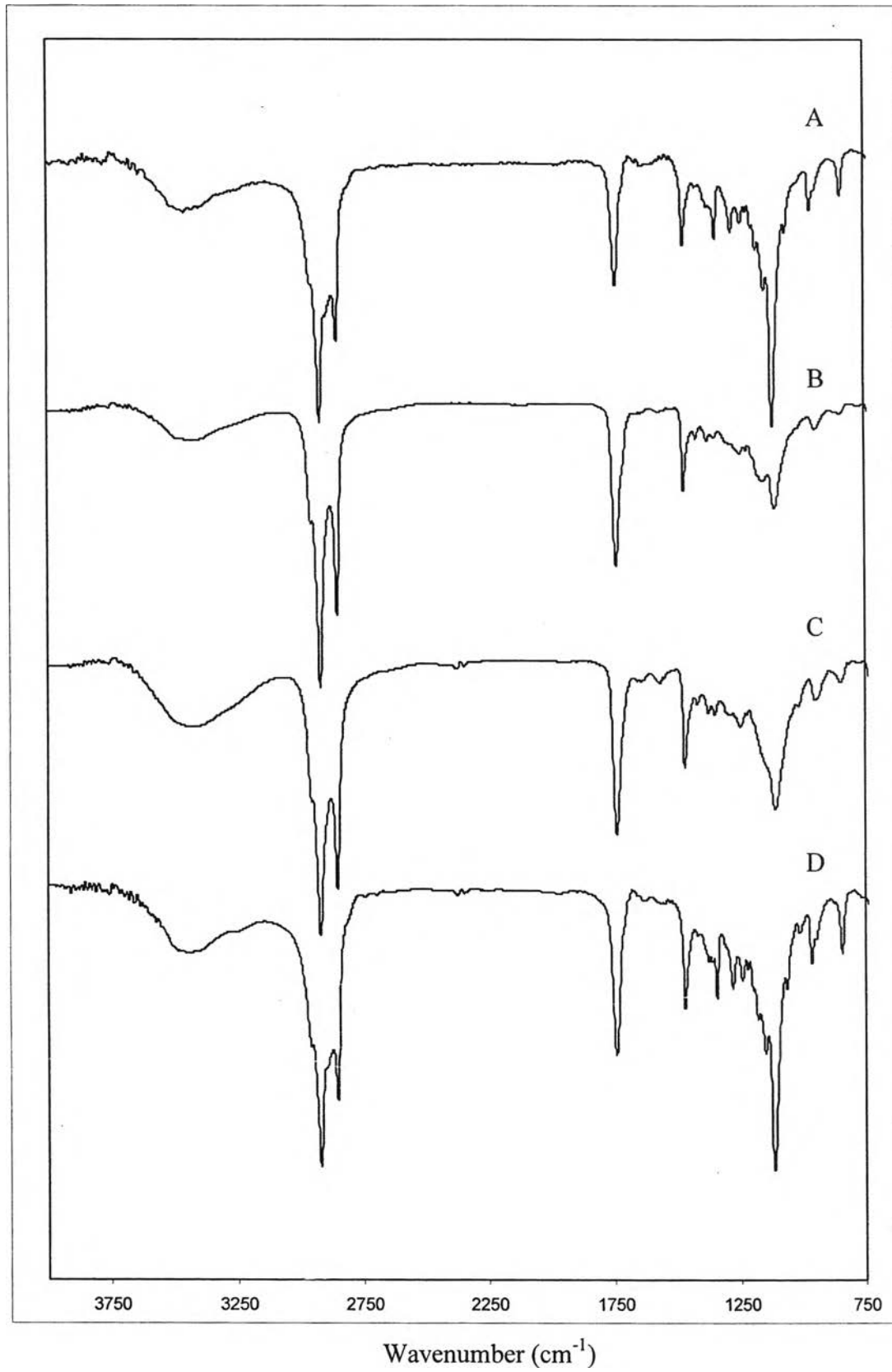

Figure 56 IR spectra of AmB-NLC containing 1% AmB(A); 2.5%AmB(B); 5%AmB(C) and physical mixture of lyophilized NLC base and 5% of AmB powder(D)

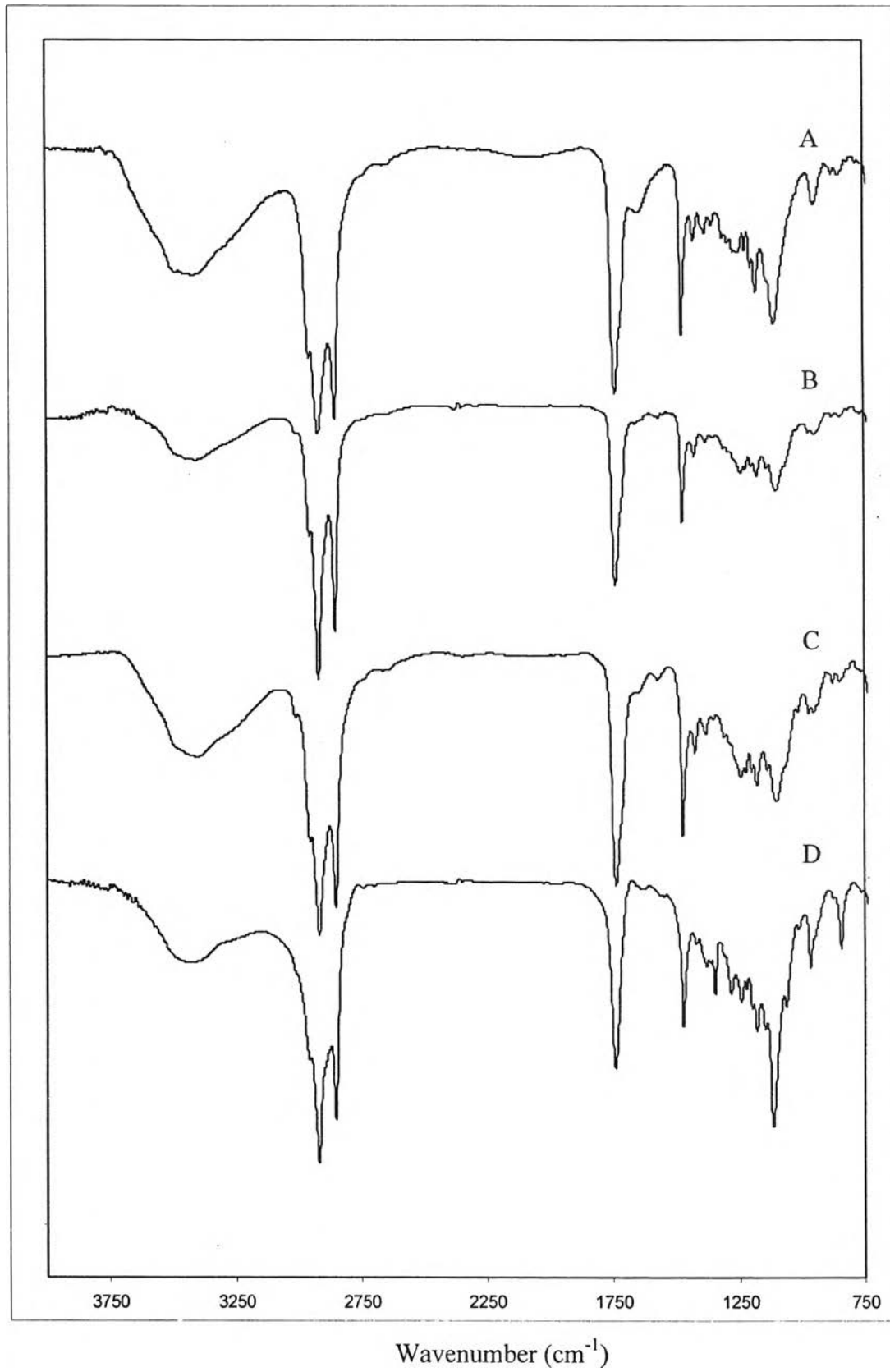

Figure 57 IR spectra of AmB-SLN-L containing 1% AmB(A); 2.5%AmB(B); 5%AmB(C) and physical mixture of lyophilized SLN-L base and 5% of AmB powder(D)

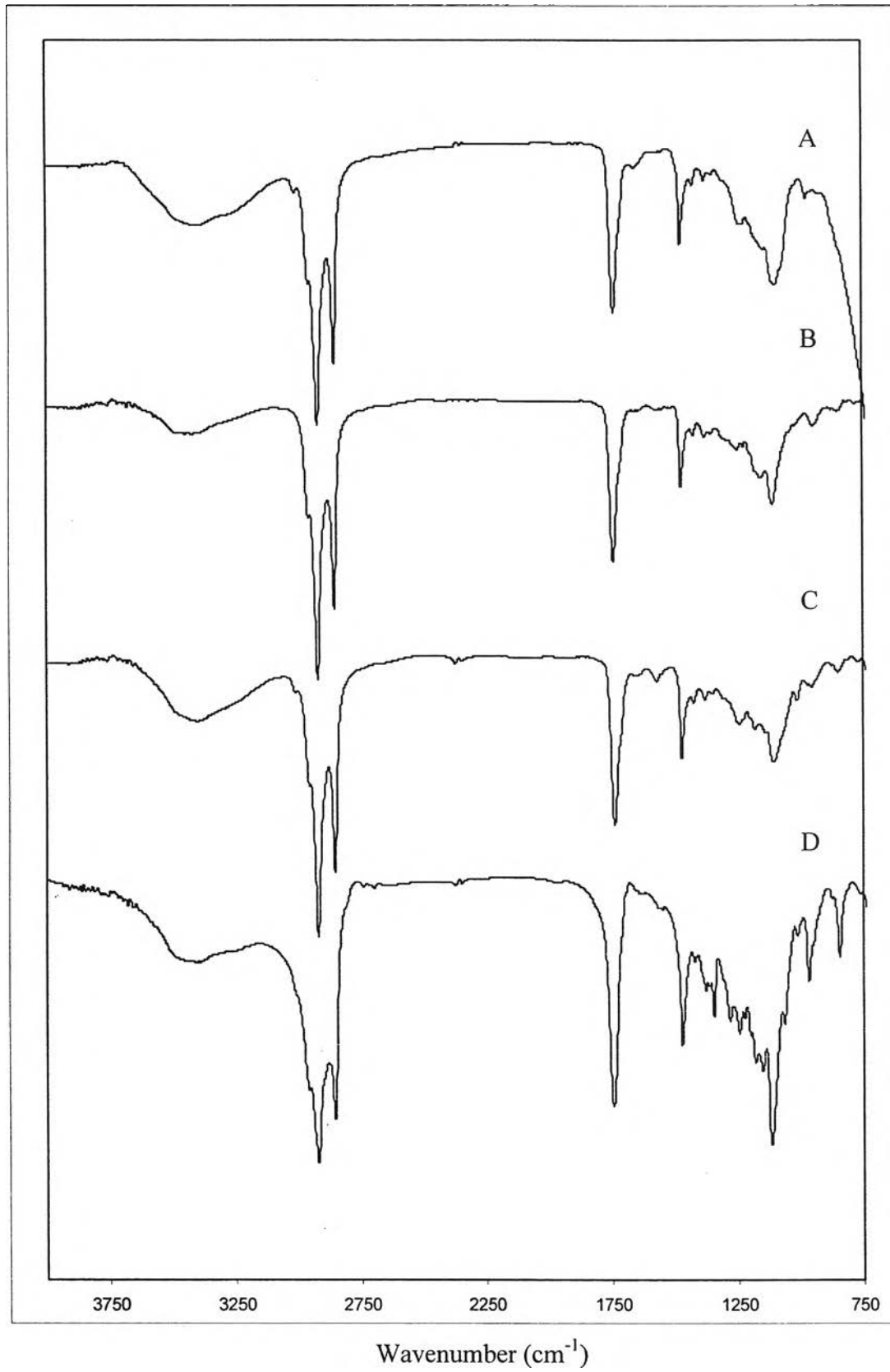

Figure 58 IR spectra of AmB-NLC-L containing 1% AmB(A); 2.5%AmB(B); 5%AmB(C) and physical mixture of lyophilized NLC-L base and 5% of AmB powder(D)

Thermal analysis

Differential Scanning Calorimetry

DSC thermograms of 1, 2.5 and 5% AmB loaded in SLN, NLC, SLN-L and NLC-L formulation are shown in Figure 59. The melting temperature and melting enthalpy determined from thermograms are summarized in Table 60. From the results, 5% of drug in all preparations showed shifting of the endothermic peak of AmB while 1 and 2.5% AmB formulations did not show any crystalline peak. It was not clearly to include that AmB in amount of 1 and 2.5% of total lipid were in amorphous form or such a small amount could not be detected under this technique. Cavalli et al. (2000a) showed the drug melting peak at 230°C was not present in paclitaxel-loaded SLN. This thermal behaviour might be ascribed to the presence of paclitaxel in an amorphous form or molecularly dispersed. Similar thermal behaviour were also noted with other drugs, such as nifedipine, phenothiazine, diazepam and camptothecin (Cavalli et al., 1995a; Cavalli et al., 1997; Yang and Zhu, 2002).

The inclusion of drug molecules in the crystal lattice was normally accompanied by the depression of the melting point. A linear correlation between melting temperature and concentration of added drug was a good indicator of complete inclusion of the drug in the lattice. In contrast, if the thermal behavior of the lipid matrix was not altered in the presence of drug, most likely the drug was not incorporated in the lipid matrix (Jennings and Gohla, 2001).

The depressions of the melting point of various formulations when the drug incorporated in 1.0, 2.5% and 5.0% are also shown in Table 60. The thermal characteristics of the lipid in each AmB formulations were not significant different when compared with different percentages of drug loaded. This indicated that the drug was not dispersed in the lipid matrix of all formulations. Contrast result of decrease in melting and crystallization temperature of the matrix lipid with increasing drug concentration has been reported for Udidecarenone (Q_{10}) loaded SLN (Bunjes et al., 2001).

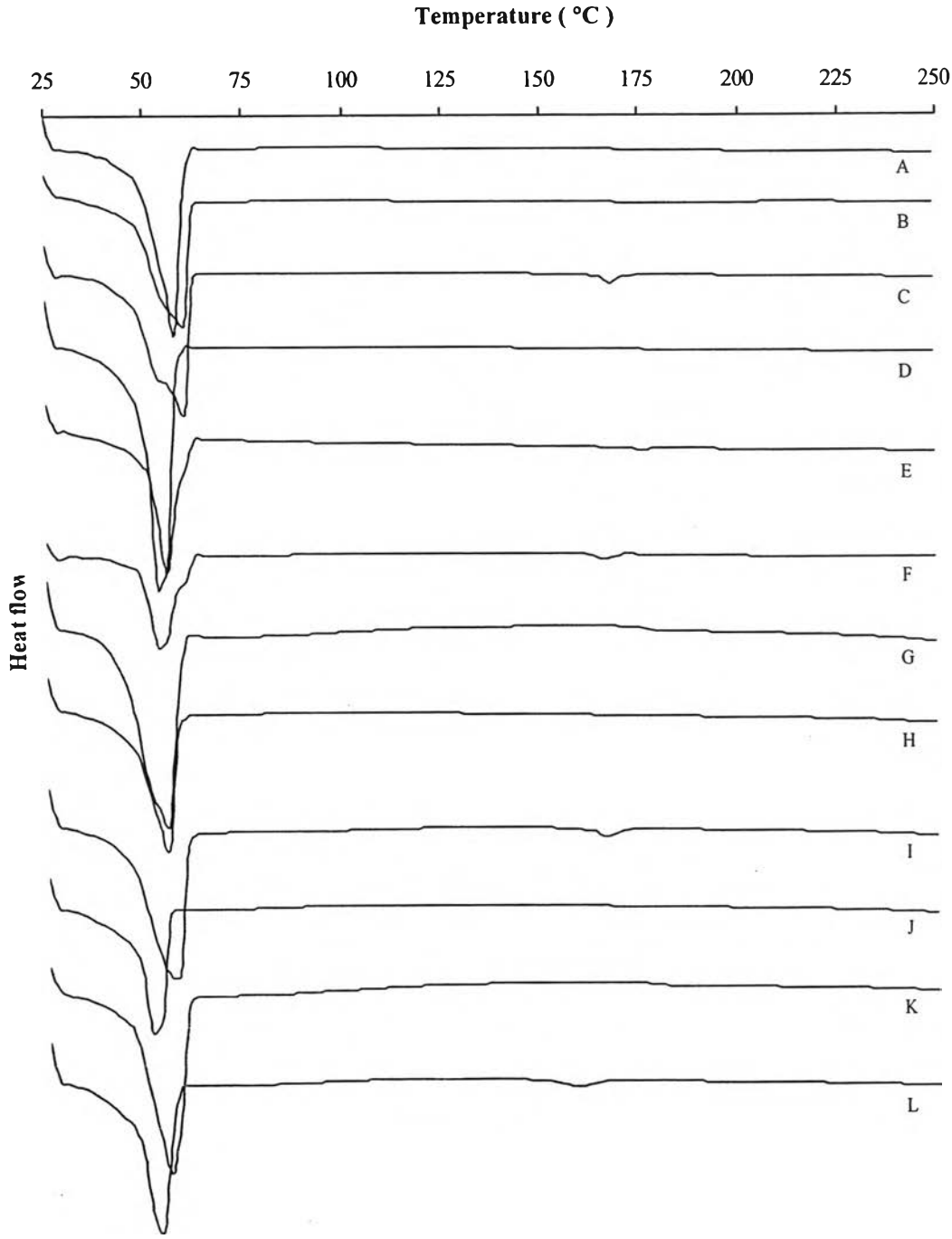

Figure 59 DSC thermograms of lipid matrices of preparations containing 1, 2.5, 5%AmB-SLN(A,B,C); 1, 2.5, 5%AmB-NLC(D,E,F); 1, 2.5, 5%AmB-SLN-L(G,H,I); 1, 2.5, 5%AmB-NLC-L(J,K,L).

Table 60 The thermal behaviours of different amount of AmB loaded in various formulations determined by DSC analysis

Formulation	% AmB loaded	Melting properties (1st peak, °C)		Energy (J g^{-1})	Melting properties (2nd peak, °C)		Energy (J g^{-1})
		Melting range	Melting peak		Melting range	Melting peak	
AmB-SLN	1.0%	48.50-60.58	58.14	-132.32	-	-	-
	2.5%	47.50-61.04	59.27	-137.68	-	-	-
	5.0%	46.53-61.20	59.58	-123.28	161.58-170.61	167.74	-2.44
AmB-NLC	1.0%	49.39-56.28	54.00	-122.60	-	-	-
	2.5%	50.10-58.31	54.93	-106.71	-	-	-
	5.0%	48.80-57.41	53.82	-105.41	162.63-169.85	165.62	-2.66
AmB-SLN-L	1.0%	43.05-58.13	55.64	-108.22	-	-	-
	2.5%	46.25-57.48	55.75	-105.16	-	-	-
	5.0%	44.61-59.88	56.22	-108.66	162.40-169.30	165.56	-2.16
AmB-NLC-L	1.0%	47.28-54.19	51.72	-63.10	-	-	-
	2.5%	44.83-54.83	51.68	-90.82	-	-	-
	5.0%	45.77-56.32	52.06	-69.31	153.55-162.33	157.74	-1.65

To evaluate whether the drug was in crystalline or amorphous forms when 5% of drug was loaded in various preparations are shown in Figure 60 and Table 61. The endothermic peak of AmB was shifted from 205°C of pure AmB in both physical mixtures and lyophilized SLN, SLN-L, NLC and NLC-L preparations; especially the latter case showed the peak at the lowest temperature. However, the AmB peak intensities of the obtained formulations were higher than their physical mixture which might probably be due to the demixing of sample preparation. The shift of endothermic peak was due to the influence of process preparation. AmB was passed through the hot high pressure homogenizer which gave the particle size much smaller than from the simple mixing. Thus, these transitions were faster for the small crystallites. In addition, the presence of oil and phospholipids as in NLC-L formulation resulted in the fastest transition of the endothermic peak. The data could indicate that the 5% of AmB loaded in these formulations showed the crystalline form which was deposited on the surface of particles or was expeled from the solid lipid. Consequently, the chemical stability of 5% drug loaded in preparations was lower than the 2.5% drug loaded.

The comparison between the degree of crystallinity of physical mixture and lyophilized SLN, SLN-L, NLC and NLC-L formulations is shown in Figure 61. Degree of crystallinity was calculated by comparing the enthalpy of the formulations with the enthalpy of bulk lipid according to zur Mülhen et al., (1998); Freitas and Müller (1999); Schubert and Müller-Goymann (2005), and Souto et al. (2005). Enthalpy of bulk lipid was being taken as 100%. Enthalpies of formulations were calculated on the basis of total weight taken. The physical mixture of all formulations had the degree of crystallinity higher than their processed ones. It was because the recrystalline process was retarded and needed time to reorder. The crystallinity of AmB formulations was ranked: AmB-SLN> AmB-SLN-L>AmB-NLC>AmB-NLC-L in both cases. It was confirmed that the presence of oil or/and phospholipid could reduce the degree of crystallinity of lipid in formulation. The finding was agreed with the previous study of Lombardi et al. (2005) that the addition of oleic acid and Miglyol reduced crystallinity of the GB-NLC and GP-NLC formulations. With regarding to the depression of melting temperature, these lipid nanoparticles formulations was ranked in the same order of the degree of crystallinity as shown in

Figure 62. The effect of oil to reduce the melting point of both AmB-SLN and AmB-SLN-L formulations was proportionally related. Thus, the presence of oil or/and

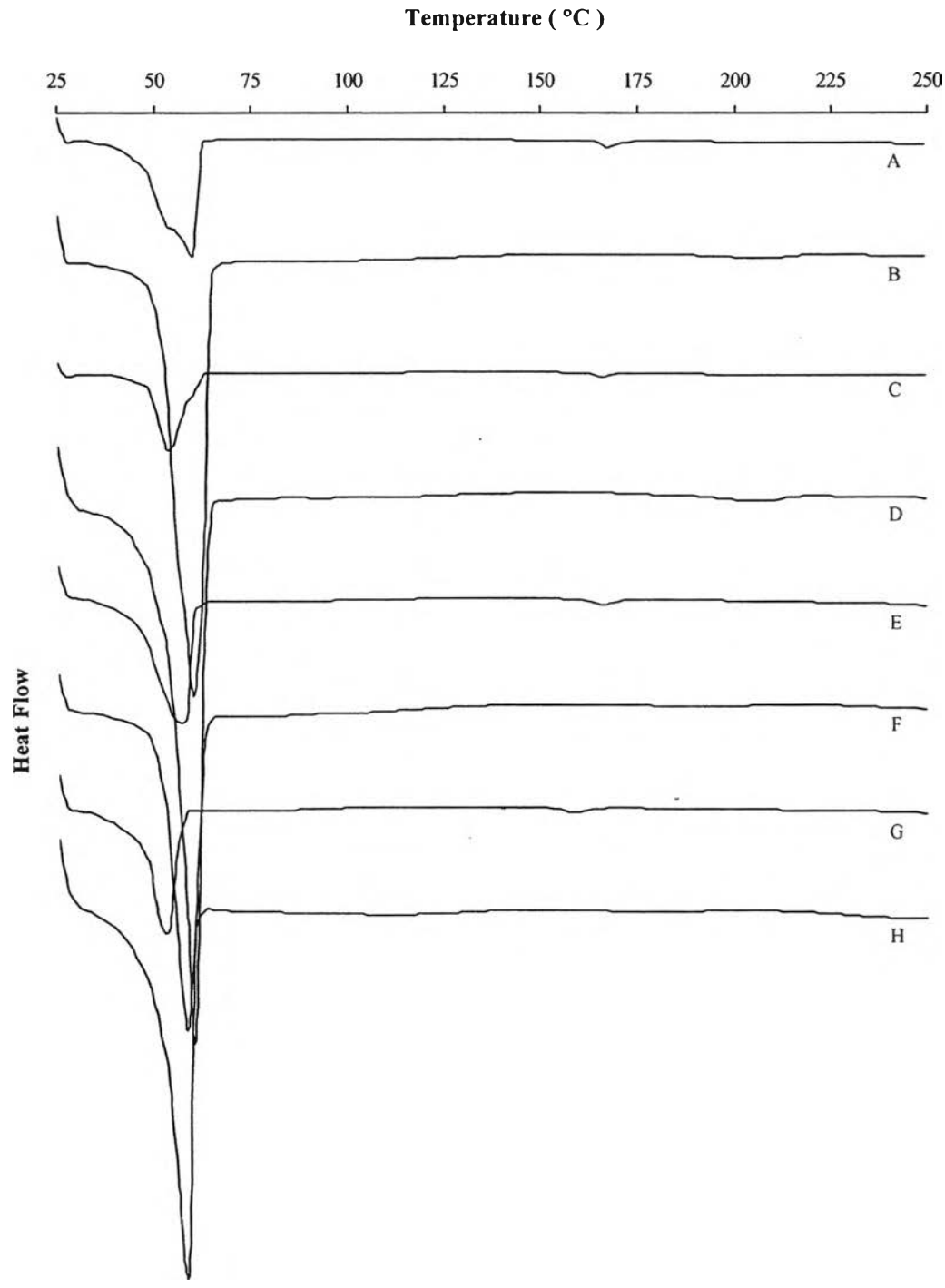

Figure 60 DSC thermograms of 5% AmB lipid matrix and physical mixture of of SLN (A,B); NLC(C,D); SLN-L(E,F) and NLC-L(G,H), respectively.

Table 61 The thermal behaviours of 5% AmB loaded in various formulations and their physical mixture determined by DSC analysis

Formulation	Melting properties (1st peak)		Energy ($J g^{-1}$)	Melting properties (2nd peak)		Energy ($J g^{-1}$)
	Melting range	Melting peak		Melting range	Melting peak	
AmB-SLN (PM)	51.04-63.45	59.00	-146.86	207.66-216.39	209.88	-1.70
AmB-NLC (PM)	53.39-62.65	58.77	-125.80	193.79-214.50	202.62	-1.67
AmB-SLN-L (PM)	51.16-61.53	57.69	-121.83	177.25-203.41	192.73	-1.99
AmB-NLC-L (PM)	48.78-59.10	56.76	-90.72	162.89-195.10	176.49	-1.51
AmB-SLN (FD)	46.53-61.20	59.58	-123.28	161.58-170.61	167.74	-2.44
AmB-NLC (FD)	48.80-57.41	53.82	-105.41	162.63-169.85	165.62	-2.66
AmB-SLN-L (FD)	44.61-59.88	56.22	-108.66	162.40-169.30	165.56	-2.16
AmB-NLC-L (FD)	45.77-56.32	52.06	-69.31	153.55-162.33	157.74	-1.65

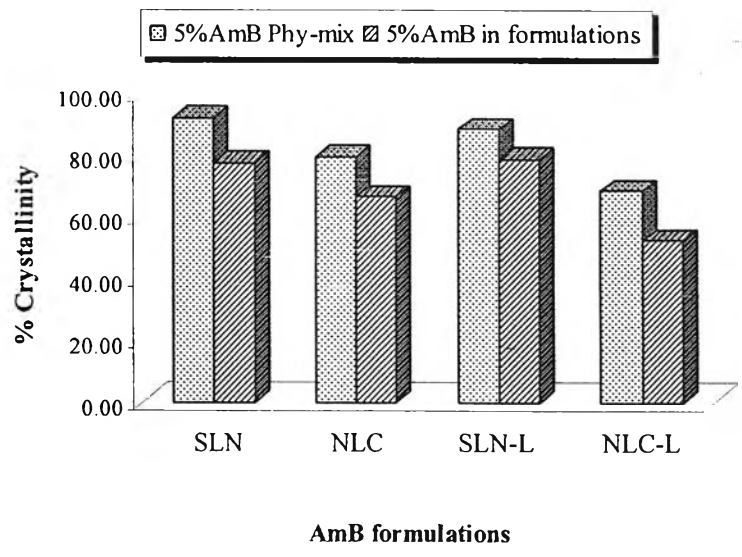

Figure 61 The comparison between the degree of crystallinity of 5% AmB physical mixture and 5% AmB loaded SLN, SLN-L, NLC and NLC-L formulations

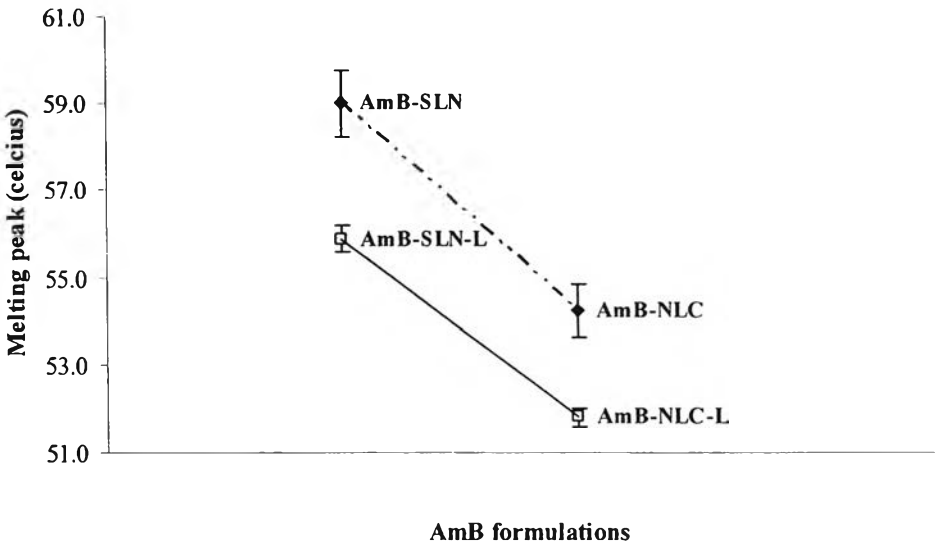

Figure 62 The depression of melting temperature of the various lipid particles formulations; each point was average from three drug loading data.

phospholipid affected the crystal lattice of the lipid, particularly the combination of oil and phospholipid had a strong effect to both melting behavior and degree of cystallinity.

Thermal analysis of lecithin-based SLN and NLC dispersion show significant influence of the phospholipids on the melting behavior of the triglycerides in term of melting peak and onset temperature. In contrast, Friedrich and Müller-Goymann (2003) reported that the thermograms of binary mixture of Softisan®100 or Softisan®142 with varying Phospholipon®90 (30-60% w/w) had no significant change on the melting behavior in terms of peak minimum and onset temperature. However, they presented the correlation between the amount of Phospholipon®90 and the melting enthalpy of lipid which agreed with this experiment. With increasing amount of Phospholipon®90 the melting enthalpy decreased linearly in consequence of non-crystallized phospholipid. In this study, the addition of phospholipid in both cases of SLN-L and NLC-L decreased the melting enthalpies of lipid of SLN and NLC, respectively. It was concluded that, the incorporation of phospholipids in the system seems to disturb the crystallization of triglycerides.

Hot stage microscopy (HSM)

Figure 63A shows the HSM microphotographs obtained from SLN containing AmB 1%, 2.5% and 5%, respectively. The melting range of the these preparations were 53°C-59°C, 54°C-60°C and 56°C-62°C, respectively. The DSC results in Table 95 show a broader melting range of GP than the HSM data.

The HSM micrographs of NLC containing 1%, 2.5% and 5% of AmB are shown in Figure 63B. The unmelted substances were at 51°C, 52°C, 52°C and the totally melt at 57°C, 59°C and 59°C, respectively. The results indicated that the drug loading in preparations did not affect the melting range of solid lipid. The onsets of melting temperature of NLC products were lower than that of SLN preparations. This was due to the behavior of MCT oil loaded in SLN that described earlier (DSC data).

Figure 63C and 63D show the microphotographs of SLN-L and NLC-L containing 1%, 2.5% and 5% of AmB, respectively. These results were in accordance with those observed by the DSC technique. They showed no alteration in melting point of GP when the amount of AmB increased. It was concluded that the drug did not disturb the crystallinity or change the melting behaviour of solid lipid.

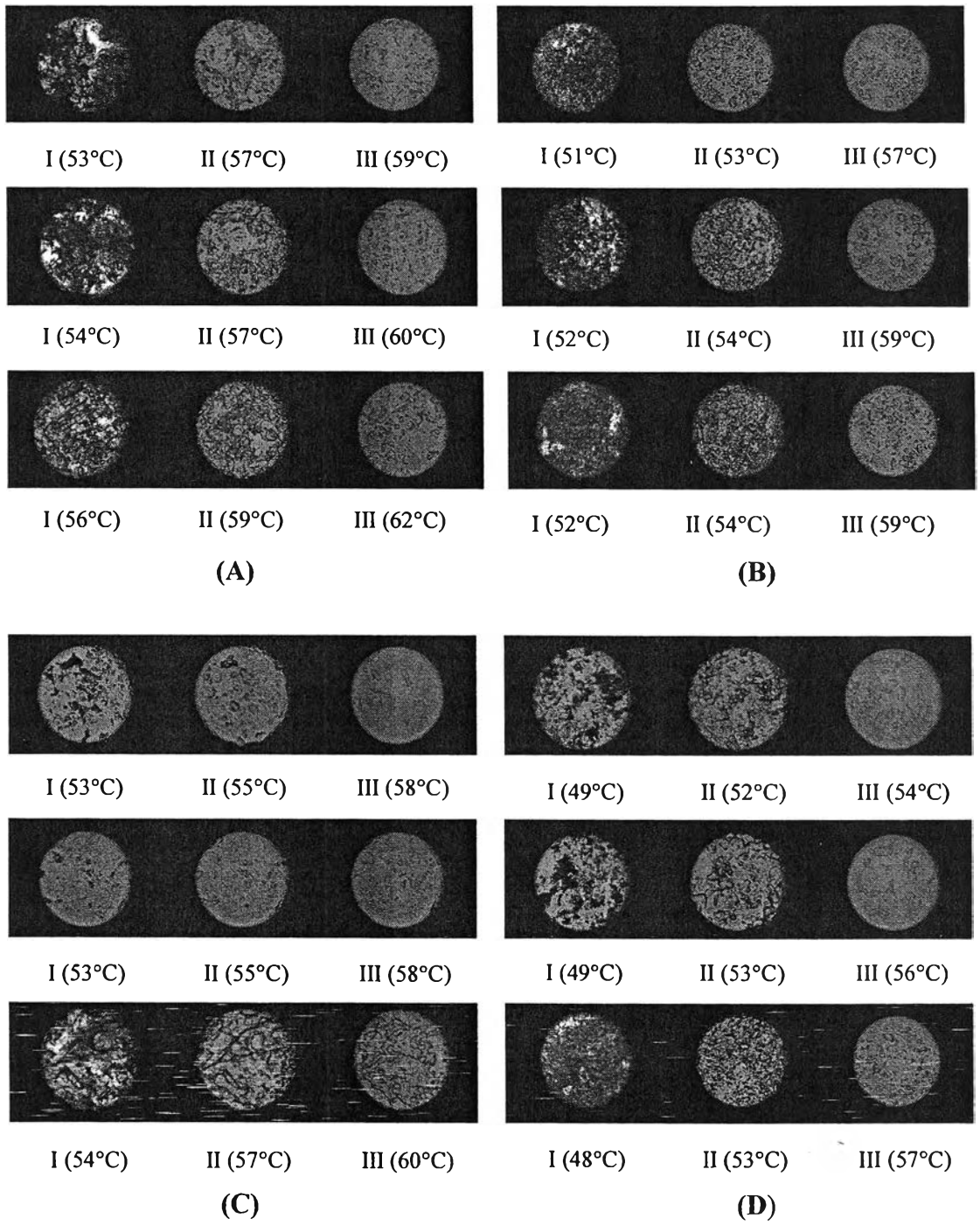

Figure 63 HSM microphotographs of (I)unmelt GP, (II) melting GP to (III) totally melt GP (magnification 40x) obtained from lyophilized 1, 2.5, 5% (top, middle, bottom) of AmB loaded SLN(A); NLC(B); SLN-L(C) and NLC-L(D).

Powder X-ray Diffractometry

The X-ray investigations suggested that good entrapment efficiency in SLN could be achieved with lipids of low crystalline order and metastable polymophs. High crystallinity or the formation of the stable polymorph could be correlated with drug expulsion from the carrier (Jennings and Gohla, 2001). The X-ray diffractogranms of physical mixture of GP+AmB, GP+AmB+P407, and the mixture of GP+AmB+P407+PL and similar to that of weight ratio in SLN and SLN-L formulations are shown in Figure 64i.

To verify the existence of AmB in GP, the mixture of GP and AmB was analyzed by the powder X-ray diffractometry. The physical mixture of GP and AmB in the same quantity as in formulation of 5% AmB loaded SLN were used to assure that the sharpening peaks of AmB could be detected by powder X-ray dfiffractometry. It is obvious that GP exhibited crystalline state. X-ray diffraction patern of physical mixture of GP and AmB was simply a superimposition of each component with the peaks of lower intensities. The existing peaks of AmB exhibited at 13.99° and 21.55° while the GP displayed at 19.48°, 21.44° and 23.36°.

For investigation of the effect of stabilizers on crystalline state of AmB, the physical mixture of GP, P407 and AmB and the mixture of GP, P407, PL and AmB were also analyzed by X-ray diffractometry. The X-ray diffraction of the physical mixture of GP, P407 and AmB showed the peaks which combined the crystalline peaks of each component. The existing peaks were strong peaks at 19.72° and 23.27° which refered to the peaks of P407, the small peaks at 21.47° and 14.03° which represented the peaks of GP and AmB, respectively. The other predominant peaks of their pure components were superimposed by the strong peaks of P407. In the same way, X-ray diffractogram of the mixture of GP, P407, PL and AmB was shown the peak pattern similarly to that of the former physical mixture. The peaks of PL were superimposed which could not be appeared.

The presenting crystalline characteristic of the drug could be observed in the physical mixture. Figure 64ii show the X-ray diffractograms of the physical mixture

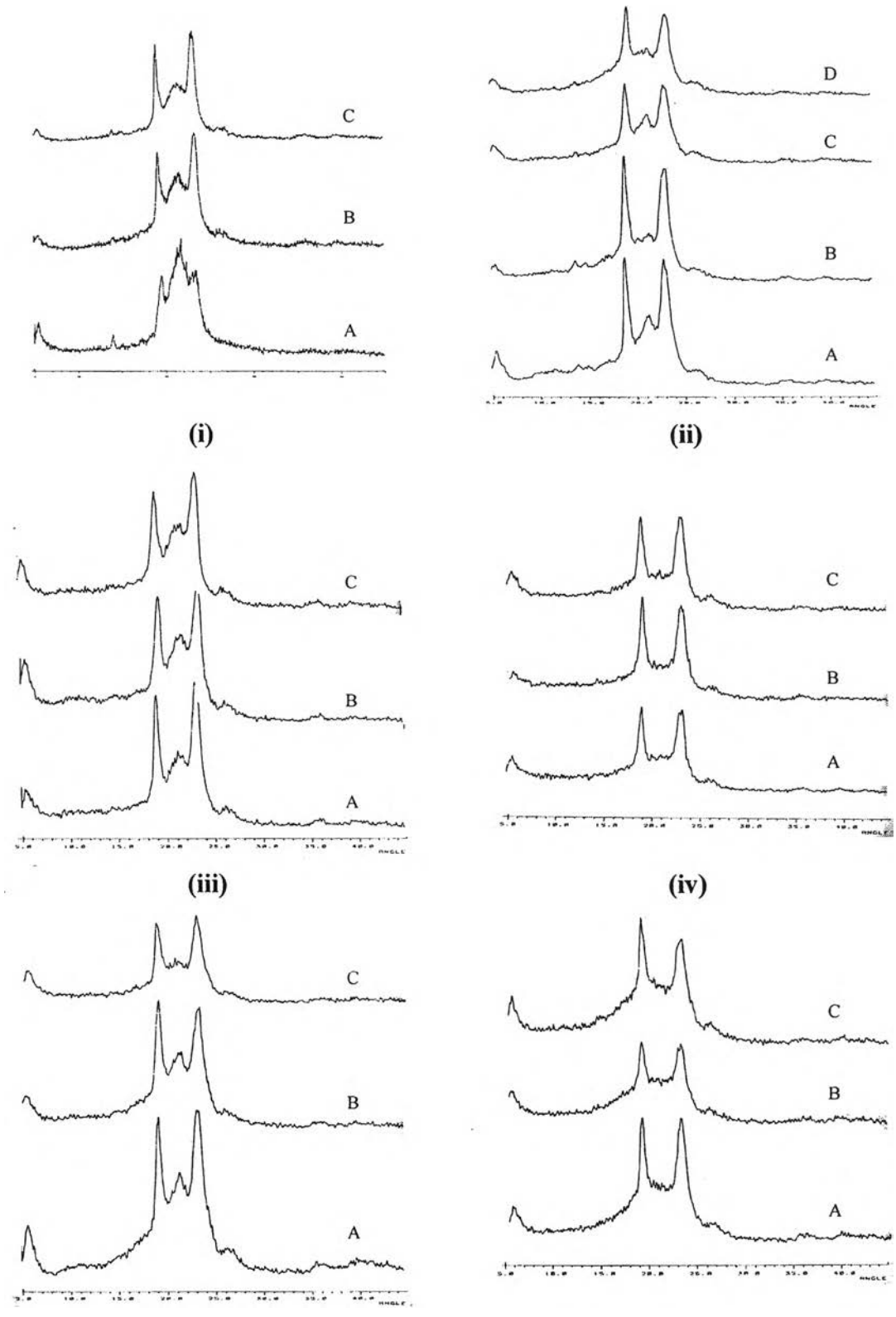

Figure 64 X-ray diffractogram of (i)PM of GP+AmB(A), GP+P407+AmB(B) and GP+P407+PL+AmB(C); (ii)PM of 5% AmB and the lyophilized base of SLN(A), NLC(B), SLN-L(C) and NLC-L(D); (iii)1, 2.5, 5% (A,B,C) of lyophilized AmB-SLN; (iv) 1, 2.5, 5% (A,B,C) of lyophilized AmB-NLC; (v)1, 2.5, 5% (A,B,C) of lyophilized AmB-SLN-L; (vi) 1, 2.5, 5% (A,B,C) of lyophilized AmB-NLC-L.

of 5% AmB calculated to the lipid and the lyophilized drug-free SLN, NLC, SLN-L and NLC-L formulations. The distinguished peaks of AmB at 14.10°, 13.94°, 13.98° and 14.06° were observed respectively. This indicated that the 5% AmB could show the crystalline peak in the physical mixture of all preparations.

The effect of drug loading in each formulation was observed in Figure 64iii-64vi as the X-ray diffractograms of 1.0%, 2.5% and 5.0% of AmB loaded in SLN, NLC, SLN-L and NLC-L formulations, respectively. The amount of drug loading did not significantly change the X-ray diffractograms of AmB-SLN formulation that still showed the lipid crystalline after preparation but affected the AmB-SLN-L formulation and altered the X-ray diffractograms. The peak that represented the crystallinilty of lipid at 21.44° was deduced when the amount of drug increased. This indicated that the drug affected the lipid recrystallization to less ordered crystals and the amorphous state would attribute to the higher drug loading. The peak at 21.44° in NLC formulation was insignificantly deduced when the drug increased while this peak was disappeared in all drug loaded NLC-L preparations. It could conclude that the amount of drug did not play a role for the recrystallization of the lipid in both cases but the addition of oil in the systems was the predominant factor to obtain the lipid in amorphous state. However, the distinguished crystalline peak of AmB in all percentage of the drug loaded of four systems disappeared. It was found that all amount of drug in solid matrix was either molecularly dispersed or amorphous from.

The physicochemical properties of AmB were detected by X-ray diffractometry and DSC techniques. The results of the drug status from two methods were not correlated. It was probably due to the difference of the principal and the sensitivity of each method.

11. *In Vitro* drug release

In vitro release studies are important to understand the *in vivo* performance of the dosage form. Drug release studies help in evaluation of sustained and prolonged release dispersion systems. For present work, 1% AmB loaded SLN, NLC and SLN-L prepared by HPH method and amphotericin B loaded SLN prepared by WME method

were selected. HPLC method was selected to determine the amount of drug in receptor compartment of modified Franz diffusion apparatus. AmB quantity was measured at the wavelength of 408 nm that was the λ_{max} of monomer AmB form in PBS and the amount of AmB released was then calculated from calibration curve.

The drug release profiles of these preparations for 24 hours are shown in Figure 65a. The release of AmB from SLN formulations was low. After 24 h, the AmB release was about 45%. Very low paclitaxel release of 20% after 24 h from SLN containing stearic acid and P188 was also reported by Chen et al. (2001).

The AmB release was ranked AmB-SLN > AmB-NLC >AmB-SLN-L. In addition, the final accumulative amount of drug after 24 hours of AmB-SLN was higher than that of AmB-NLC and AmB-SLN-L, respectively. This might be resulted from the entrapment efficiency and aggregate species of these preparations. AmB-NLC showed the burst release at the initial stage and sustained release subsequently which was corresponding to the finding of Hu et al. (2005). It was due to that the oil was not homogenously distributed in nanoparticles. Because of the different melting point between solid lipid and liquid lipid, the solid which owned higher melting point could crystallize first, forming a liquid lipid-free or little lipid core, finally, most of the liquid lipid was located at the outer shell of the nanoparticles which resulted to drug burst release at the initial stage. The drug in monomer form or oligomer form could pass through the membrane easier than in the aggregated form. In comparision, AmB-SLN-L had large amount of the aggregated species and the highest of drug entrapment efficiency among these preparations; therefore, not only the drug release rate but also the cumulative amount of drug release was the lowest.

The effect of composition in preparations in vitro drug release is shown in Figure 65b and 65c. Both 2.5% and 5% of drug loading in SLN, NLC and SLN-L displayed the pattern of drug release similar to 1% of drug loading. It is noticed and confirmed that the entrapment of efficiency and the aggregate species of the drug from these preparations had an influence to the drug release mechanism. Indeed, for the in vitro release of AmB from 5% of drug loaded in these formulations, they showed an interesting biphasic release. After 6 hr, there were cumulative release of

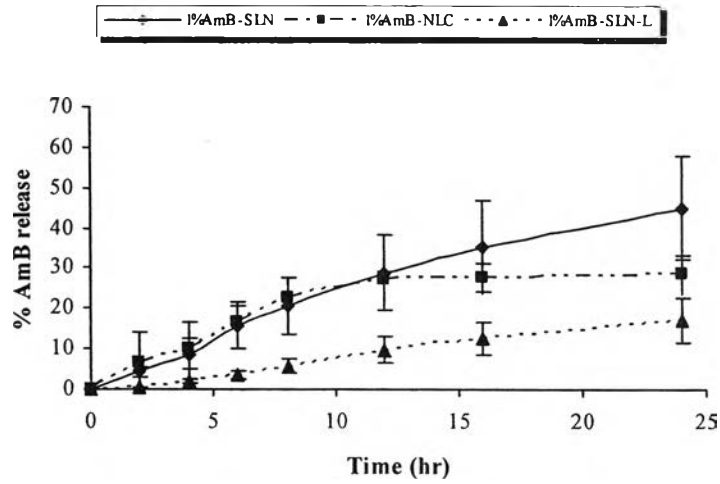

(a)

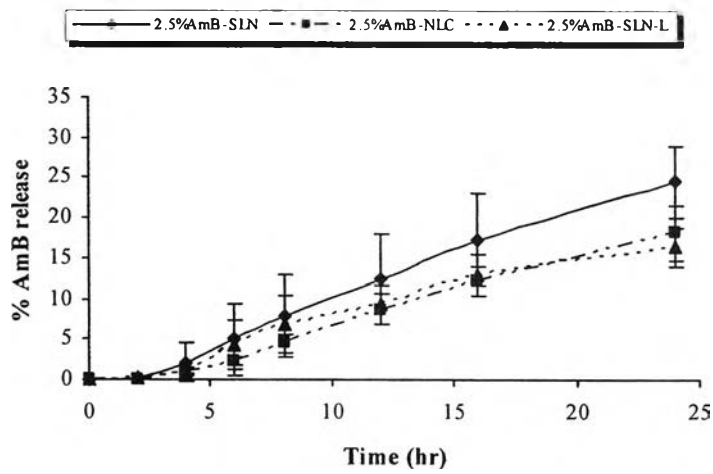

(b)

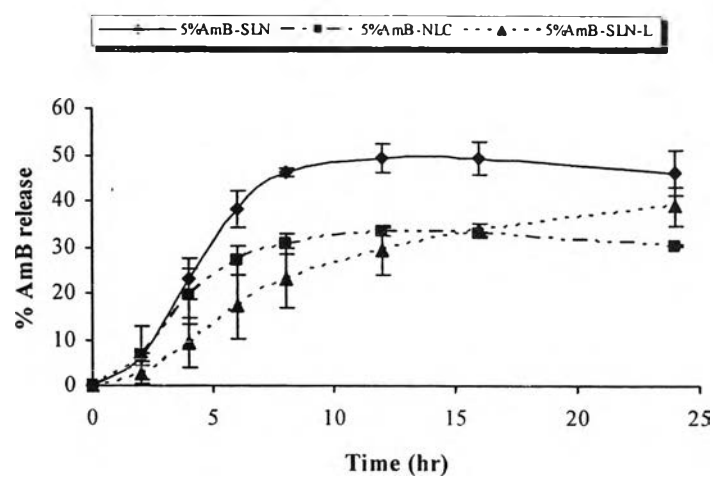

(c)

Figure 65 The release profile of AmB in SLN, NLC and SLN-L formulations 1.0%(a), 2.5%(b), 5%(c).

41.47, 26.41 and 19.44% of the drug for SLN, NLC and SLN-L, respectively. Afterward, the drug release followed a steady pattern. This finding was in accordance with the previous study of Cortesi et al. (2002) on the release of cromoglycate from liposphere produced with P407. The release pattern of AmB from egg albumin nanospheres described by Santhi et al. (1999) also showed an interesting biphasic release with total percentage of drug released of 97% after 24 h.

Figure 66a shows the drug release profile of various amount of AmB loaded SLN to investigate the effect of drug loading. The profiles indicated that 5% drug loaded SLN had the highest drug release rate followed by 1% and 2.5% drug loaded, respectively. The cumulative amount of drug release in 24 hr of 5% and 2.5% drug loaded SLN were equal whereas was the lowest with 1% drug loaded. This result might be described in the term of the drug entrapment. From Table 56, the drug entrapment efficiency of 1% drug loaded SLN was lower than that of 2.5% loaded SLN. Therefore, the release of the former was higher than the latter. The 5% drug loaded preparation presented the highest crystallinity of free drug or the drug conjugated to the copolymer side chain in the continuous phase as described in DSC analysis. The release of 5% drug loaded SLN was the highest due to the large amount of the drug in the continuous phase could be freely passed through the membrane.

For the NLC and SLN-L preparations, the effect of drug loading on the release rate is displayed in Figure 66b and 66c, respectively. As expected, the release rate of the drug from NCL formulation increased when the drug entrapment was decreased. Therefore, the drug release rate of 1% drug loaded NLC was faster than that of 2.5% drug loaded NLC formulations. In case of 1% and 2.5% drug loaded SLN-L, the percentage release of the drug was practically identical due to the non significant difference in drug entrapment efficiencies ($p>0.05$). Again, 5% drug loaded of both cases showed the fastest release when compared to 1% and 2.5% drug loaded.

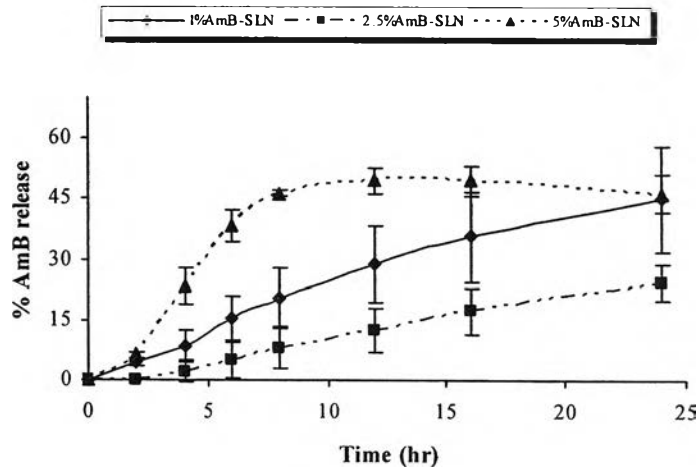

(a)

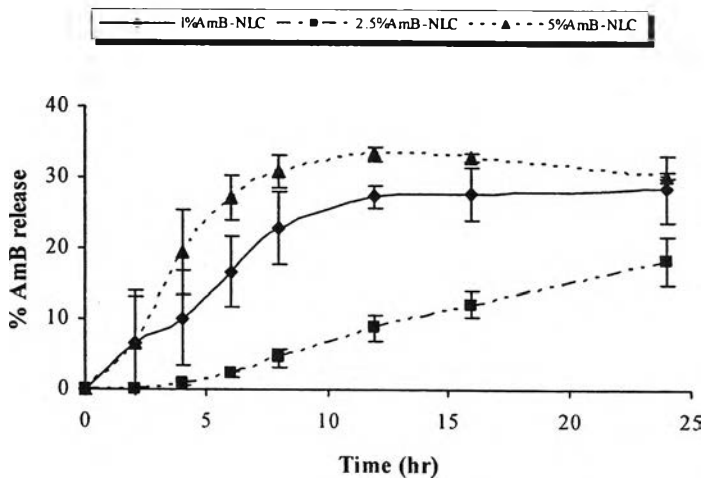

(b)

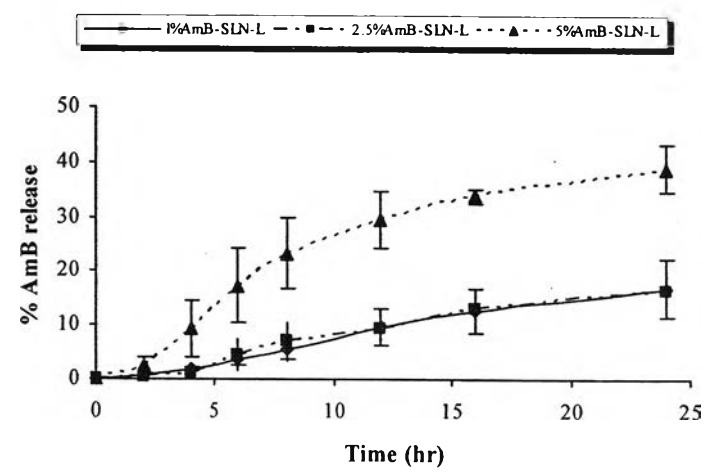

(c)

Figure 66 The release profile of formulations containing 1.0%, 2.5% and 5.0% AmB loaded SLN (a); NLC (b); SLN-L (c).

From the release profiles, it might be conjectured that since the outer shell of SLN was composed of P407, and quite a lot of drug was released in the form of a burst. The core of the SLN mainly consisted of GP and a portion of drug which complexed with lecithin was released more gradually. However the characterization of the drug location needed to be further investigated by NMR and ESR techniques (Wang et al., 2002) and also determined by fluorescence and parelectric spectroscopy (Lombardi et al., 2005).

12. Biopharmaceutical characterizations of formulations

12.1 Hemolytic activity

Formulations of good physical and chemical stability were chosen for hemolysis study. There were AmB-SLN containing CreRH and either Gly or PEG preapared by WME method and AmB-SLN, AmB-NLC, AmB-SLN-L and AmB-NLC-L containing GP with either Tw20, CreRH, P407 or M52 as stabilizer prepared by HPH method. These formulations were diluted with isotonic PBS pH 7.4 to various concentrations of AmB in the range of 1-40 mcg/ml. Generally, the *in vitro* hemolytic test served as a screening method for toxicity of lytic agent contained in intravenous formulation.

The hemolytic activity of WME1 and WME3 compared with Fungizone® are shown in Figure 67b. The systems of GP+CreRH+Gly and GP+CreRH+PEG showed hemolysis response upon increasing concentration up to 2.14% and 4.72% hemolysis at the concentration of 40 μg/ml, respectively. In contrast, Fungizone®, a mixture of AmB with a detergent, deoxycholate caused 50% hemolysis at the concentration of 10 μg/ml and 100% hemolysis at about 40 μg/ml as shown in Figure 67a. These two formulations had aggregate species of AmB as described earlier which would lead to hemolyse the erythrocytes. However, the high entrapment efficiency of these formulations of higher than 95% in the SLN had an effect on the release of drug from preparations; thus, the less interaction between the drug and RBC, the lower in hemolytic activity was observed.

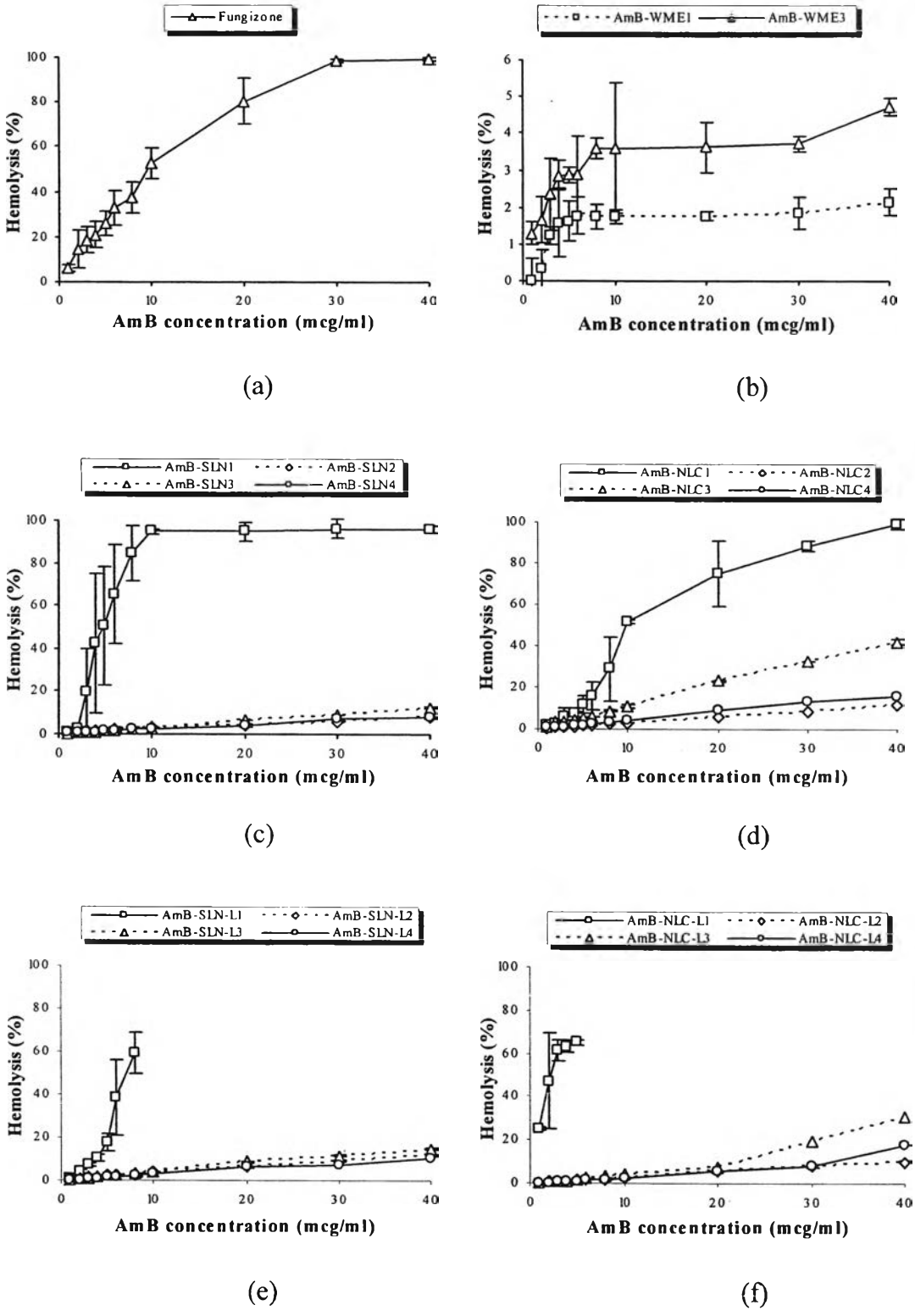

Figure 67 Hemolysis of sheep RBC at the varied levels of AmB in formulations; (a): Fungizone; (b): AmB-SLN prepared by WME method; (c), (d), (e), (f): AmB-SLN, AmB-NLC, AmB-SLN-L and AmB-NLC-L prepared by HPH method.

Hemolysis of AmB-SLN dispersions obtained from HPH method are shown in the Figure 67c. The results from AmB encapsulated in SLN2, SLN3 and SLN4 comprised of GP+CreRH, GP+P407 and GP+M52, respectively were similar ($p > 0.05$) that caused 7.5-12.5% hemolysis even at the AmB concentration of 40 μg/ml whereas Fungizone® causing 100% hemolysis at about 40 μg/ml. AmB-SLN1 which used Tw20 as stabilizer had high hemolytic activity of 95% at just a level of 10 μg/ml AmB. Therefore, some non-ionic surfactants as stabilizer in solid lipid nanoparticles could reduce the toxicity when compared the conventional form, Fungizone®. Another hypothesis suggested that AmB could gradually release from the SLN since some drug was incorporated in the solid lipid core; hence, the slow release of AmB from SLN might be due to the solid-like nature of their cores. Similar result that used AmB incorporated into PEO-PBLA micelle was reported by Yu et al. (1998). In addition, the low hemolytic activity may also reflect the release of monomeric AmB from AmB-SLN as opposed to Fungizone® which was released as both aggregated and monomeric, since monomeric AmB is less hemolytic than the aggregated forms of the drug (Brajtburg et al., 1996). From spectroscopic data, AmB-SLN1 that used Tw20 as stabilizer had the highest amount of AmB in aggregate form. Moreover, it was suggested that the highest percent hemolysis was also due to its shortest alkyl chain compared to the other surfactant solutions. Therefore, molecules of Tw20 were easily adsorbed onto the erythrocyte. In addition, Tw20 might have higher critical micelle concentration, thus there was more free surfactant monomers interacting with the erythrocytes (Aroonrat, 2001).

The hemolysis response of showed that AmB-SLN3 that used P407 as stabilizer had slightly higher hemolysis activity than AmB-SLN2 and AmB-SLN4 at the same AmB concentration. This was probably due to the least percentage of entrapment that AmB was entrapped in the chain of block copolymer rather than the surface or the core of particles led to higher interaction with the erythrocytes.

Figure 67d shows the effect of AmB loading on the hemolytic activity of NLC1, NLC2, NLC3 and NLC4 formulations. The hemolytic activities of most NLC formulations were slightly higher than those of SLN formulations. There were 2 possible hypotheses. Firstly, NLC formulations had more AmB aggregated form than

SLN preparations thus caused higher hemolytic response. Secondly, the flexibility and less rigid structure of NLC formulation would result in higher mobility of drug while vibrating. Therefore, the chance of interaction between drug and the surface of RBCs was more than that of SLN formulations.

Hemolytic activities of AmB loaded in SLN-L are shown in Figure 67e. Due to its poorly soluble in water and the oil phase thus the drug was located in the interfacial lecithin layer (Müller et al., 2004). Hemolytic activity of SLN-L formulation stabilized by Tw20 in high concentrations was not detected due to too turbid to measure by spectroscopic method. The hemolytic response of all preparations of AmB-SLN-L was not different from AmB-SLN; therefore, adding lecithin in the preparations did not affect the hemolytic activity. This result could be described into 2 main reasons as previously described. The degree of aggregation of AmB-SLN-L was significantly higher than those of AmB-SLN. In contrast, the drug entrapment of AmB-SLN was lower than those of AmB-SLN-L. Although AmB-SLN-L formulations had high quantity of the aggregate form of the drug but it stayed in the inner phase that could little effect interactive with the cell membrane of RBC. Lower toxicity of spray-dried AmB-phospholipid composite particles was also reported due to the association of AmB with phospholipid in their hydrated forms, either the liposomes or the complexes that AmB molecules may be immobilized by adjacent phospholipids and their transfer to RBC would be unfavorable (Kim et al., 2001).

Figure 67f displays the hemolytic activity of AmB loaded in NLC-L formulations (NLC-L1, NLC-L2, NLC-L3, and NLC-L4). The hemolytic activity of NLC-L were slightly higher than that of SLN-L while the ranking order of hemolytic response of the NLC-L formulations was the same as that of NLC formulations. Again, as the result of AmB-NLC formulations, it was clearly concluded that the oil incorporated in the system played the role for hemolytic activity. With regarding to the entrapment efficiencies of the latter three formulations, the ranking was NLC-L3 < NLC-L4 < NLC-L2. That meant the drug localized in the surface of particles or continuous phase could freely interact with RBC cause hemolytic response. The

assessment of cytotoxicity of SLN by hemolytic activity was also investigated by Schubert and Müller-Goymann (2005).

The cytotoxicity of unloaded SLN of triglycerides, soya lecithin, poloxamers and poloxamine as surfactants was lower than that of polyalkylcyanoacrylate and polylactic/polyglycolic acid nanoparticles using HL60 cell line differentiated to granulocytes particularly SLN containing lecithin had no cytotoxic effect at all, thus allowing their use as *in vivo* colloidal drug carriers. In addition, the nature of the lipid matrix had no effect on cell viability (Müller et al., 1997; Müller and Olbrich, 1999).

12.2 AmB susceptibility testing

Invasive fungal infections have increased over the past to decades causing formidable morbidity and mortality among immunocompromised hosts, especially patients with AIDS. The frequency of nosocomial fungal infections has also increased amongst cancer, organ transplant, burn and surgical patients. Due to the life threatening nature of these infections and reports of the drug resistance, susceptibility testing of yeast pathogens has become very important.

Methods used for susceptibility testing of yeasts include disc diffusion, agar dilution and broth dilution procedures. Numerous in vitro factors such as media, buffer, inoculum, incubation and end point criteria can affect results significantly. However, in this study, the broth macrodilution method by observing the turbidity changes was selected to study due to its simplicity and uncomplicated procedure. Although disc and agar-well diffusion tests have been used, these techniques have not been widely applied. Such methods exhibit poor reproducibility and have difficulties with drug stability and solubility.

Comparison of the MICs and MFCs of various AmB formulations (AmB-WME, AmB-SLN, AmB-NLC and AmB-SLN-L) obtained by broth macrodilution technique against *C. albicans*, *C. neoformans*, *A. fumigatus* and *P. marneffei* is shown in Table 62. The temperature of incubation was set to 25°C for *P. marneffei* contrast to that of 37°C for other fungi, because it showed better growth at such temperature.

Table 62 *In vitro* activities of various AmB formulations against important medical fungi

Formulations	*C. albicans*		*C. neoformans*		*A. fumigatus*		*P. marneffei**	
	a	b	a	b	a	b	a	b
AmB	0.25	0.5	0.25	1	0.5	16	0.06	4
Fungizone	0.25	1	0.25	0.5	0.5	8	0.06	4
AmB-WME	0.06	0.25	0.06	0.125	0.25	> 16	0.06	4
AmB-SLN	0.06	0.25	0.06	0.5	0.25	4	0.125	2
AmB-NLC	0.06	0.25	0.125	0.25	0.25	4	0.06	2
AmB-SLN-L	0.06	0.25	0.06	0.125	0.25	4	0.06	4

a,b: MIC, MFC (μg/ml); *: incubation at room temperature (25°C)

The *in vitro* anifungal activity of different types of AmB formulations was comparable to AmB itself and Fungizone, AmB in deoxycholate sodium, based on measurement of MICs and MFCs. AmB in buffered medium inhibited the growth of tested pathogenic fungi at the same concentration level of Fungizone® of equal or less than two-folds dilution. MFCs for *C. albicans* and *C. neoformans* were equal to the MICs or two folds higher while four-six folds higher were observed for *A. fumigatus* and *P. marneffei*. The best fungicidal activity was for *C. albicans* and *C. neoformans* (0.5-1.0 μg/ml) followed by *P. marneffei* (4.0 μg/ml) and *A. fumigatus* (8.0-16 μg/ml). In contrast, the pathogenic fungi could be ranked by the inhibitory activity as follows: *P. marneffei* (0.06 μg/ml), *C. albicans* and *C. neoformans* (0.25 μg/ml) and *A. fumigatus* (0.5 μg/ml).

For all AmB formulations, the MIC and MFC against *C. albicans* and *P. marneffei* were the same as AmB itself or Fungizone®. Whereas the MICs and MFCs of these formulations against *A. fumigatus* were similar except AmB-WME formulation which shown the highest MFC (> 16 μg/ml). In case of *C. neoformans*, the best formulations were AmB-WME and AmB-SLN-L which showed the minimum inhibited and killed concentrations less than the parent compound and commercial product in two folds dilution. Therefore, it was concluded that the optimal AmB formulations were AmB-NLC-L and AmB-SLN-L. They had the best fungicidal for *C. neoformans* (MFC 0.125-0.25 μg/ml) followed by *C. albicans* (MFC 0.25

μg/ml), *P. marneffei* and *A. fumigatus* (MFC 2-4 μg/ml). On the other hand, pathogenic fungi could be ranked by inhibitory activity for *C. albicans, C. neoformans* and *P. marneffei* (MIC 0.06 μg/ml) followed by *A. fumigatus* required at least 0.25 μg/ml of AmB to be inhibited. Nevertheless, all of the selected AmB lipid nanoparticles were equal and more effective than both AmB itself and Fungizone®, particularly 2 two folds dilution for *C. albicans* and *C. neoformans*.

The results indicated that solid lipid preparations containing AmB could improve antifungal activity in term of MIC and MFC. This might be influenced by the sustained release of AmB from the solid matrix in formulations and the release of drug in monomeric state. AmB at a low degree of aggregation, probably a dimer, preferentially binds with ergosterol, the sterol of fungal cell membranes whereas higher aggregated AmB, nonselective form, has little tendency to bind ergosterol. The explanation was in accordance with Lavasanifar et al. (2002b) who described the effect of aggregation state of AmB. AmB encapsulated stably in PEO-*b*-PHSA micelles might be released gradually and/or in a monomeric state which are non-toxic for mammalian cells, but cause the leakage of fungal cells. From Figure 53, the aggregated species of AmB in AmB-WME was the highest among the AmB formulations that related to this hypothesis. As expected, the MFC of AmB against *A. fumigatus* in AmB-WME was higher than those obtained by the other three formulations, Fungizone® and its AmB, respectively. However, in long-term assays, the antifungal activity of Fungizone® and lipid-based AmB formulations was seen to depend upon the concentration of the drug, the stability of the formulation, the fungal strain being tested, and the incubation period (Brajtburg and Bolard, 1996).